Exploring Targets of Allogeneic T cell Activation in Mouse Models of GvHD

Exploring Targets of Allogeneic T cell Activation in Mouse Models of GvHD

By
Jewel Imani, BSc (Hons)

A Thesis
Submitted to the School of Graduate Studies in
Partial Fulfillment of the Requirements for the Degree
Doctor of Philosophy

McMaster University

Doctor of Philosophy
(Medical Sciences)

McMaster University
Hamilton Ontario

Title: Exploring Targets of Allogeneic T cell Activation in Mouse Models of GvHD

Author: Jewel Imani, BSc (Hons)

Supervisor: Dr. Mark Larché

Number of Pages xiii,181

Abstract

Allogeneic Hematopoietic stem cell transplants (HSCT) are used for the treatment of bone marrow aplasias. Allogeneic HSCT is performed by treating the patient with chemotherapy drugs and irradiation and then transplanting hematopoietic stem cells from a healthy donor to restore the immune system and hematopoietic cells. Allogeneic HSCTs has the added benefit of the graft vs leukemia effect (GvL), whereby donor allogeneic T cells are able to mount immune responses against any residual cancer cells. However, alloreactivity towards the mismatched minor and major histocompatibility antigens the patient's healthy tissues leads to graft vs host disease (GvHD). This process is also mediated by Macrophages, Dendritic cells, B cells. Furthermore, a decrease in the number of NK, B, and T regulatory cells exacerbates GvHD. This leads to a state of systemic inflammation, tissue damage and multiorgan fibrosis. Current therapies designed to suppress the immune system have been shown to be efficacious in preventing GvHD but patients become susceptible to infection or experience cancer relapse through the elimination of the GvL response as well.

In this thesis, we explore two strategies for targeting T cell activation in two mouse models of GvHD. In the first model, we examined the contribution of donor-derived complement C5 on the induction GvHD. We observed that recipient mice were only protected from GvHD when donor cells were deficient for complement protein C5.

Our second strategy involves selective targeting of alloreactive T cells using peptide immunotherapy. For this approach, we first developed a humanized mouse model of

GvHD whereby cells from donor mice expressing human class II HLA were reconstituted into recipient mice expressing human class I HLA. We then tested peptide immunotherapy using peptides derived from the human class I HLA. Our initial results were inconclusive and require further optimization.

Acknowledgments

The past 8 years have been an amazing adventure, I have had many amazing experiences, met so many new people and made life-long friends along the way. First and foremost, I want to thank my two co-supervisors Dr. Mark Larché and Dr. Peter Margetts, I would not be here today had you not given me this great opportunity. Starting a new project and creating two animal models was not an easy task and I want to say thank you for placing your trust in me to tackle it. Your continued support, guidance and most importantly patience were invaluable and crucial when times were tough, experiments failed or I was being less than productive. I also want to thank my committee members, Dr. Inman, and Dr. Kolb. Thank you for all the support, feedback and guidance throughout the years and helping me to become a better researcher. To all the members of the Lab, especially Lesley and Cheryl for providing support for all the random times I need help with something.

I want to thank Daniel Moldaver, Jennifer Wattie and Mantej Bharhani for welcoming me into the lab with open arms and teaching me everything I needed to know to hit the ground running. To Niroo, Neha, Chris and Tiffany, Lindsay and Shyam, my first friends in Hamilton. It was great getting to know all of you, exploring the city and surviving the lab together.

To my roommates, Ameet, Adrian, Julie & Patrick. Living with you guys was an absolute blast, from our guitar hero adventures to our weekly trips to Snooty Fox. You guys were the best roommates I've had in 8 years. Chris Hynes, my best friend, and brother from another mother, I can confidently say you've had the greatest influence on my life. Thanks for introducing me to the world of music festivals and teaching me how to stay positive during tough times. I wouldn't have been able to finish this Ph.D. without you keeping me grounded, always believing in me and pushing me to keep fighting. To my oldest friend Mark Zhou, thanks for your continued support and always checking in on me. Playing paintball and airsoft with you was the catharsis I needed after long hours in the lab.

Tarandeep Singh, I want to thank you for keeping me sane, providing an ear for support and a shoulder to lean on during tough times. To Ehab Ayaub, you taught me the value of hard work and determination, that you can spend all your time in the lab and still have a life. Your incredible life story inspires me to be my best every day. To Iris Wang and Tom Mu, thank you for being my second set of parents and always looking out for me. To all the other friends I've made along the way, I wish I could name each and every one of you, but I want you to know that you all had a positive influence on me.

I also want to say thank you to Dr. Jonathan Bramson for giving me the opportunity to be TA Immunology and Dr. Martin Stampfli for placing your trust in me and letting me lead the Team of Immunology. Hopefully, I didn't get you into too much trouble with the

department from all the student complaints. I also want to thank you for the continued support and gentle nudging to finish my Ph.D.

To Dr. Kjetil Ask, working in your lab has been an absolute pleasure. Your continued support, guidance, and positive attitude makes research fun and engaging.

To my sister Flora and brothers Nadeem and Naheed, I'm sorry for being gone for 8 years but I'm so proud of the people you grew up to be. Finally, I must say thank you to my parents, you instilled in me the values of honesty, integrity and hard work. Everything I have accomplished and will ever accomplish is thanks to your unwavering support and guidance.

Table of Contents

List of Tables and Figures

None

List of Abbreviations and Symbols

ACK – ammonium chloride potassium
aGvHD – acute Graft vs Host Disease
AML – acute myeloid leukemia
ALL - acute lymphoblastic leukemia
APC – antigen presenting cell
BM – bone marrow
BOS - bronchiolitis obliterans
C – compliance
C3a – complement protein 3 subunit a
C5 – complement protein 5
C5a – complement protein 5 subunit a
C5aR – C5a Receptor
C5b – complement protein 5 subunit b
CD – cluster of differentiation
CML – chronic myeloid leukemia
cGvHD – chronic graft vs host disease
CST – quasi-static compliance
CTL – cytotoxic T lymphocyte
DAF – decay accelerating factor
DN – double negative
DC – dendritic cell
ECM – Extra Cellular Matrix
ETP – Early thymic progenitor
G – tissue resistance
H – tissue elastance
H&E – hematoxylin and eosin
HLA – human leukocyte antigen
HSC – hematopoietic stem cells
HSCT – hematopoietic stem cell transplantation
IFN-γ – Interferon gamma
IGF-1 – insulin-like growth factor 1
IL – interleukin
IP – intraperitoneal
iNOS - inducible nitric oxide synthase
iTreg – inducible T regulatory cell
MCP – 1 – monocyte chemoattract protein 1
mTEC – medullary thymic epithelial cell
MAC – membrane attack complex
MHC – major histocompatibility complex
miHC – minor histocompatibility complex
MLR – mixed lymphocyte reaction
MM – multiple myeloma
nTreg – natural T regulatory cell
PBS – phosphate buffered saline
PDGF-β – platelet-derived growth factor
PRR - pattern recognition receptors
R – resistance
RBC – red blood cell
Rn – conducting airway resistance
RO – retro-orbital
SLE – systemic lupus erythematosus
TBI – total body irradiation
TGF-β – transforming growth factor beta
Th1 – T helper cell type 1
Th2 – T helper cell type 2
Th17 – T helper cell type 17
TNF-α – tumor Necrosis Factor-alpha

Preface

This work encompassing the past 8 years of my Ph.D. has resulted in the generation of two mouse models of GvHD with 2 accompanying manuscripts and 1 project that requires further work. This work has been assembled as "sandwich thesis" following the guidelines outlined by the school of graduate studies. In Chapter 1. We explore the history of graft vs host disease, the mechanisms of disease activation and associated tissue pathology and finally examine how the development and regulation of T cells promote the GvHD response following allogeneic transplant.

Chapter 2. Donor-derived C5 is required for induction of murine Pulmonary GvHD following hematopoietic stem cell transplant

Jewel Imani, Ehab E. Ayaub, Jennifer Wattie, Iris Wang, Mark D. Inman, Martin Kolb, Peter Margetts, and Mark Larché

Explores the role of donor-derived complement C5 in the induction pulmonary manifestations of GvHD following allogeneic HSCT in a mouse model. This body of work encompasses experiments that were conducted between September 2012 and May 2017 and is currently being prepared for submission.

Chapter 3. Immune responses to HLA-A2 drive multiorgan pathology in a humanized murine model of Graft versus Host Disease

Imani. J, Wattie. J, Inman. MD, Kolb. M, Margetts. P, Ball, ST, Larché. M

Describes the creation of a mouse model of GvHD whereby donor cells exclusively expressing human HLA-DRB*0401 were used to reconstitute recipient mice which express human class I HLA-A2*0201. These mice develop GvHD of lung, skin, and liver as early as day 60 post-HSCT. This body of work encompasses experiments that were conducted between April 2013 and September 2017 and is currently being prepared for submission

Chapter 4. Examining the efficacy of peptide therapy in a humanized model of Graft vs Host Disease

Imani. J, Inman. MD, Kolb. M, Margetts. P, Larché. M

Explores the use of peptide-based therapies to induce transplant tolerance in the humanized mouse model of GvHD described in **Chapter 3.** This body of work encompasses experiments that were conducted between November 2015 and March 2017. The results of this work were inconclusive and require further optimization of the treatment protocols.

Chapter 5. Summarizes and discusses the major findings from chapter 2-4 in the context of current therapeutic strategies for treating GvHD. We also examine the potential clinical implications of the data and future directions.

Chapter 1. Introduction

A historical perspective of bone marrow transplants and GvHD

The routine use of bone marrow transplants for treatment of leukemia arose following the end of the second world war and the beginning of the atomic age. Researchers discovered that the bone marrow was the most radiation sensitive organ in the body; exposure to ionizing radiation damages the DNA and disproportionally affects the rapidly dividing cells of the bone marrow. This subsequently affects the immune system through loss of hematopoietic stem cells (HSC). Furthermore, it was also discovered that there is a link between exposure to radiation and an increased incidence of bone marrow aplasias. In the search for a treatment, early studies in mice revealed that the lethal effects of radiation exposure could be overcome by reconstitution with intravenous or intraperitoneal injections of syngeneic spleen or bone marrow cells[1-3]. It was later discovered that a single progenitor cell (HSC) within the bone marrow was responsible for expanding and replacing the hematopoietic cells in the irradiated recipient mice[4]. In one of the first studies examining the ability of hematopoietic stem cell transplants (HSCT) to treat leukemias, Barnes et al[5] hypothesized that if leukemia cells were as sensitive to radiation exposure as normal bone marrow cells, then irradiation followed by transplantation of syngeneic cells could cure leukemia. However, if the radiation does not destroy all the leukemia cells, then transplant of allogeneic bone marrow would confer additional protection against any residual leukemia cells. To test their hypothesis, the researchers reconstituted CBA/H mice with allogeneic bone marrow from A/H mice; they observed that three of five mice were cured of leukemia but subsequently died from an unknown syndrome of weight loss and diarrhea which they termed “wasting syndrome” (GvHD). In

contrast, nine of ten mice reconstituted with syngeneic CBA/H bone marrow survived; the one death being attributed to a relapse of leukemia. This study was the first recorded case of GvHD and the graft vs leukemia (GvL) effect, the phenomenon whereby allogeneic donor cells are able to mount immune responses against leukemia cells. It was later discovered that induction of GvHD was a result of genetic disparities between donor and recipient[6], and these differences were later shown to be linked to the major histocompatibility complex (MHC)[7].

These discoveries allowed clinicians to develop strategies of radiation therapy whereby patients with hematological malignancies would be irradiated and then rescued by administration of bone marrow. The first series of HSCTs for the treatment of leukemia in humans were conducted by Dr. Donnall Thomas at the University of Washington in 1957[8]. In this study, six patients were treated with radiation and chemotherapy and then administered bone marrow from a healthy donor. Without adequate knowledge of the immune system and establishment of proper transplant protocols, only two patients engrafted and all six died within 100 days from engraftment failure or recurrent leukemia. The first successful HSCT for the treatment of leukemia was conducted in 1959 whereby two patients were reconstituted with bone marrow from their homozygous twins. However, these patients died shortly after from relapse of their leukemia[9]. This study indicated that irradiation followed by syngeneic (or autologous) HSCT was insufficient to completely eradicate leukemia cells. As a result, researchers reverted back to using allogeneic bone marrow to reconstitute irradiated leukemia patients as these types of transplants were already shown to be effective in murine models[5]

Further research using canine models investigated the role of total body irradiation (TBI)[10-13], myeloablation stratagies[14-16], optimal doses of donor cells to use[17,18], and manipulation of the donor cells to promote engraftment and reduce GvHD[19]. The findings from these studies were adopted in the clinic to improve the outcomes of patients treated for aplastic anemia and hematological malignancies using HLA-matched sibling marrow donors[20]. By 1977, Dr. Donnall treated 54 patients with acute myeloid leukemia (AML) and 46 patients with acute lymphoblastic leukemia (ALL) with HSCT. However, only 13 patients were alive without disease after 5 years[21]. Through continued improvements, a cure rate of 50% was achieved for AML patients by 1979[22]. By 1990, over 2000 HSCT transplant had been performed and the key to a successful transplant relied partially on the GvL effect. In the beginning, HSCTs were originally used to treat leukemias, but today they are routinely used for the treatment of various diseases including AML, ALL lymphoma, myeloma, myeloproliferative neoplasms, immune deficiencies (ADA deficiency), immune dysregulation syndromes (HLA), metabolic disorders such as leukodystrophies and hematologic disorders like aplastic anemia and thalassemia[23]. Despite continuous improvements for the last 60 years including drug therapies designed to suppress the immune system, development of GvHD remains a challenge for successful allogeneic HSCT.

Etiology of Graft vs Host Disease

Graft vs Host disease (GvHD) is an unwanted side effect of HSCT. Allogeneic T cells within the donor graft recognize leukemia associated and leukemia-specific antigens on

malignant cells in the recipient and mount immune responses such that all residual cancer cells are eliminated. However, the T cells also recognize antigens derived from healthy host cells and initiate destruction immune responses towards those cells as well. This leads to a state of systemic inflammation within the recipient and leads to significant tissue damage. The long-term disease eventually leads to irreversible fibrosis of the major organ systems, particularly in the lungs, skin, and liver.

GvHD was discovered in murine models following a series of hematopoietic stem cell transplants aimed at treating radiation-induced bone marrow aplasia's. Researchers discovered that transplantation of allogeneic bone marrow cells was successful in eliminating leukemia cells but the mice died of an unknown wasting syndrome[5]. At the time the researchers were unsure of the pathology occurring in these mice but shortly after, Billingham and Brent[24] later described a case of runt disease in newborn mice injected with allogeneic adult lymphoid tissues. The runt disease was characterized by splenomegaly, defects in growth, and early deaths. They determined that this phenotype was a result of a graft vs host reaction. T cells were later implicated as the primary drivers of this disease following transplantation of T-cell depleted bone marrow in animal models[25]. Further research using mice[26,27] and canine models characterized much of disease classifications and immunological basis for disease including the role of T cells, B cells, antigen presenting cells (APC) and MHC. These animal models have also helped characterize the two main types of disease; acute GvHD (aGvHD) and chronic GvHD (cGvHD). These two subtypes are classified in part by their pathogenesis and the degree of organ involvement. Acute GvHD has been reported to occur in up to 50% of allogeneic

HSCT patients and is characterized by involvement of the gastrointestinal tract (GI tract), skin, and liver, but can also affect the kidneys[28], salivary glands[29], oral epithelium[30], and thymus[31]. Chronic GvHD occurs in up to 50% of patients and is characterized by significant morbidity and mortality as a result disease in the lung, skin, liver, GI, brain, heart, kidney, pancreas, tendon, and mucosal surfaces[32,33].

Acute Graft vs Host Disease

Studies in murine models have defined the processes that lead to aGvHD, the current paradigm of the disease pathogenesis can be segmented into three phases. 1) activation of APCs, 2) activation of donor T cells 3) destruction of host tissues by alloreactive T cells[34]. In the first phase, radiation and chemotherapy drugs (methotrexate, cyclophosphamide) are used as a conditioning regimen to prepare the host by destroying the cancer cells and bone marrow reservoir, freeing up space for the donor cells to engraft. The conditioning also causes significant damage to healthy host tissues; ionizing radiation damages the DNA leading to cell death, the damaged cells and tissue-resident macrophages release reactive oxygen/nitrogen species and pro-inflammatory cytokines such as TNF-α and IL-1[35]. In the GI tract, the multipotent stem cells in the intestinal crypts and gastric glands are destroyed[36] and as a result, there are no new cells to replace the epithelial cells of the lumen wall as they are turned over, effectively creating holes in the GI tract wall. Microbial byproducts are then able to translocate through these gaps and enter the lamina propria where they are recognized by and activate tissue-resident macrophages and dendritic cells (DC)[37,38]. The activated macrophages and DCs release

pro-inflammatory cytokines (IL-1, TNF-α, IFN-γ, IL-6); which promotes antigen presentation by nonprofessional APCs[39] and enhances the presentation by regular APCs through upregulation of co-stimulatory molecules CD80 and CD86[40].

The second phase of disease begins as the transplanted donor T cells migrate into secondary lymphoid organs[41]. It is thought that the Peyer's patches within the GI are the initial sites of donor T cell activation as mice deficient in this structure are protected from aGvHD[42]. Host APCs in the Peyer's patches present host-derived antigens to donor T cells through the direct antigen presentation pathway[43]. Donor CD8+ are activated into cytotoxic T Lymphocytes (CTL) and CD4+ T cells are activated and differentiate into various T helper (Th) subsets. Both Th1[44] and Th17[45] cell have been shown to be sufficient for disease initiation as depletion of both cell types is required for preventing aGvHD in mouse models[46]. In the final phase, activated T cells are guided to host tissues through chemokine signalling. The Th1 cells promote aGvHD symptoms through the release of pro-inflammatory cytokines that further activate neutrophils, natural killer cells, monocytes, inflammatory macrophages, and donor T cells[47]. Host cells are directly killed by the CTLs but can also be induced to undergo apoptosis through TNF-α and IL-1 signalling[47].

Thymic Damage

The Thymus is responsible for the development of T cells as well as facilitating the elimination of autoreactive T cells and producing immuno-suppressive natural T regulatory cells (nTreg). Damage to the thymus may cause a dysregulation in T cell

development such that autoreactive T cells can be generated or fewer nTregs are produced. Removal of the thymus in the neonate mice was shown to induce multi-organ autoimmune disease[48,49]. Furthermore, in a mouse model of thymic dysfunction, C3H/HeN mice were lethally irradiated and injected with T-cell depleted, MHC II-deficient donor cells from C57BL/6 mice, the recipient mice developed features of cGvHD including, immune cell infiltration of the salivary glands, inflammation, weight loss, and sclerodermatous skin fibrosis[50]. In the context of GvHD, damage to the thymus can occur from the conditioning regiment or during aGvHD whereby alloreactive CD8+ T cells migrate to the thymus and damage the medullary thymic epithelial cells (mTEC) [31,51-53] leading to De novo production of autoreactive T cells that can then interact with donor B cells resulting in autoantibody production[52,54]

Chronic GvHD

Chronic GVHD is a late stage event of HSCT characterized by multiorgan tissue damage and fibrosis. It usually occurs after aGvHD but can also occur in the absence of it. Unlike aGvHD however, the process involved in the induction of cGvHD are complex and involve multiple arms of the immune system including, alloreactive and dysregulated T cell, B cell, DC, Macrophages, and Neutrophils. The current paradigm for induction of cGVHD can also be segmented into 3 phases[55,56]. 1) Early inflammation similar to that observed in the first stage of aGvHD. As a consequence of the conditioning regiment and activation of donor T-cells that leads system inflammation, damage to tissues including to vascular endothelial cells promotes migration of donor immune cells into target organs. 2)

Chronic inflammation from the conditioning regiment and drug-induced loss of regulatory T cells, B cells, and NK cells. This is compounded by the de novo production of autoreactive T-cells resulting from regiment and aGvHD induced thymic damage. 3) Tissue damage from dysregulated immune responses leads fibroblast activation and differentiation into collagen-secreting myofibroblasts[57]. In the context of T cells, use of depleting anti-T cell antibodies[58,59] or post-transplant high dose cyclophosphamide[60,61] has been shown to reduce the incidence of cGvHD therefore, targeting donor T cell activation or bolstering the number of T regulatory cells may represent two strategies for targeting cGVHD.

Tissue Fibrosis

The end stage manifestation of cGvHD is the damage and fibrosis of organs including lung, skin, and liver[62]. Progressive fibrosis in the skin negatively affects mobility; while in the lungs, fibrosis of the bronchioles leads bronchiolitis obliterans (BOS) and respiratory failure[63,64]. Fibrosis is defined as the excessive production and deposition of collagen and ECM components by activated myofibroblasts. Myofibroblast can develop from fibroblasts, fibrocytes or transdifferentiate from epithelial and endothelial cells by proinflammatory and profibrotic cytokines[65]. While deposition of collagen and ECM is a part of the normal wound repair response to tissue damage, progressive fibrosis can occur as a result of chronic inflammation, a feature in many diseases including cGvHD. The normal wound repair process begins with inflammation, at sites of tissue injury damaged cells release proinflammatory cytokines (TNF-α, IL-1) and chemokines (CXCL8 and

CXCL1). This recruits and activates neutrophils, monocytes, and mast cells; neutrophils remove infectious and noninfectious foreign material and damaged matrix components. Mast cells release tryptase, which promotes the breakdown of connective tissue allowing recruited cells to infiltrate the tissues and induces fibroblast proliferation[66]. These cytokines also activate tissue-resident macrophages that further release IL-1, IL-6, TNF-α, TGF-β, iNOS, PDGF-β, and IGF-1 that promotes endothelial & epithelial cell proliferation, angiogenesis, and fibroblast activation, leading to collagen and ECM deposition[67]. In the context of HSCT and GvHD, chronic inflammation leads to dysregulated wound repair such that myofibroblasts are constitutively activated, leading to progressive fibrosis.

Clinical Manifestations of GvHD

Lung

Lung manifestations of cGvHD occur in up to 50% of HSCT patients with mortality occurring in 15% of patients[68]. The primary pathologies of lungs are BOS, interstitial pneumonia, and fibrosis. BOS is caused by mononuclear cells infiltration into the terminal bronchioles, chronic inflammation then leads to the destruction of alveolar cells and subsequent deposition of collagen and ECM into the airway lumen[69]. Interstitial pneumonia is caused by mononuclear cell infiltration of the alveolar septa and perivascular areas, chronic inflammation can lead to pulmonary edema, interstitial thickening, and fibrosis[70]. Patients can present with dyspnea, wheezing cough,

subcutaneous emphysema, and obstructive or restrictive changes in pulmonary function tests. Lung biopsies or CT Scans can diagnose BOS and interstitial pneumonia, but pulmonary function tests can also be used as indirect indicators of disease. Patients with BOS have increased respiratory resistance and interstitial pneumonia patients have decreased lung compliance.

Skin

The skin is affected in both acute and chronic GvHD. Skin manifestations begin immediately following HSCT as activated T cells are recruited into the skin. CD4+ T cells have been shown to migrate into the dermis while CD8+ T cells migrate into the epidermis[71]. These T cells induce inflammation that causes edema as well as structural damage to the skin. The most common manifestation is pruritic maculopapular skin rash. Severe aGvHD is characterized by erythroderma, epidermolysis leading to bullae formation, and dyskeratosis within keratinocytes. Langerhan cells may become depleted and acantholysis can occur in the stratum basale, basal cells may also become necrotic or undergo vacuolar degeneration. In late-stage cGvHD, the skin changes can be classified as sclerodermatous, marked by inflammatory plaques over the extremities while the junction between the epidermis and dermis may be obliterated and replaced by dense deposition of collagen and ECM[33]. Diagnosis of GvHD in the skin requires histopathological analysis, however, histology is not always pathognomonic and often requires differential diagnosis due to the heterogeneity of the changes that can occur[72].

Liver

The primary symptom of liver disease is jaundice; a result of lymphocyte infiltration followed by inflammation and damage to the bile canaliculi and bile ducts that leads to cholestasis[73,74]. Histological analysis reveals necrosis of the biliary cells and basement membrane thickening[75]. However, this phenotype can also be a result of veno-occlusive disease, infection or sepsis and therefore requires differential diagnosis[76].

GI Tract

GI tract involvement is primarily a feature of aGvHD but fibrosis in the esophagus can occur during cGvHD[77]. The entire length of the GI tract is susceptible to disease but prominent lesions in the cecum, ileum, and ascending colon, stomach, duodenum, and rectum have been reported. This can result in dysfunctional motility, mechanical obstruction, and issues with food absorption. Diarrhea is the primary symptom of GI involvement, but it can also be a result of the conditioning regiment. At the onset of disease, patients can lose up to 10 liters of water per day and it can become bloody later on. Clinical symptoms include nausea, vomiting, abdominal pain, distention, paralytic ileus, and intestinal bleeding. Endoscopic analysis reveals edema, mucosal sloughing, and diffuse bleeding throughout the entire GI tract[74]

The Immune System

The mammalian immune system has evolved over millions of years as a mechanism to provide host defense as well as regulate homeostasis. Loosely defined, it is a collection of bone marrow-derived cells and organ systems that work together to mount immune responses to danger signals but also regulates its self to prevent collateral damage to host tissues. The environment is filled with pathogenic bacteria, viruses, parasites, toxic substances, and allergens; broadly speaking, the immune system is able to recognize these pathogens through the detection of pathogen-specific structures such as surface proteins, lipids or carbohydrates. This then initiates a coordinated immune response towards clearing the pathogen. The first part of immune protection begins with physical barriers designed to prevent the invasion of pathogens. These include the epithelial cells of the skin and GI tract and secreted mucus in GI, respiratory and urinary tracts. If pathogens manage to overcome these barriers, humoral factors such as complement proteins, defensins, and ficolins are present to initiate immune responses[78]. The final step is the recognition of the pathogen by innate immune cells such as neutrophils, eosinophils, mast cells, basophils, macrophages, and DCs. These cells express germline-encoded pattern recognition receptors (PRR) that recognize molecular structures expressed by many pathogens. Upon recognition, these cells become activated and start releasing proinflammatory cytokines and chemokines that recruit more immune cells to the sites of infection. Activated DCs and macrophages then initiate the adaptive arm of the immune response. Unlike the innate immune cells, the T cells and B cells of the adaptive immune system express T-cell receptors (TCR) and B-cell receptors (BCR) that have restricted

antigen specificity. This is accomplished through somatic recombination of the receptor genes such that each T-cell and B-cell receptor has a unique specificity. The adaptive immune response begins when APCs phagocytose pathogens at the site of infection and travel to local lymph nodes and present antigens to naïve T cells and B cells. Unlike the receptors of the innate cells which directly recognize pathogens, the TCR only recognizes peptides when they are presented by MHC molecules on the APC. Upon activation, the T cell undergoes clonal expansion and then migrates back into the tissue to carry out its effector function. In contrast, B cells can recognize whole antigens and are activated following engagement of the BCR by the antigen and receiving T cell help. The activated B cell will differentiate into a plasma cell and secrete its BCR in the form of an antibody. The antibodies confer protection by binding to the pathogen and acting as opsonins for macrophages or activating the complement pathway.

T cells

The two main types of T cells are the CD8+ T cells which directly target virus-infected or malignant cells and CD4+ T cells whose function is to provide support to other immune cells and/or responses through the release of specific cytokines. All T cells can be characterized by their surface expression of the TCR. Each T cell expresses a unique TCR that has specificity for a limited range of peptides presented in the context of MHC. The TCR is composed of an α and β (or γδ) polypeptide chain that is non-covalently associated with a CD3 molecule and a CD4 or CD8 co-receptor. Each polypeptide chain is composed of a variable domain involved in recognition of peptides and a structural

domain that forms part of the cell membrane anchor. Unlike the germline-encoded receptors utilized by innate immune cells, the genes that encode the TCR exist in a fragmented state in the DNA. These genes are composed of multiple variable (V), diversity (D) and joining (J) segments that recombine with one another through DNA splicing during T cell development. In the β chain locus, 1 of the many V segments will recombine with one random D segment and one random J segment to form the variable domain, in contrast, in the α, γ, and δ chain loci, one V segment will recombine with one J segment to form the variable domain.

T cell Development

T cell development begins following the migration of early thymic progenitor cells (ETP) from the bone marrow into the cortico-medullary junction of the thymus[79]. The thymus provides the necessary microenvironment for the development of ETPs into mature T cells. In the beginning, the ETPs do not the express the TCR, CD3 or CD4/CD8 and are termed double negative (DN). The developing DN cells then undergo four stages of development to become a mature naïve T cell[80]. At the DN1 stage, the cells reside in the medulla and are $CD44^{+}CD25^{-}$. CD25 is expressed in the DN2 stage as the cells migrate into the cortex of the thymus where RAG1 and RAG 2 proteins facilitate gene rearrangements in the β, γ, δ chains. If the γ, δ chains recombine first, the developing cell will develop into a γδ T cell, otherwise, it will develop into αβ T cell if the β chain rearranges first. At the DN3 stage, the developing T cell migrates into the subcapsular region of the thymus and the rearranged β chain associates with an invariant pre-TCR

surrogate α-chain and CD3 to form a pre-TCR complex on the cell surface[81]. The cell then interacts with cortical thymic epithelial cells and receives positive stimulation signals that stop further gene rearrangements and induces cell proliferation. The cell then temporarily enters the DN4 stage as both CD44 and CD25 are downregulated. In the next stage of development, the cell begins rearrangement of the α chain and expresses both CD4 and CD8 and is termed double postive[82]. Following successful rearrangement of the α chain, the cell will express the complete TCR and undergo positive and negative selection prior to entering the peripheral circulation as a mature naïve T cell.

T Cell Tolerance

Following the development of ETPs to mature naïve T cells, the T cell expresses a TCR that recognizes peptides in the context of MHC. However, as the gene rearrangements that occurred to produce the TCR are random, there is a potential that the T cell may recognize self-antigen in the context of self MHC and initiate autoimmune responses. To prevent this from occurring, the new T cells undergo positive selection to promote survival of those T cells that recognize self-peptide in the context of self MHC with low affinity but negatively select any T cell that recognizes self-peptide in the context of self MHC with high affinity. This process is mediated in the thymus through central tolerance mechanisms as well as in the periphery through peripheral tolerance mechanisms.

Central Tolerance

Central tolerance begins at the double positive stage of T cell development, the developing T cell starts interacting with cortical thymic epithelial cells in the cortex. If the newly formed TCR is unable to recognize self-peptide in the context of self MHC, the cell will undergo apoptosis from neglect. If however, it can recognize MHC, it is positively selected to survive. Additionally, if the TCR recognizes MHC class I, the CD4 co-receptor will be downregulated; and if the TCR recognizes MHC II, then CD8 will be downregulated[83]. The newly formed single positive T cell then migrates back into the medulla and starts interacting with mTECs and BM-derived DCs and macrophages. If the T cells recognize self-peptide in the context of self MHC with high affinity, the cells are negatively selected to ensure tolerance to self. In the thymus, the main mechanisms of tolerance include clonal deletion, clonal diversion, and receptor editing. Clonal deletion of autoreactive T cells occurs following interaction of the T cells with thymic APCs, in the mTECs, the autoimmune regulator (AIRE) promotes expression of tissue-specific antigens for presentation to the T cells [84,85], while DCs cross present tissue-specific antigens acquired from the mTECs[86,87]. When self-antigens are presented to the T cells in the context of self MHC with high affinity, signal transduction into the T cell leads to apoptosis[83]. During clonal diversion, mTECs[88] and thymic DCs[89] convert autoreactive T cells into $CD4^+CD25^+FoxP3^+$ nTregs. Natural Tregs have the ability to suppress immune responses through various mechanisms including, production of anti-inflammatory cytokines (TGF-β and IL-10), direct suppression through cell to cell contact and modulating the function of APCs[90]. It is currently not well understood what factors

determine if an autoreactive T cell is deleted or diverted, but one hypothesis suggests the strength and duration of the TCR to peptide: MHC interaction is involved; with stronger signals leading to deletion and weaker signals leading to nTreg conversion. The cytokine microenvironment is likely to be involved as well, as the absence of TGF-β and IL-2 signalling was shown to inhibit nTreg production[91]. Finally, in receptor editing, the autoreactive T cell is instructed to undergo further V-J gene rearrangements in the α chain such that the peptide specificity of the TCR will change[92,93].

Peripheral Tolerance

Central tolerance mechanisms are used to eliminate T cells with specificity for self-antigens. However, the thymus does not express the entire repertoire of self-antigens, therefore circulating T cells undergo another round of tolerance in the periphery. When T cells are activated, they are presented peptides in the context of MHC but also require co-stimulation. In the absence of any co-stimulation, the T cell becomes hyporesponsive to further antigen stimulation and is deemed "anergized"[94] or it can be converted into an induced T regulatory cell (iTreg) in the presence of TGF-β, IL-2, and retinoic acid. Additionally, tolerogenic DCs can provide inhibitory signals such as PD-L1 and PD-L2 which binds to PD-1 receptor on the T cell and attenuates the activation pathways[95]. T cells have also been shown to be become anergized by stromal fibroblastic reticular cells and follicular DCs of the lymph nodes as well as lymphatic endothelial cells which have all been shown to express tissue-specific antigens[96].

T cell Priming

Following positive and negative selection, the mature naïve T cell circulates throughout the lymphatic and blood vessels in search of a peptide antigen sufficient to induce activation. As the T cells are tolerant to self, the peptides are derived from infectious pathogens (or innocuous allergens or food proteins). The T cells are activated or "primed" by APCs in secondary lymphoid tissues such as lymph nodes. The APC must provide two signals to completely activate the T cell; the first is the presentation of peptides in the context of MHC and the second signal is co-stimulation.

Antigen Presentation

Class I Presentation

In humans, MHC is also known as the human leukocyte antigen (HLA). CD8+ T cells are presented peptides in the context of class I HLA. These class I HLA molecules are expressed on APCs and all nucleated cells. Within the class I locus, there are 3 major HLA genes (HLA-A, B, and C) which are co-dominantly expressed on each cell. Therefore a single cell will express 6 unique class I HLA molecules (3 paternal & 3 maternal). Each of these genes encodes a single α-chain polypeptide which associates with an invariant β2-microglobulin protein[97]. The α chain contains 3 domains, the α1, and α2 interact to form a groove that allows peptides to bind and the α3 domain which anchors the polypeptide in the cell membrane and interacts with the CD8 co-receptor on the T cell. The peptides presented on class I molecules are generated endogenously by the proteasome, a large protein complex in the cytoplasm that cleaves and degrades proteins

into smaller peptide frgaments[98]. The peptides are transported into the endoplasmic reticulum and guided onto the class I molecule binding groove by the tapasin, calreticulin and ERP57 proteins[99]. The β2 microglobulin molecule then associates with the class I molecule and the entire complex is shuttled to the cell surface through the goli complex. While most peptides are derived from within the cell, exogenous antigens can also be presented on class I molecules through cross-presentation of antigens that are endocytosed[100]. At the cell surface, the peptide: MHC complex forms a structure that is able to engage the TCR on a CD8+ T cell and provide signal 1 for T cell priming.

Class II Presentation

Class II HLA molecules are expressed on monocytes, macrophages, B cells, and DCs but can be induced on epithelial and endothelial cells by IFN-γ. There are three major class II HLA molecules (HLA-DR, HLA-DQ, HLA-DP), which are also co-dominantly expressed. Each class II HLA is composed of an α and β polypeptide chain, each containing 2 extracellular domains[97]. The peptide binding groove is formed by the α1 and β1 domains of each respective polypeptide chain. Whereas the α2 and β2 domains provide structural support and a binding site for the CD4 molecule. Unlike the class I HLA molecules, peptides presented on class II HLA are derived from extracellular sources. There include antigens derived from bacteria, viral particles, parasites, and apoptotic or necrotic cells. APCs acquire these antigens following recognition by PRRs and subsequent phagocytosis. The phagosomes fuse with lysosomes to form a phagolysosome whereby the antigens are processed into peptide fragments through

proteolysis[101]. Concurrently, the class II HLA molecules are synthesized in the ER and stabilized by calnexin while the binding groove is blocked by an invariant chain protein to prevent endogenous peptides from binding. The entire complex dissociates from calnexin and is transported to the class II loading compartment[102]. The peptide containing endosome then fuses with the class II loading compartment and the invariant chain is degraded by proteases leaving behind a small peptide (CLIP) in the binding domain. HLA-DM then facilitates the unloading of CLIP and loading of antigen peptide into the class II binding groove[103] The complete peptide: MHC complex is then shuttled to the cell surface membrane where it can engage the TCR on CD4+ T cells.

Co-Stimulation

T cell priming occurs following engagement of the TCR to the peptide: MHC complex, but the T cell must also receive co-stimulation signals which act to fully activate the T cell. While there are numerous co-stimulatory molecules the APC can express, during T cell priming, there are a limited number of co-stimulatory receptors expressed on the naïve T cell[104]. CD28 is the prototypical receptor that binds to CD80/CD86 on the APC [105] but other co-stimulatory receptor-ligand pairs include HVEM, and CD27 that receive co-stimulatory signals from LIGHT[106], and CD70[107] respectively (see Ref[104] for a list of T cell costimulatory molecules). Following engagement of CD28, phosphatidylinositol 3-kinase (PI3K) interacts with the cytoplasmic domain of CD28 and protein kinase B (AKT), this initiates a cascade of cytoplasmic signalling pathways which leads to activation of nuclear transcription factor-κB and promotes T cell activation and

proliferation[108]. Recently it has been shown that complement proteins can provide co-stimulation signals as well.

Complement C5 Protein

The complement system was initially discovered as a set of plasma proteins that augment the opsonization of bacteria by antibodies, but it can also function in the absence of antibodies as well. There are numerous complement and regulatory proteins that are produced and secreted by the liver in response to inflammation. In general, the complement proteins are secreted in an inactive state; and a number of these complement proteins are proteases that cleave and activate the other members of the complement system. Once activated, the complement system confers protection through three independent pathways. 1) complement component C3b covalently binds to the surface of pathogens and act as opsonins for phagocytosis. 2) The cleavage products C3a, C4a, and C5a act as chemoattractants and inflammatory mediators to recruit and activate immune cells at sites of infection. 3) The complement proteins C5b-C9 form a membrane attack complex (MAC) by inserting themselves into the membrane of bacteria and creating pores that effectively kill the bacteria. In the recent years, the complement proteins have also been shown to be involved in tissue regeneration, angiogenesis, mobilization of stem cells and regulation of the adaptive immune responses[109]. Specifically, complement proteins C3a and C5a have been shown to be prominent co-stimulators of T cell activation[110-113].

Effector T cells

Following priming and activation by the APCs, the T cells are classified as effector T cells and are able to impart their function to ongoing immune responses.

CD8+ T cells

Once activated, A CD8+ T cell is known as a cytotoxic T lymphocyte (CTL) because it directly kills its target cell, these include virally infected cells and malignant cells. The CTLs rapidly proliferate under IL-2 stimulation and then migrate to sites of infection in the periphery. At the site of infection, CTLs recognize target cells through recognition of the same peptide: MHC class I complex originally expressed by the APC that activated it. Upon engagement of the TCR to the peptide: MHC complex, the target cell upregulates FAS ligand. Binding of FAS on the CTL to FAS ligand induces caspase-dependent apoptosis in the target cell. CTLs can also kill target cells through release of lytic granules that contain perforin and granzyme. The perforin molecule inserts into the target cell membrane and creates pores that allows granzyme to enter the cell. Granzyme can also be endocytosed and then released into the cytoplasm by perforin. Inside the cell, the granzyme also induces caspase-dependent apoptosis[114].

CD4+ T cells

Unlike CTLs, CD4+ T cells do not generally directly kill target cells, rather they provide support to other cells through the release of specific cytokines. Th1 cells release IFN-γ,

IL-2, TNF-β which promote inflammation and upregulates CTL responses. IFN-γ promotes IL-12 production in macrophages and DCs to promote further activation of CTLs. Th2 cells can release IL-4, IL-5, IL-6, IL-10, and IL-13, these cytokines inhibit Th1 responses and promote antibody production and class switching of immunoglobulin isotypes (IgG, IgM, IgA, IgE) in B cells[115]. While CD4+ T cells have been classified dichotomously as Th1 or Th2, other subtypes have also been described including IL-17 producing Th17 cells, IL-9 producing Th9 cells, Il-22 producing Th22 cells, Treg cells, and T follicular helper cell.

Regulatory T cells

Regulatory T cells are key modulators of T cells and fundamental in preventing the rise of T cell-mediated autoimmune diseases. Regulatory T cells can be generated in the thymus (nTreg) or in the periphery (iTreg). Both these T cells are characterized by expression of the transcription factor FoxP3, CD25, and CD4 and suppress T cell responses through cell to cell contact-mediated or contact independent mechanisms. Contact-mediated mechanisms include the expression of inhibitory receptors that block co-stimulation of T cells and contact independent mechanisms involves secretion of anti-inflammatory cytokines IL-10 and TGF-β.

Peptide Immunotherapy

The use of peptides to target antigen-specific T cells was first demonstrated in *in vitro* studies whereby human T cell clones specific for influenza A hemagglutinin were rendered unresponsive to antigen stimulation following pretreatment with influenza A hemagglutinin derived peptides[116]. This protocol of administering antigen-derived peptides to tolerize antigen-specific T cells has since been applied with various success for the treatment of cat[117], house dust mite[118], tree pollen[119], and bee venom[120] allergies. It has also been investigated in models of autoimmune diseases such as systemic lupus erythematosus[121], systemic sclerosis[122,123], arthritis [124], and diabetes[125,126]. In the clinic, use of peptide therapy for the treatment of type 1 diabetes patients was associated with IL-10 and Il-13 producing Th2/regulatory T cells[127]. A similar observation was made in trials of rheumatoid arthritis treatment, peptide therapy resulted in increased IL-4 and IL-10 producing T cells and reduced Th1 cells and increased Foxp3 expression in CD4+CD25+ cells indicating peptide therapy also increased regulatory T cells production[128,129].

Tolerization of antigen-specific T cells is thought to occur following the administration of peptides in the absence of adjuvants. Once administered, the peptides are distributed throughout the body and bind to class II MHC/HLA molecules on DCs and non-professional APCs. In the absence of inflammation, the APCs are unable to mature and therefore antigen-specific T cells are presented peptides without co-stimulation. In this situation, the T cells are anergized while some are converted into iTregs[129,130].

Principles of Allorecognition

Activated T cells have an incredible ability to cause damage. As such, T cells undergo significant regulation in order to prevent the rise of T cell-mediated autoimmune diseases[131]. This includes positive and negative selection in the thymus and peripheral tolerance to eliminate autoreactive T cells. As a result, mature naïve T cells have the ability to recognize self-peptides in the context of self MHC, but the binding affinity is insufficient to induce activation and therefore the T cell is considered tolerant to self. The TCR makes contact with both the peptide and MHC molecule and the affinity of binding is determined largely by hydrogen bonding and ionic interactions forces between the amino acid side chains of TCR, peptide, and MHC; replacement of self-peptide for a pathogenic peptide (in the case of an infection) shifts the binding affinity such that sufficient CD3 signalling then leads to the T cell becoming activated. Conversely, a change in the MHC molecule can also shift the binding affinity and activate the T cell, but as each individual contains a defined set of MHC genes, mature T cells are restricted and tolerant to self MHC as well.

However, due to the degeneracy of the TCR, it may also bind to MHC molecules of another individual. As these T cells were never negatively selected against the another individuals MHC, interaction with recipient APCs in the context of transplantation may lead to donor T cell activation. It is estimated that 1-20% of all naïve T cells are alloreactive to any given mismatched MHC haplotype[132]. There are an estimated 19 000 protein-coding genes in the human genome[133], while many of these may be conserved due to functional and structural constraints, many genes have multiple allelic versions that

correspond to differences in the amino acid sequence of the protein. When bone marrow and immune cells are transplanted across two individuals, protein sequence differences (miHC) between donor and recipient alleles of any given gene may be seen as non-self by the donor T cells. By far, the genes with the greatest allelic diversity are the MHC or HLA genes. Within the population, there are over 650 different HLA-A alleles, 1000 HLA-B alleles, and 350 HLA-C alleles. In the class II HLA locus, there are at least 16 α chain and 118 β chain alleles for HLA-DP, 25 α chain and 72 β chain alleles for HLA-DQ and 560 β chains in for HLA-DR[78]. As each individual expresses a unique MHC haplotype, this ensures at least a few individuals within the population will be able to bind and induce immune responses to any given pathogenic peptide. However, in the case of haplo-identical HSCT, the donor-recipient pair will at least one HLA mismatch. Following HSCT, peptides derived from recipient miHC and HLA are presented to donor T cells as non-self and activates the T cell. Conversely, the mismatched MHC can also present recipient miHC peptide to the donor T cells and activate them. Clinically, following HSCT, donor T cells are initially activated directly by recipient APCs. In this case, recipient miHC and HLA derived peptides are presented by recipient HLA molecules and activate cross-reactive donor T cells. In late-stage GvHD, donor T cells are indirectly activated by donor APCs; in this case, recipient miHC and HLA derived peptides are presented in the context of self HLA[134,135].

Central Aims

GvHD is a complex disease, it occurs when donor T cells recognize miHC or MHC antigens derived from a mismatched donor. Once activated, the T cell initiates a cascade of immune responses that generate CTLs, proinflammatory Th1 cells and Th2 cells that promote activation of autoantibody-producing B cells, macrophages, and myofibroblasts that secrete collagen and ECM. At each step of this pathway, there is an amplification of the GvHD response and redundancy in the signalling pathways such that targetting any specific part of the pathway is unlikely to completely ablate the entire GvHD response. However, as donor T cell activation initiates this whole process, it represents the ideal target to prevent GvHD. Furthermore, as activation of T cells requires 2 signals from the APC. 1) Presentation of peptides and 2) co-stimulation. **We hypothesize that interrupting any of these two signals will effectively prevent activation of the donor T cells and subsequently inhibit the induction GvHD.**

Complement protein C5 is a potent inflammatory mediator that has been shown to be a potent co-stimulator of T cell and it is also involved in the rejection of solid organ transplants. As such, targetting C5 may represent one approach to inhibiting induction of GvHD though blockage of co-stimulation. In **Chapter 2,** we explore the role of complement protein C5 in the induction of GvHD. Specifically, we examined the contribution of donor-derived complement protein C5. We reconstituted BALB/c mice with donor bone marrow and spleen cells from MHC matched but minor mismatched

B10.D2 mice that were either $C5^-$ or $C5^+$. We found that recipient mice were only protected from developing GvHD when the donor cells were deficient for C5.

An alternative approach to preventing GvHD is to selectively target those T cells that recognize peptides derived from recipient MHC molecules; therefore there would no T cells to recognize recipient-derived peptides. We hypothesize that delivery of peptides derived from mismatched MHC molecules will anergize antigen-specific donor T cells as well as promote the generation of iTregs that will further downregulate immune responses. For clinical relevance, we first developed a humanized mouse model of GvHD described in **Chapter 3.** Briefly, donor cells from transgenic C57BL/6 mice that exclusively express human class II HLA-DRB1*0401 were transplanted into transgenic C57BL/6 mice that express human class I HLA-A2*0201. We found recipient mice developed multiorgan GvHD as early as day 60 post-transplant.

In **Chapter 4**, we investigated the use of peptide immunotherapy as a means to anergize or clonally deleted only those T cells that recognize peptides derived from HLA-A2*0201. We found that peptide therapy, in this case, was ineffective at preventing the GvHD phenotype.

Collectively, **Chapters 2-4** explore 2 strategies for inhibiting GvHD by targeting mechanisms of donor T cell activation.

Chapter 2. Donor-derived C5 is required for induction of murine Pulmonary GvHD following hematopoietic stem cell transplant

Donor-derived C5 is required for induction of murine Pulmonary GvHD following hematopoietic stem cell transplant

Donor C5 is required for induction of murine GvHD

Jewel Imani,[1-2] Ehab E. Ayaub,[1-2] Jennifer Wattie,[1] Iris Wang,[1-2] Mark D. Inman,[1] Martin Kolb,[1] Peter Margetts,[3] and Mark Larché[1-2]

[1] Department of Medicine, Firestone Institute for Respiratory Health, The Research Institute of St. Joe's Hamilton, McMaster University, Hamilton, ON, Canada

[2] Department of Medicine, Division of Clinical Immunology & Allergy, McMaster Immunology Research Center, McMaster University, Hamilton, ON, Canada

[3]Department of Medicine, Division of Nephrology, McMaster University, Hamilton ON, Canada

Corresponding author: Dr. Mark Larché, Department of Medicine, McMaster University and The Research Institute of St. Joe's Hamilton, Firestone Institute for Respiratory Health, Hamilton Health Sciences, Rm 4H20, 1200 Main street W, Hamilton Ontario L8N 3Z5, Ph# (905) 525-9140 ext. 21284; Fax# (905) 521-4971, E-mail: larche@mcmaster.ca

Category: Transplantation & Immunobiology and Immunotherapy scope

Key Points: Donor cell-derived complement C5 is required to induce pulmonary GvHD in a murine model of allogeneic hematopoietic stem cell transplant

Abstract

Graft vs host disease (GvHD) is an unwanted side effect of allogeneic hematopoietic stem cell transplantation (HSCT). Lung manifestations of the disease are characterized by inflammation and fibrosis. Activation of infiltrating alloreactive donor T-lymphocytes requires recipient and donor antigen presenting cells (APC) but also involves complement C5a. Herein, we investigated the role of donor cell-derived complement C5 in the induction and progression of pulmonary manifestations of GvHD in a murine model. Bone marrow and spleen cells from C5 sufficient B10.D2 $^{(H1)}$ or C5 deficient B10.D2$^{(H0)}$ donor mice were transplanted into BALB/c recipient mice. Recipient mice were sacrificed on days 30, 60 and 90 post-transplant; airway physiology was assessed to track changes in lung compliance and resistance, and histology was used to track morphological changes.

BALB/c mice transplanted with C5 sufficient donor cells had increased perivascular infiltration, lung resistance and decreased lung compliance at day 60 post-transplant. By day 90 the inflammation subsided, and lung resistance was reduced giving way to increased collagen in the airways as lung compliance continued to decrease. In contrast, mice transplanted with C5 deficient cells were protected from lung inflammation, airway fibrosis and changes in lung resistance and compliance.

Transplantation of C5 sufficient bone marrow and spleen cells induced lung GvHD symptoms, whereas transplantation of C5 deficient donor cells did not. As recipient mice are C5 sufficient, this implies that induction of GvHD is dependent on donor-derived C5 and represents a new opportunity for targeted intervention in HSCT.

Introduction

Allogeneic hematopoietic stem cell transplantation (HSCT) is used to treat hematologic diseases such as myeloid or lymphoid leukemia; however, an unwanted side effect is the development of Graft vs Host Disease (GvHD). This occurs following recognition of mismatched major or minor histocompatibility antigens (MHC or miHC) on recipient tissues by allogeneic donor lymphocytes, which then mount immune responses towards the host tissues. The disease can manifest as either acute or chronic GvHD (aGvHD & cGvHD) characterized in part by the degree of tissue involvement[1,2]. Acute GvHD is characterized by systemic inflammation and tissue damage which can manifest as diarrhea, weight loss, and significant mortality. In contrast, cGvHD is characterized by immune dysregulation and fibrosis of organs including skin, liver, gastrointestinal tract, oral mucosa, and lungs[3]. GvHD occurs in up to 80% of HSCT patients, with lung manifestations arising in up to 50% of patients and an associated mortality rate of 15%[4]. The etiology of GvHD is poorly understood, however, studies in human and animal models have implicated various cellular and molecular pathways in disease progression. Beginning with the conditioning regiment, total body irradiation and chemotherapy drugs are first used to destroy cancer cells in the recipient, but this inadvertently causes tissue damage and activates host immune cells. Activated host macrophages and dendritic cells release pro-inflammatory cytokines IL-1, TNFα, and IFN-γ; activating neutrophils and enhancing presentation by antigen presenting cells (APCs)[5]. Following HSCT, donor lymphocytes migrate into secondary lymphoid organs[6] while macrophages[7] and DCs[8] are activated by the proinflammatory microenvironment and migrate into peripheral tissues to

acquire host antigens. The APCs then traffic to local lymph nodes and present alloantigens and activate donor T cells[8]. Upon expansion, the cytotoxic $CD8^+$ T cells migrate to the periphery and attack host tissues including damage to the medullary thymic epithelium that can lead to a decrease in natural T regulatory cell production and dysfunctional negative selection, promoting the generation of de novo autoreactive T cells[9]. Activation of donor CD4+ T cells leads to differentiation into Th1 cells that exacerbates aGvHD symptoms through the release of pro-inflammatory cytokines that further activate neutrophils, natural killer cells, monocytes, inflammatory macrophages and non-cognate activation of additional donor T cells[10]. Induction of cGVHD is more complex and less well understood compared to aGvHD; early activation of donor T-cells which leads to tissue damage is followed by a state of chronic inflammation in part due to decreased regulation from T, B, and NK regulatory cells. Furthermore, the de novo produced autoreactive T-cells expands uthe antigenic targets of disease beyond the mismatches in MHC and miHC between donor and recipients. Consequently, cGvHD can target and affect multiple organs in the body[11,12].

As a regulator of both aGvHD and cGvHD, modulation of T cell activation and function represents an ideal target to inhibit the induction and progression of GvHD. Canonically, T cells are activated by APCs through antigen presentation and co-stimulation through receptors such as CD28 and CD40L. However, complement proteins are have been shown to be involved in modulating T cell activation also.[13-15] During T cell/APC interactions, both cell types produce C3, C5 and their receptors C3aR and C5aR; bidirectional

signalling then leads to activation of both the APC and T cell[16,17]. Conversely, deficiency of decay accelerating factor (DAF) in the APC promotes increased T cell proliferation[18]. In the context of GvHD, complement C3a has been shown to mediate the polarization of Th1/Th17 T cells in murine and human cutaneous GvHD[19]. Additionally, transplantation of T cells deficient for C3a and/or C5a receptor reduced GvHD scores in murine models, conversely, transplantation of $Daf1^{-/-}$ bone marrow cells exacerbated GvHD[20]. This observation was attributed to C5a production[16]. Furthermore, pharmacological blockade of the C5a receptor on human T cells reduced GvHD scores in a xenograft model of GvHD[21]. Furthermore, as the early stages of GvHD is modulated by host APCs[22,23] but later stages of the disease are modulated by donor APCs[24,25]. Targeting the interaction between donor APC and alloreactive T-cells may be an ideal target for inhibiting GvHD induction and/or progression.

In light of this, we investigated the role of donor-derived complement C5 in the development of pulmonary manifestations of GvHD in a mouse model. We transplanted $C5^{+}$ B10.D2 or $C5^{-}$ B10.D2 bone marrow and spleen cells into MHC matched but miHC antigen mismatched $C5^{+}$ BALB/c recipient mice. Our findings suggest that donor-derived complement C5 is necessary to induce pulmonary manifestation of GvHD.

Methods

Murine Model of GvHD

Six-eight-week-old female $Qa2^-$ BALB/cByJ mice (Jackson Laboratory) were sub-lethally irradiated with 650 RADs and transplanted with $2x10^6$ red blood cell (RBC)-free spleen cells and $1x10^6$ RBC-free bone marrow (BM) cells from female $C5^+Qa2^+$ B10.D2-*Hc*^{l} *H2*^{d} *H2-T18*^{c}/nSnJ, or $C5^-Qa2^+$ B10.D2-*Hc*^{0} *H2*^{d} *H2-T18*^{c}/nSnJ (Jackson Laboratory). BM cells were recovered by grinding femurs and tibias with a mortar and pestle in cold PBS and filtering the suspension through a 40 µm cell strainer. Spleen cells were recovered by rupturing the spleen in cold PBS and filtering the suspension through a 40 µm cell strainer. BM and spleen cells were treated with ACK (Ammonium-Chloride-Potassium) red blood cell lysis buffer and washed twice with 5 ml of cold PBS. BM and spleen cells were suspended in 200 µl of saline and injected retro-orbitally into recipient mice under gaseous isoflurane anesthesia. Mice were housed in ultraclean level 2 facilities until study endpoint. Mice were euthanized on day 30, 60 and 90 post-transplant to assess airway physiological and morphological changes within the lungs. BALB/c mice transplanted with syngeneic cells or saline were used as control groups.

Assessment of Donor Cell Engraftment

Blood was collected from recipient mice every 3 weeks starting on day 21 post-transplant to assess donor cell engraftment. Red Blood cells were lysed with ACK and the cells were washed twice with cell staining buffer (Biolegend Cat# 420201), blocked with Rat Anti-

Mouse CD16/CD32 (BD Pharmingen Cat# 553141) and stained with FITC Anti-mouse Qa2 (Biolegend Cat# 121709), PE Anti-Mouse CD4 (BD Pharmingen Cat# 553730) and PerCP Anti-mouse CD8a (BD Biosciences Cat# 553036). Stained cells were captured on a BD LSR Fortessa cell analyzer (BD Biosciences) and data were analyzed using Flowjo 10 (Flowjo. LLC).

Assessment of Airway Physiology

On day 30, 60 and 90 post-transplant mice were sedated with an intraperitoneal injection (IP) of 10 mg/kg xylazine hydrochloride followed by IP injection of 30 mg/kg sodium pentobarbital. A tracheotomy was performed and a 19-gauge cannula was inserted into the trachea; the mice were attached to rodent mechanical ventilator (Flexivent, SCIREQ) and IP injected with 20 mg/kg pancuronium bromide to paralyze and inhibit respiratory effort. Mice were ventilated with 10 ml/kg of air at150 breaths per minute in between forced oscillation waveform maneuvers. The flow, volume, and pressure within the airways was recorded and the raw data was fit to the single compartment model to assess total airway resistance (R), constant phase model to assess parameters associated with conducting airway resistance (Rn), tissue resistance (G) and tissue elastance (H), and the *Salazar-Knowles equation* to assess quasi-static compliance (CST)[26,27].

Lung Histology

The left lobe of each lung was inflated with 10% formalin at a pressure of 20cm H20,

placed in formalin for 48 hours and then dissected into superior, middle and inferior sections. The sections were embedded in paraffin wax, cut into 4 µm sections and stained with hematoxylin and eosin (H&E) and Masson's trichrome blue. H&E and trichrome stained images were captured at 200x resolution using an Olympus VSI 120 microscope system (Olympus).

Analysis of Perivascular Infiltration

Photoshop (Adobe) was used to select and crop out each blood vessel and surrounding perivascular areas from H&E stained whole lung section images. The perivascular area was then selected, and the parenchyma and blood vessel lumen was masked out. The masked images were imported into ImageJ and a script was used to count all dark staining nuclei within the selected perivascular area. A circularity threshold of 0.5 was used to exclude the irregular shaped nuclei of endothelial cells. A second script was used to count the total area of the selected perivascular area. The total cell count was then divided by the area of the perivascular area to enumerate the average number of infiltrating cells.

Quantification of Peribronchiolar Fibrosis

Collagen deposition was quantified from Masson’s trichrome blue stained whole lung section images. Photoshop CC (Adobe) was used to select and mask out the lung parenchyma and lumen of each airway. The masked images were imported into ImageJ and a script was used to colour threshold the image to select the blue stained areas (Hue

130-215, Saturation 20-255, Brightness 170-255). A second script was used to measure the area of the airway. The blue stained area was divided by the total area of the airway to determine the percent blue stained area of each airway.

Immunohistochemistry

Immunohistochemistry staining was performed by the core histology facility (McMaster University). Paraffin-embedded whole lung sections were stained with 1:800 rat anti-Mouse CD4 (ebioscience Cat# 149766) and 1:1000 rat anti-Mouse CD8 (ebioscience Cat# 14080880) on a Bond RX (Leica) and captured at 200x resolution using an Olympus VSI 120 microscope (Olympus).

Statistics

All statistical tests were completed using a one-way ANOVA with a Dunnett's multiple comparisons test to compare the means of each group against the mean of the $C5^-$ transplant group. Data is represented as ± SEM; A P value less than 0.05 was considered significant

Study approval

The animal utilization protocols described herein were developed and approved in conjunction with the McMaster Animal Research Ethics Board. Mice were housed in

ultraclean level 2 facilities at McMaster University central animal facility, Hamilton Ontario Canada.

Results

Equivalent engraftment of donor $C5^+$ and $C5^-$ B10.D2 cells, into BALB/c recipients.

To assess engraftment of donor cells into recipient mice, Qa2+ donor cells from $C5^+$ B10.D2, $C5^-$ B10.D2 and control BALB/c mice were used to reconstitute irradiated $Qa2^-$ BALB/c mice. Beginning at 21 days post-transplant, peripheral blood from the recipient mice was collected every 3 weeks and stained for CD4, CD8, and Qa2 to differentiate between donor and recipient T cells **(Figure 1A)**. CD4+Qa2+ and CD8+Qa2+ cells from both $C5^+$ and $C5^-$ donor mice were detectable at 21 days post-transplant **(Figure 1B, F)**. The number of Qa2+ stained cells as a proportion of the total CD4+ and CD8+ populations increased over time with donor cell engraftment in these groups reaching near 100% reconstitution by 42 days **(Figure 1C, G)**. In contrast, mice transplanted with syngeneic donor cells were slower to engraft, on average these mice reached near 100% reconstitution by day 63 **(Figure 1D, H)**. Overall this shows that any differences between mice transplanted with $C5^+$ or $C5^-$ donor cells are not attributed to a failure of donor cell engraftment.

Reduced perivascular inflammation in the lungs of BALB/c mice transplanted with $C5^-$ donor cells

H&E staining of whole lung sections revealed BALB/c mice transplanted with $C5^-$ allogeneic B10.D2 cells consistently had reduced recruitment of inflammatory cells into perivascular areas compared to mice transplanted with allogeneic $C5^+$ or syngeneic cells. From day 30 to 90, no discernible perivascular infiltration was observed in the lungs of mice transplanted with $C5^-$ cells, nor in the syngeneic transplant or saline groups. In contrast, there was perivascular infiltration in mice transplanted with $C5^+$ allogeneic cells across all time points, indicating that perivascular inflammation in this model was donor C5-dependent **(Figure 2A)**. Using Fiji ImageJ, the number of inflammatory cells in the perivascular area of each blood vessel was enumerated and represented as the number of cells/ area (um^2) of the perivascular area. On day 30, there was no difference in perivascular infiltrate between mice transplanted with $C5^-$ allogeneic cells and saline, but there was a significant difference compared to the groups transplanted with $C5^+$ allogeneic cells and syngeneic cells **(Figure 2B)**. This difference between the $C5^+$ and $C5^-$ transplant groups remained on day 60 while significance compared to the syngeneic group was lost **(Figure 2C)**, suggesting that donor C5 is involved in the recruitment of inflammatory cells. Perivascular inflammation in the $C5^+$ group subsided by day 90 but remained higher than the other groups **(Figure 2D)**.

Reduced perivascular recruitment of CD4+ and CD8+ cells in the lungs of BALB/c mice transplanted with $C5^-$ donor cells

BALB/c mice transplanted with allogeneic $C5^-$ B10.D2 bone marrow and spleen cells consistently had reduced recruitment of CD4+ and CD8+ cells into the perivascular areas compared to wildtype C5+ groups. To characterize the perivascular infiltrate, whole lung sections were immunostained for CD4 and CD8. Within the $C5^-$ transplant groups, there was limited to no staining of CD4 positive cells across all time points with no discernible difference between $C5^-$ and saline group. BALB/c mice transplanted with syngeneic cells had marginally increased CD4 staining while mice transplanted with $C5^+$ allogeneic donor cells had substantial CD4 staining across all time points **(Figure 3)**. Examination of the CD8 staining in the same tissue sections revealed a similar staining pattern across all the groups and time points **(Figure 4)**.

Reduced late stage airway fibrosis in BALB/c mice transplanted with B10.D2 $C5^-$ bone marrow and spleen cells

BALB/c mice transplanted with $C5^-$ allogeneic B10.D2 cells were protected from deposition of collagen into the airways. To assess lung fibrosis, we performed a sircol assay from mice sacrificed on day 90. We did not observe any difference between any of the experimental groups **(Supplemental Figure 1)**. To segment the fibrotic areas of the lung, whole tissue sections were stained with Masson's trichrome blue; quantification of blue trichome stain of whole lungs sections from mice transplanted with $C5^+$ allogeneic cells revealed no discernable morphological changes or collagen deposition in the parenchyma at day 30 and 60, but a statistically significant difference at day 90 (**Supplemental Figure 2A-C).** High-resolution analysis revealed progressively more

collagen staining from day 30 to 90 post-transplant in the peribronchiolar regions of mice transplanted with $C5^+$ allogeneic cells, which was not present in the $C5^-$ transplant or control groups **(Figure 5A)**. Quantification of collagen deposition in the peribronchiolar region of the airways revealed a marginal increase in collagen deposition at day 30 between the mice transplanted with $C5^+$ allogeneic cells, $C5^-$ allogeneic cells and saline but not mice transplanted with the syngeneic donor cells **(Figure 5B)**. At day 60 there was no difference between the groups **(Figure 5C)**. However, at day 90 there was a marked and significant increase in collagen deposition in the peribronchiolar region in mice transplanted with $C5^+$ allogeneic cells compared to all the other groups **(Figure 5D)**. In contrast, no increase was observed between mice transplanted with $C5^-$ allogeneic cells and those transplanted with syngeneic cells across all time points. These findings confirm the dependency on donor-derived complement C5 in the development of conducting airway fibrosis.

Mice transplanted with $C5^-$ donor cells have decreased total lung, conducting airway and tissue resistance.

BALB/c mice transplanted with $C5^-$ allogeneic B10.D2 cells had reduced total lung resistance, conducting airway resistance and tissue resistance compared to mice transplanted with $C5^+$ allogeneic cells. To investigate the role of complement C5 dependent GvHD-related lung airway physiology, we assessed lung function of mice transplanted with allogeneic $C5^+$ cells, allogeneic $C5^-$ cells, syngeneic cells, and saline. At each time point mice were placed on a mechanical ventilator to assess respiratory

mechanics. The ventilator applied forced oscillation waveforms and recorded the subsequent changes in flow, volume, and pressure within the airways. On day 30, 60 and 90 there was no difference in the total lung, conducting airway and tissue resistance between mice that were transplanted with allogeneic $C5^-$ cells, syngeneic cells, or saline **(Figure 6A, D, G)**. In contrast, compared to the $C5^-$ transplant group, mice transplanted with $C5^+$ allogeneic cells had significantly increased total lung, conducting airway and tissue resistance on day 60 **(Figure 6B, E, H)**. However, by day 90 the difference between the groups was diminished **(Figure 6C, F, I)**.

Mice transplanted with $C5^-$ donor cells have increased lung compliance

BALB/c mice transplanted with $C5^-$ allogeneic B10.D2 cells had increased lung compliance compared to mice transplanted with $C5^+$ allogeneic cells. Lung compliance was measured using the rodent mechanical ventilator. The lung was inflated with a fixed volume of air and the corresponding changes in pressure were recorded. A relatively large rise in pressure due to a small volume of ventilated air indicates that the lung is stiffer and more "fibrotic" and has a correspondingly low lung compliance value. The pressure-volume data is plotted as a pressure-volume (PV) loop. A shift in the PV loop downward and to the right indicates a lung that is stiff and suggestive of lung fibrosis. At day 30, 60 and 90 the PV loops for mice transplanted with $C5^-$ allogeneic cells were similar to and fell on top of the loops for mice transplanted with syngeneic cells or saline. In contrast, the loops for the mice transplanted with $C5^+$ allogeneic cells were the lowest and furthest to the right on day 60 and 90 **(Figure 7A-C)**. Upon fitting the expiratory branch of each

PV loop to the *Salazar-Knowles equation*[27], the quasi-static compliance for the whole lung was determined for each mouse.

There was no difference in quasi-static compliance between mice transplanted with $C5^-$ allogeneic cells or syngeneic cells at all time points. However, there was a difference between the $C5^-$ group and saline group on day 30 and 60 **(Figure 7D, E)**. In contrast, mice transplanted with $C5^+$ allogeneic cells had significantly lower lung compliance compared to the $C5^-$ group on day 60 and 90 **(Figure 7E, F)**. Segmenting the compliance data to specifically assess the lung parenchyma, we observed a significant decrease in tissue elastance in the $C5^-$ group compared to the $C5^+$ and syngeneic groups on day 60 only **(Figure 7G-I)**.

Discussion

To investigate, the contribution of donor-derived complement C5 protein in the induction and progression of pulmonary GvHD, we adapted a mouse model of GvHD whereby by allogeneic bone marrow and spleen cells from $C5^+$ or $C5^-$ B10.D2 donor mice were used to reconstitute sub-lethally irradiated recipient $C5^+$ BALB/c mice.

Following total body irradiation, damage to the alveoli and capillaries in the lungs leads to increased vascular permeability and pulmonary edema[28] and a subsequent accumulation of inflammatory cells[29]; particularly neutrophils resulting in diffuse alveolar damage.[4] Reactive oxygen/nitrogen species further damage parenchymal cells and

promote macrophage release of pro-inflammatory cytokines TNF-α, IL-1 and chemotactic factors TGF- β, PDGF- β, IGF-1, and MCP-1. Fibroblasts are recruited by these chemotactic factors and are converted into collagen-secreting myofibroblasts culminating in lung fibrosis[30]. In light of this, we used mice transplanted with syngeneic donor cells as radiation controls. In addition to radiation-induced lung injury, mice transplanted with allogeneic donor cells develop GvHD; characterized by infiltration of inflammatory cells; leading to the destruction of alveolar cells and subsequent deposition of collagen into the airways leading to the development of bronchiolitis obliterans[31,32]. Following the transplant, donor cells engraft between day 7-21 post-transplant.[33] Therefore, we did not expect to see lung pathology on day 30. Indeed, at 21 days we observed only 50% of blood CD4+ and CD8+ cells were of donor origin and accordingly we did not observe differences in pulmonary function tests or morphology between mice transplanted with allogeneic $C5^{+}$, allogeneic $C5^{-}$ or syngeneic cells on day 30. However, with near full donor reconstitution occurring by day 63, we observed an increase in perivascular filtration and recruitment of CD4+ and CD8+ cells in mice transplanted with $C5^{+}$ allogeneic cells. With this we also observed an increase in total lung, conducting and tissue resistance and a decrease in quasi-static compliance. In contrast, these parameters did not change in the syngeneic group. The constant phase model allows segmentation of lung mechanics and determines the conducting airway resistance (Rn), a reflection of changes in airway lumen diameter; tissue resistance (G), reflecting changes in tissue properties or localized heterogeneity; and tissue elastance (H), reflecting changes in mechanical properties of the parenchyma. While the model allows tracking of changes in

central airways and parenchyma; changes in G & H are affected by heterogeneous constriction of small airways and morphological changes in parenchymal tissues[26]. Wagers et al[34] and Lundblad et al[35] demonstrated that bronchoconstriction in smaller airways can occur through liquid bridging and give rise to an increase in G and H. Herein, we observed an increase in perivascular inflammation in the $C5^+$ transplant group at day 60 accompanied by an increase of the total, conducting and tissue resistance and no change in the tissue elastance. By day 90 these observations were largely resolved. We hypothesize that G & H were transiently increased at day 60 as a result of increased lung inflammation and pulmonary edema and resolved as inflammation subsided by day 90. We also propose that the decrease in lung compliance in the $C5^+$ transplant group at day 90 was a result of airway but not parenchymal fibrosis. Mice transplanted with $C5^+$ allogeneic cells had nearly twice as much airway collagen deposition compared to the syngeneic group and but only a small increase in whole lung collagen staining. In summary, transplantation of allogeneic $C5^+$ donor cells into BALB/c mice induced GvHD within 90 days post-transplant. In contrast, mice transplanted with $C5^-$ allogeneic donor cells were protected from developing GvHD. From day 30 to 90, there was no difference in lung mechanics between these mice and mice transplanted with syngeneic donor cells. Similarly, we did not observe late stage airway fibrosis is these mice.

Complement C5 is a member of the complement cascade of proteins produced mainly by the liver. However, during T cell priming C5 is locally produced by both the APC and T cell[16-18]. C5 is extracellularly hydrolyzed into C5b and C5a, a potent proinflammatory mediator and chemoattractant for neutrophils and lymphocytes[36]. Binding of C5a to both

APCs and T cells provide costimulatory signals, promotes proliferation and effector functions[17,21,37]. In the context of hematopoietic stem cell transplantation, allogeneic T cells may be indirectly activated by donor APCs, or directly activated by host APCs. While studies in other murine models of GvHD have shown alloreactive donor T cells to be activated by host APCs[22,23]. It has been reported that host APCs primarily activate allogeneic T cells in the early stages of disease but are replaced by donor APCs in the later stages of the disease[25]. Furthermore, Matte et al[23] demonstrated that while GvHD begins with recipient APCs initially activating allogeneic T cells, donor APCs are required to maintain the ongoing disease. In the context of the current model, we hypothesize that developmental of GvHD is dependent on C5 produced locally by donor APCs. Accordingly, mice transplanted with $C5^-$ allogeneic donor cells had decreased perivascular inflammation from day 30 to 90. These mice were also protected from changes in airway physiology and lung morphology. Interestingly, compared to the syngeneic group, these mice had less perivascular inflammation on day 30 and 60, suggesting that deficiency of C5 in donor cells is sufficient to protect mice from radiation-induced lung injury as well. In our model, recipient BALB/c mice were systemically C5 sufficient but were only protected from developing GvHD when the donor allogeneic cells were C5 deficient, implying that GvHD is dependent on C5 produced locally by the APC; independent of the C5 status of the host.

In summary, transplantation of $C5^+$ allogeneic donor bone marrow and spleen cells into irradiated BALB/C mouse lead to the development of pulmonary GvHD; specifically, early-stage inflammation followed by late-stage airway fibrosis similar to bronchiolitis

obliterans. In conjunction with these morphological changes, there were accompanying changes in lung mechanics. In contrast, when transplants were performed with allogeneic $C5^-$ bone marrow and spleen cells, recipient mice were protected from developing pulmonary inflammation and subsequent airway fibrosis. We propose that deficiency in C5 within the donor cells prevents adequate activation of allogeneic donor T cells by donor APCs, thereby preventing the downstream cascade of signalling events and alloresponses culminating in lung fibrosis. Finally, we propose that the dependency of donor-derived C5 on GvHD induction represents a new target for the development of donor cell-targeted therapeutic interventions leading to more successful hematopoietic stem cell transplant protocols.

Acknowledgments. We thank the central animal facility (McMaster University, ON, Canada) for their exceptional care and monitoring of the mice and the core histology facility for their staining services. We thank Kjetil Ask for use of the VSI 120 microscope system. We thank Daniel Moldaver for providing animal training and all the members of the Larché lab for their continued guidance and support. This work supported by the Scleroderma Society of Ontario, a non-profit organization that supports scientific research.

Authorship

Contributions: Conception and design of study: JI, MI, MK, PM and ML; Conducted experiments: JI, EAA, JW, IW; Analysis and interpretations of Data: JI, EAA, JW, MI,

MK, PM and ML; Drafting the manuscript: JI; Edited and revised manuscript: JI, ML. All authors read and approved the final version.

Conflicts of interest disclosure: The authors declare no financial conflicts of interest

The current affiliation for EAA is Division of Pulmonary and Critical Care Medicine, Brigham and Women's Hospital, Harvard Medical School, Boston, MA.

Correspondence: Dr. Mark Larché, Department of Medicine, McMaster University Health Sciences Centre, Rm 4H20, 1280 Main Street W, Hamilton Ontario L8S 4L8; e-mail: larche@mcmaster.ca

References

1. Bauerlein CA, Riedel SS, Baker J, et al. A diagnostic window for the treatment of acute graft-versus-host disease prior to visible clinical symptoms in a murine model. *BMC Med*. 2013;11:134.
2. Min CK. The pathophysiology of chronic graft-versus-host disease: the unveiling of an enigma. *Korean J Hematol*. 2011;46(2):80-87.
3. Schroeder MA, DiPersio JF. Mouse models of graft-versus-host disease: advances and limitations. *Dis Model Mech*. 2011;4(3):318-333.
4. Wah TM, Moss HA, Robertson RJ, Barnard DL. Pulmonary complications following bone marrow transplantation. *Br J Radiol*. 2003;76(906):373-379.
5. Roncarolo MG, Battaglia M. Regulatory T-cell immunotherapy for tolerance to self antigens and alloantigens in humans. *Nat Rev Immunol*. 2007;7(8):585-598.
6. Wysocki CA, Panoskaltsis-Mortari A, Blazar BR, Serody JS. Leukocyte migration and graft-versus-host disease. *Blood*. 2005;105(11):4191-4199.
7. Alexander KA, Flynn R, Lineburg KE, et al. CSF-1-dependant donor-derived macrophages mediate chronic graft-versus-host disease. *J Clin Invest*. 2014;124(10):4266-4280.
8. Markey KA, Banovic T, Kuns RD, et al. Conventional dendritic cells are the critical donor APC presenting alloantigen after experimental bone marrow transplantation. *Blood*. 2009;113(22):5644-5649.
9. Wu T, Young JS, Johnston H, et al. Thymic damage, impaired negative selection, and development of chronic graft-versus-host disease caused by donor CD4+ and CD8+ T cells. *J Immunol*. 2013;191(1):488-499.
10. Teshima T, Ordemann R, Reddy P, et al. Acute graft-versus-host disease does not require alloantigen expression on host epithelium. *Nat Med*. 2002;8(6):575-581.
11. Cooke KR, Luznik L, Sarantopoulos S, et al. The Biology of Chronic Graft-versus-Host Disease: A Task Force Report from the National Institutes of Health Consensus Development Project on Criteria for Clinical Trials in Chronic Graft-versus-Host Disease. *Biol Blood Marrow Transplant*. 2017;23(2):211-234.
12. Zeiser R, Blazar BR. Pathophysiology of Chronic Graft-versus-Host Disease and Therapeutic Targets. *N Engl J Med*. 2017;377(26):2565-2579.
13. Kemper C, Atkinson JP. T-cell regulation: with complements from innate immunity. *Nat Rev Immunol*. 2007;7(1):9-18.
14. Longhi MP, Harris CL, Morgan BP, Gallimore A. Holding T cells in check--a new role for complement regulators? *Trends Immunol*. 2006;27(2):102-108.
15. Suresh M, Molina H, Salvato MS, Mastellos D, Lambris JD, Sandor M. Complement component 3 is required for optimal expansion of CD8 T cells during a systemic viral infection. *J Immunol*. 2003;170(2):788-794.
16. Lalli PN, Strainic MG, Yang M, Lin F, Medof ME, Heeger PS. Locally produced C5a binds to T cell-expressed C5aR to enhance effector T-cell expansion by limiting antigen-induced apoptosis. *Blood*. 2008;112(5):1759-1766.
17. Strainic MG, Liu J, Huang D, et al. Locally produced complement fragments C5a and C3a provide both costimulatory and survival signals to naive CD4+ T cells. *Immunity*. 2008;28(3):425-435.

18. Heeger PS, Lalli PN, Lin F, et al. Decay-accelerating factor modulates induction of T cell immunity. *J Exp Med*. 2005;201(10):1523-1530.
19. Ma Q, Li D, Carreno R, et al. Complement component C3 mediates Th1/Th17 polarization in human T-cell activation and cutaneous GVHD. *Bone Marrow Transplant*. 2014;49(7):972-976.
20. Kwan WH, Hashimoto D, Paz-Artal E, et al. Antigen-presenting cell-derived complement modulates graft-versus-host disease. *J Clin Invest*. 2012;122(6):2234-2238.
21. Cravedi P, Leventhal J, Lakhani P, Ward SC, Donovan MJ, Heeger PS. Immune cell-derived C3a and C5a costimulate human T cell alloimmunity. *Am J Transplant*. 2013;13(10):2530-2539.
22. Shlomchik WD, Couzens MS, Tang CB, et al. Prevention of graft versus host disease by inactivation of host antigen-presenting cells. *Science*. 1999;285(5426):412-415.
23. Zhang Y, Shlomchik WD, Joe G, et al. APCs in the liver and spleen recruit activated allogeneic CD8+ T cells to elicit hepatic graft-versus-host disease. *J Immunol*. 2002;169(12):7111-7118.
24. Matte CC, Liu J, Cormier J, et al. Donor APCs are required for maximal GVHD but not for GVL. *Nat Med*. 2004;10(9):987-992.
25. Benichou G, Takizawa PA, Olson CA, McMillan M, Sercarz EE. Donor major histocompatibility complex (MHC) peptides are presented by recipient MHC molecules during graft rejection. *J Exp Med*. 1992;175(1):305-308.
26. Irvin CG, Bates JH. Measuring the lung function in the mouse: the challenge of size. *Respir Res*. 2003;4:4.
27. Hantos Z, Daroczy B, Suki B, Nagy S, Fredberg JJ. Input impedance and peripheral inhomogeneity of dog lungs. *J Appl Physiol (1985)*. 1992;72(1):168-178.
28. Ghafoori P, Marks LB, Vujaskovic Z, Kelsey CR. Radiation-induced lung injury. Assessment, management, and prevention. *Oncology (Williston Park)*. 2008;22(1):37-47; discussion 52-33.
29. Giridhar P, Mallick S, Rath GK, Julka PK. Radiation induced lung injury: prediction, assessment and management. *Asian Pac J Cancer Prev*. 2015;16(7):2613-2617.
30. Morgan GW, Breit SN. Radiation and the lung: a reevaluation of the mechanisms mediating pulmonary injury. *Int J Radiat Oncol Biol Phys*. 1995;31(2):361-369.
31. Kitko CL, White ES, Baird K. Fibrotic and sclerotic manifestations of chronic graft-versus-host disease. *Biol Blood Marrow Transplant*. 2012;18(1 Suppl):S46-52.
32. Worthy SA, Flint JD, Muller NL. Pulmonary complications after bone marrow transplantation: high-resolution CT and pathologic findings. *Radiographics*. 1997;17(6):1359-1371.
33. Duran-Struuck R, Dysko RC. Principles of bone marrow transplantation (BMT): providing optimal veterinary and husbandry care to irradiated mice in BMT studies. *J Am Assoc Lab Anim Sci*. 2009;48(1):11-22.
34. Wagers S, Lundblad LK, Ekman M, Irvin CG, Bates JH. The allergic mouse model of asthma: normal smooth muscle in an abnormal lung? *J Appl Physiol (1985)*. 2004;96(6):2019-2027.
35. Lundblad LK, Thompson-Figueroa J, Allen GB, et al. Airway hyperresponsiveness in allergically inflamed mice: the role of airway closure. *Am J Respir Crit Care Med*. 2007;175(8):768-774.
36. Manthey HD, Woodruff TM, Taylor SM, Monk PN. Complement component 5a (C5a). *Int J Biochem Cell Biol*. 2009;41(11):2114-2117.

37. Moulton RA, Mashruwala MA, Smith AK, et al. Complement C5a anaphylatoxin is an innate determinant of dendritic cell-induced Th1 immunity to Mycobacterium bovis BCG infection in mice. *J Leukoc Biol*. 2007;82(4):956-967.

Figure Legends

Figure 1. Equivalent engraftment of donor B10.D2 cells from C5 sufficient, and C5 deficient mice. Irradiated BALB/c(Qa2$^-$) mice transplanted with 2x10^6 spleen and 1x10^6 bone marrow cells from Qa2+C5+, Qa2+C5- or Qa2+ syngeneic donor mice. Blood was collected every 3 weeks starting 21 days post-transplant and stained for CD4, CD8, and Qa2. (A) Representative flowjo gating strategy for assessing Qa2+ donor cells in BALB/c mice transplanted with C5+ sufficient cells from day 42 post-transplant. Percentage of Qa2+ stained CD4 blood cells from C5 sufficient, C5 deficient and syngeneic donor mice from (B) day 21(n=5) (C) day 42(n=5) (D) day 63(n=5) and (E) day 84(n=5). Percentage of Qa2+ stained CD8 blood cells from C5 sufficient, C5 deficient and syngeneic donor mice from (F) day 21 (G) day 42 (H) day 63 and (I) day 84.

Figure 2. Reduced perivascular inflammation in the lungs of BALB/c mice transplanted with C5 deficient donor cells. Irradiated BALB/c(Qa2$^-$) mice transplanted with 2x10^6 spleen and 1x10^6 bone marrow cells from C5+, C5-, syngeneic donor mice or saline. Recruited inflammatory cells in the perivascular area were enumerated from H&E stained lungs sections. The data is representative of 2-3 independent experiments pooled together. 750x750 pixel representative images were cropped from original x200 magnification whole lung images. The images were enhanced in photoshop by increasing brightness by 35% and contrast by 50%. C5+ transplant group (n=5, 7, 10), C5- transplant group (n=4, 5, 10), syngeneic group (n=10, 10, 15) and saline (n=5, 5, 10). (A)

Representative images from each experimental group from day 30 (right column), day 60 (middle column) and day 90 (left column). There is significant perivascular infiltration in C5+ transplanted group compared to the C5- transplant at (B) day 30 and (C) day 60 but not day (D) day 90. The data were analyzed using a one-way ANOVA with a Dunnett's multiple comparisons test to compare the means of each group against the mean of the C5- transplant group and represented as +/- SEM; **p≤*0.01;* ***p≤*0.0005;* **** *p≤0.0001.*

Figure 3. Reduced perivascular recruitment of CD4+ cells in the lungs of BALB/c mice transplanted with C5 deficient donor cells. Irradiated BALB/c(Qa2$^-$) mice transplanted with 2x10^6 spleen and 1x10^6 bone marrow cells from C5+, C5-, syngeneic donor mice or saline. Whole lung sections were immunostained for CD4. Data are representative images from each experimental group. 1500x1500 pixel images were cropped from original x200 magnification whole lung images. There is substantial perivascular infiltration of CD4+ in C5+ transplanted groups on day 30 (right column), day 60 (middle column and Day 90 (left column) but not in the C5- transplant or control groups.

Figure 4. Reduced perivascular recruitment of CD4+ and CD8+ cells in the lungs of BALB/c mice transplanted with C5 deficient donor cells. Irradiated BALB/c(Qa2$^-$) mice transplanted with 2x10^6 spleen and 1x10^6 bone marrow cells from C5+, C5-,

syngeneic donor mice or saline. Whole lung sections were immunostained for CD8. Data are representative images from each experimental group. 2000x2000 pixel images were cropped from original x200 magnification whole lung images. There is substantial perivascular infiltration of CD8+ cells in C5+ transplanted groups on day 30 (right column), day 60 (middle column and Day 90 (left column) but not in the C5- transplant or control groups.

Figure 5. Reduced late stage airway fibrosis in BALB/c mice transplanted with B10.D2 C5 deficient bone marrow and spleen cells. Irradiated BALB/c(Qa2$^-$) mice transplanted with 2x10^6 spleen and 1x10^6 bone marrow cells from C5+, C5-, syngeneic donor mice or saline. Whole lung sections were stained with Masson's trichrome for collagen. (A) Representative images from each experimental group are shown. 2000x2000 pixel images were cropped from original x200 magnification whole lung images. C5+ transplant group (n=5, 7, 10), C5- transplant group (n=4, 5, 10), syngeneic group (n=10, 10, 15) and saline (n=5, 5, 10). There was increased peribronchiolar trichrome staining at (top right column) day 90 in the C5+ transplant group. Trichrome staining in the peribronchiolar areas was quantified for each time point. There was no difference between any of the experimental groups at (B) day 30 and (C) day 60 post-transplant. (D) Mice transplanted with C5 sufficient cells had twice as much trichrome stained peribronchiolar area compared to the C5- transplant and control groups. The data were analyzed using a one-way ANOVA with a Dunnett's multiple comparisons test to

compare the means of each group against the mean of the C5- transplant group and represented as +/- SEM; ***p≤*0.0005.*

Figure 6. Mice transplanted with C5 deficient donor cells have decreased total lung, conducting airway and tissue resistance. Irradiated BALB/c(Qa2$^-$) mice transplanted with 2x10^6 spleen and 1x10^6 bone marrow cells from C5+, C5-, syngeneic donor mice or saline. On days 30, 60, and 90 post-transplant, a mechanical ventilator was used to assess (A-C) total lung resistance, (D-F) conducting airway resistance, (G-I) tissue resistance. There was no difference in the three measured parameters between any of the experimental groups on day 30 (A, D, G). The data is representative of 2-3 independent experiments pooled together. C5+ transplant group (n=5, 7, 10), C5- transplant group (n=4, 5, 10), syngeneic group (n=10, 10, 15) and saline (n=5, 5, 10). There is a significant difference between the C5+ and C5- transplant groups for all three measured parameters at (B, E, H) day 60 but there is no difference at between any group at (C, F, I) day 90. The data were analyzed using a one-way ANOVA with a Dunnett's multiple comparisons test to compare the means of each group against the mean of the C5- transplant group and represented as +/- SEM; *p≤*0.05;* **p≤*0.01;* ***p≤*0.0005.*

Figure 7. Mice transplanted with C5 deficient donor cells have increased lung compliance. Irradiated BALB/c(Qa2$^-$) mice transplanted with 2x10^6 spleen and 1x10^6 bone marrow cells from C5+, C5-, syngeneic donor mice or saline. On days 30, 60, and 90 post-transplant, a mechanical ventilator was used to generate pressure-volume (PV) loops and assess, lung compliance and tissue elastance. The data is representative of 2-3 independent experiments pooled together. C5+ transplant group (n=5, 7, 10), C5-

transplant group (n=4, 5, 10), syngeneic group (n=10, 10, 15) and saline (n=5, 5, 10). Each loop was plotted from averaged values from each mouse in the group. A shift in the loop downward and to the right indicates and a stiffer lung. Mice transplanted with C5 sufficient cells had slightly stiffer lungs at (B) day 60 and a substantial increase in lung stiffness at (C) day 90. (D-F) Mice transplanted with C5+ sufficient cells had decreased lung compliance across all time points, while there was no difference in lung compliance between mice transplanted with C5 deficient and syngeneic cells. (H) Mice transplanted with C5 deficient cells were also protected from increased tissue elastance at day 60. The data were analyzed using a one-way ANOVA with a Dunnett's multiple comparisons test to compare the means of each group against the mean of the C5- transplant group and represented as +/- SEM; *p≤*0.05;* ***p≤*0.0005*.

Figure 1

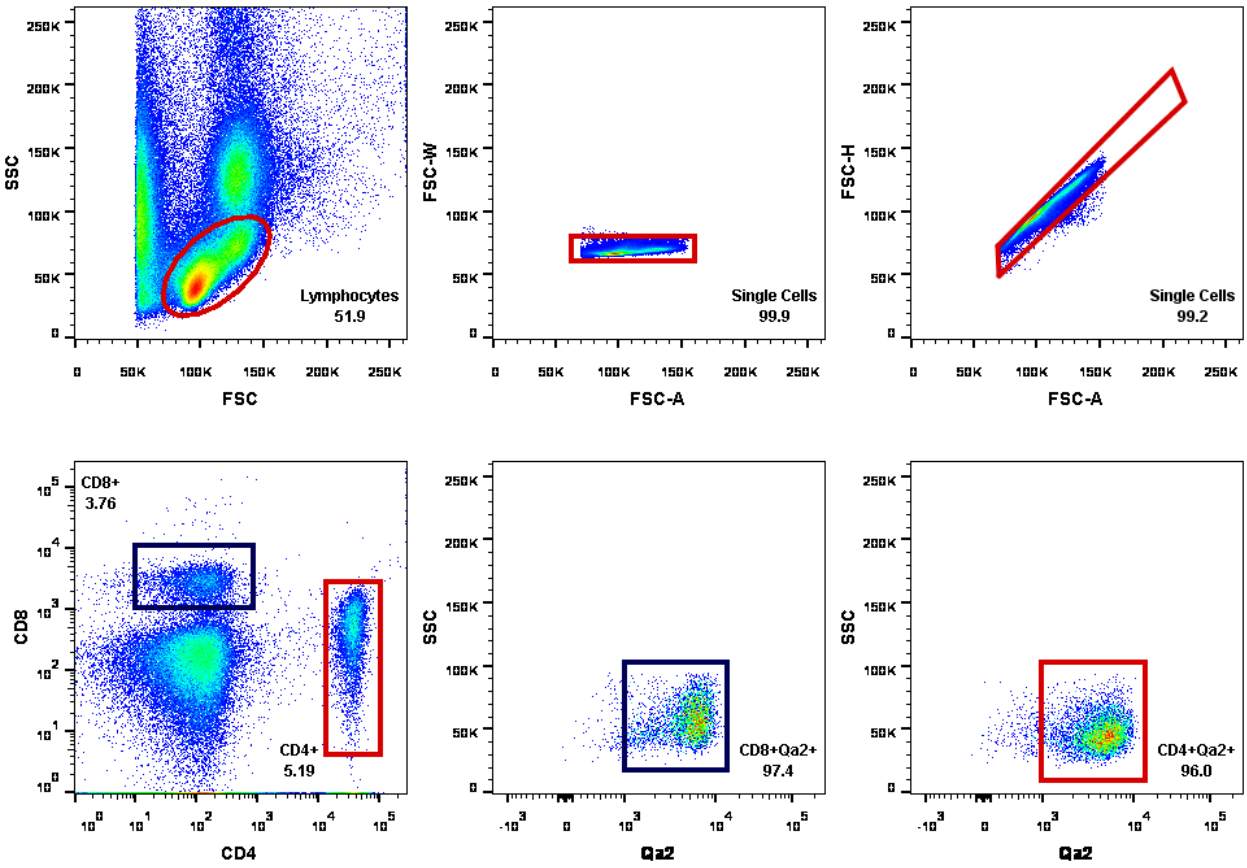
SSC
FSC
Lymphocytes
51.9
FSC-W
FSC-A
Single Cells
99.9
FSC-H
FSC-A
Single Cells
99.2
CD8
CD4
CD8+
3.76
CD4+
5.19
SSC
Qa2
CD8+Qa2+
97.4
SSC
Qa2
CD4+Qa2+
96.0

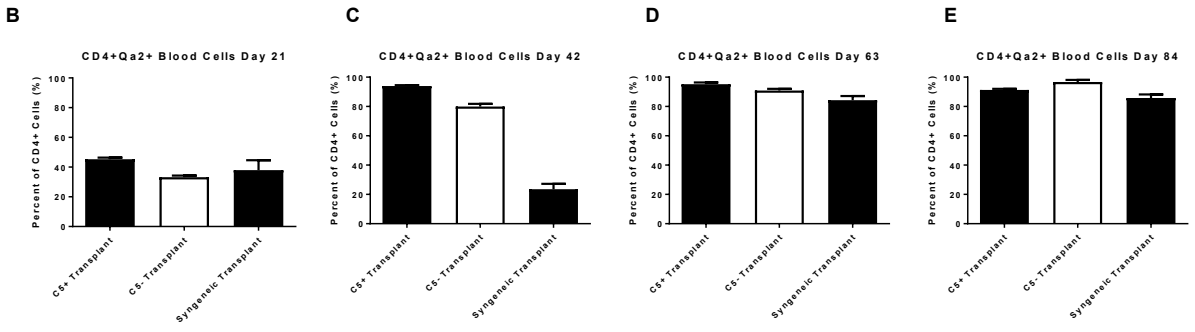
B
CD4+Qa2+ Blood Cells Day 21
C
CD4+Qa2+ Blood Cells Day 42
D
CD4+Qa2+ Blood Cells Day 63
E
CD4+Qa2+ Blood Cells Day 84
Percent of CD4+ Cells (%)
C5+ Transplant
C5- Transplant
Syngeneic Transplant

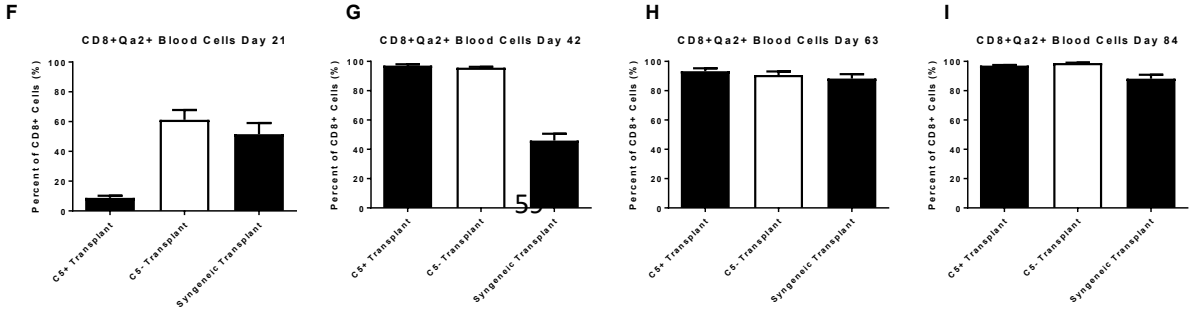
F
CD8+Qa2+ Blood Cells Day 21
G
CD8+Qa2+ Blood Cells Day 42
H
CD8+Qa2+ Blood Cells Day 63
I
CD8+Qa2+ Blood Cells Day 84
Percent of CD8+ Cells (%)
C5+ Transplant
C5- Transplant
Syngeneic Transplant

Figure 2

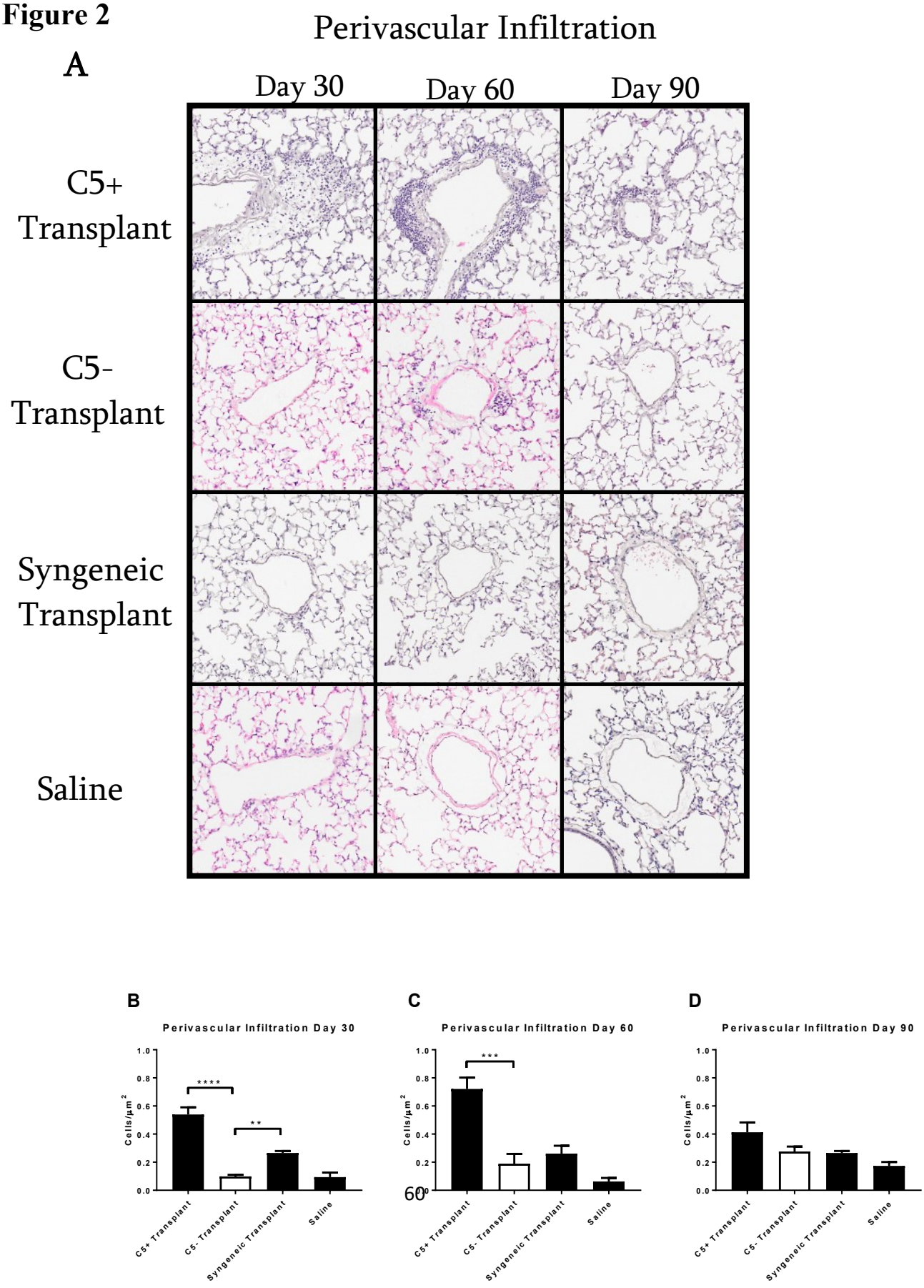
A
Perivascular Infiltration
Day 30
Day 60
Day 90
C5+ Transplant
C5- Transplant
Syngeneic Transplant
Saline
B
Perivascular Infiltration Day 30
C
Perivascular Infiltration Day 60
D
Perivascular Infiltration Day 90
Cells/µm²
C5+ Transplant
C5- Transplant
Syngeneic Transplant
Saline

Figure 3

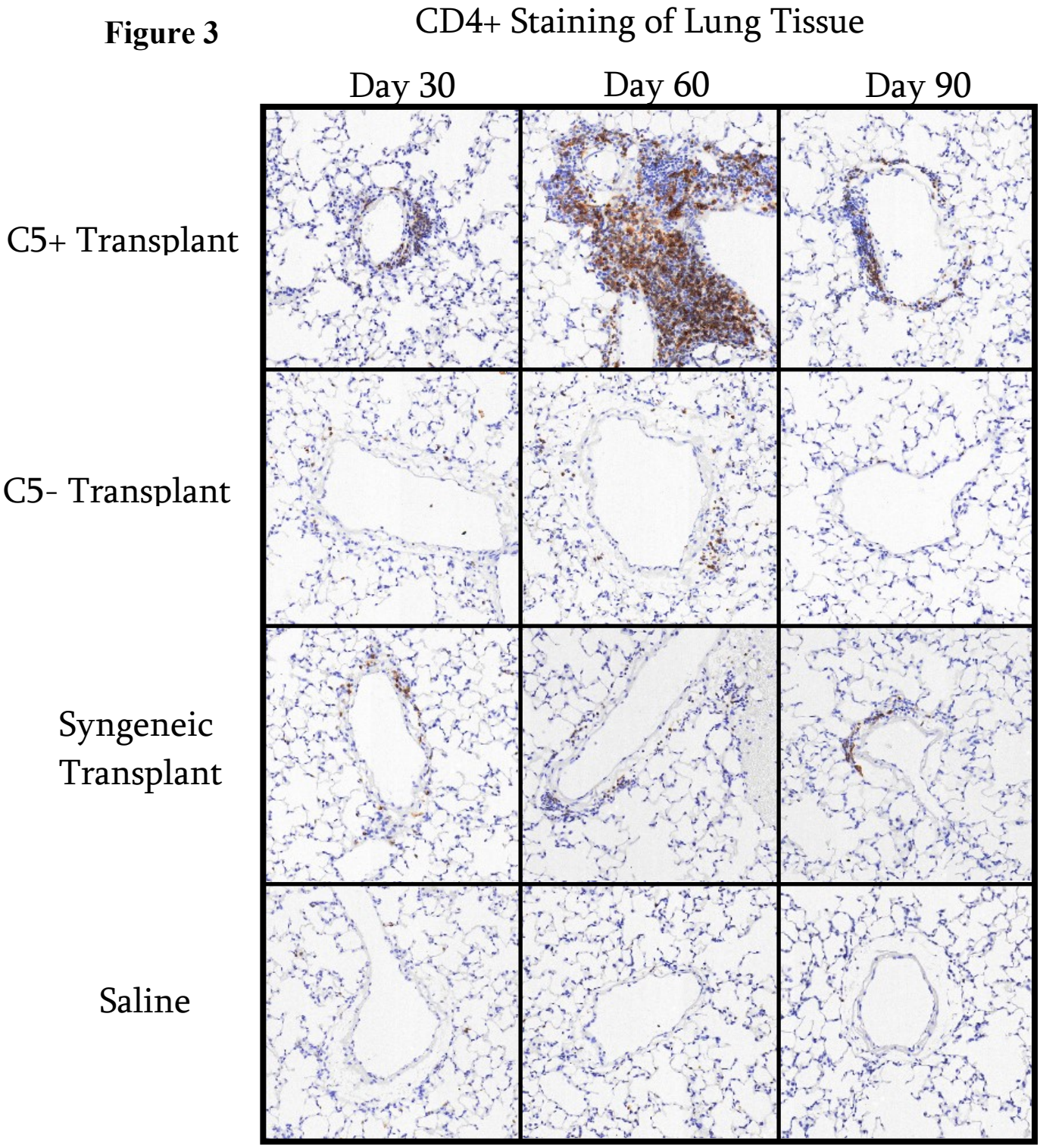
CD4+ Staining of Lung Tissue
Day 30
Day 60
Day 90
C5+ Transplant
C5- Transplant
Syngeneic Transplant
Saline

Figure 4

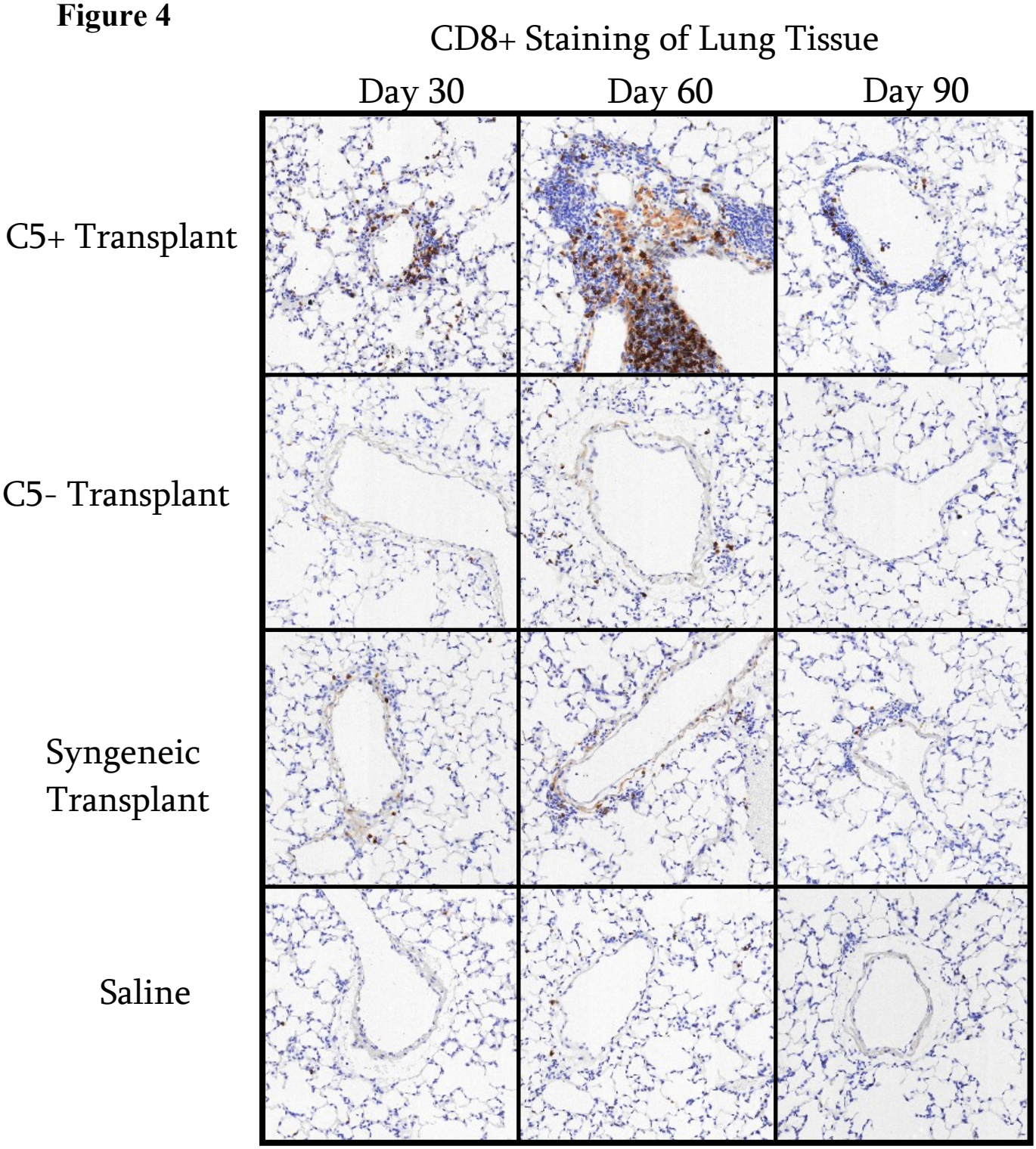
CD8+ Staining of Lung Tissue
Day 30
Day 60
Day 90
C5+ Transplant
C5- Transplant
Syngeneic Transplant
Saline

Figure 5

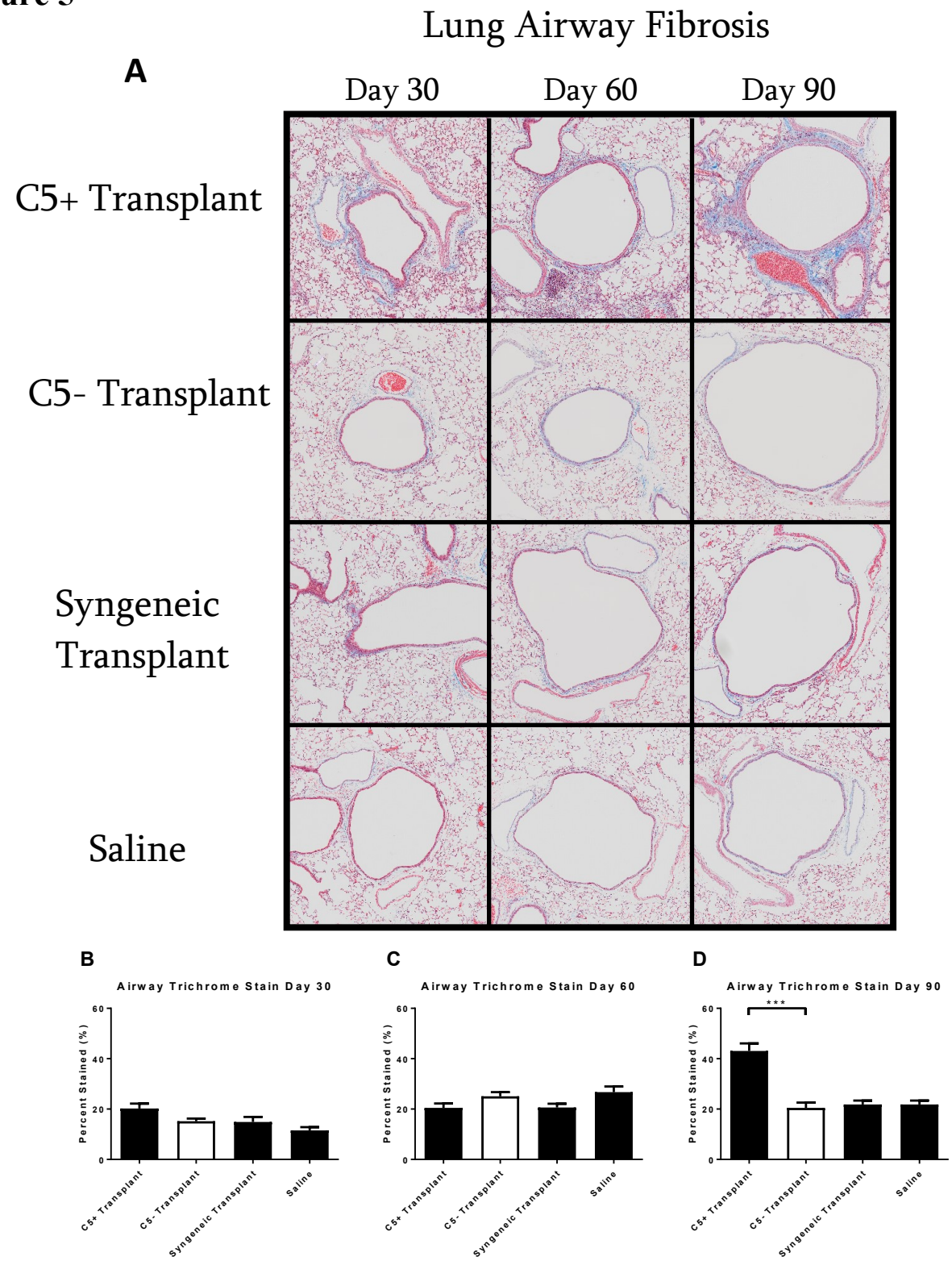
Lung Airway Fibrosis
A
Day 30
Day 60
Day 90
C5+ Transplant
C5- Transplant
Syngeneic Transplant
Saline
B
Airway Trichrome Stain Day 30
C
Airway Trichrome Stain Day 60
D
Airway Trichrome Stain Day 90
***
Percent Stained (%)
0
20
40
60
C5+ Transplant
C5- Transplant
Syngeneic Transplant
Saline

Figure 6

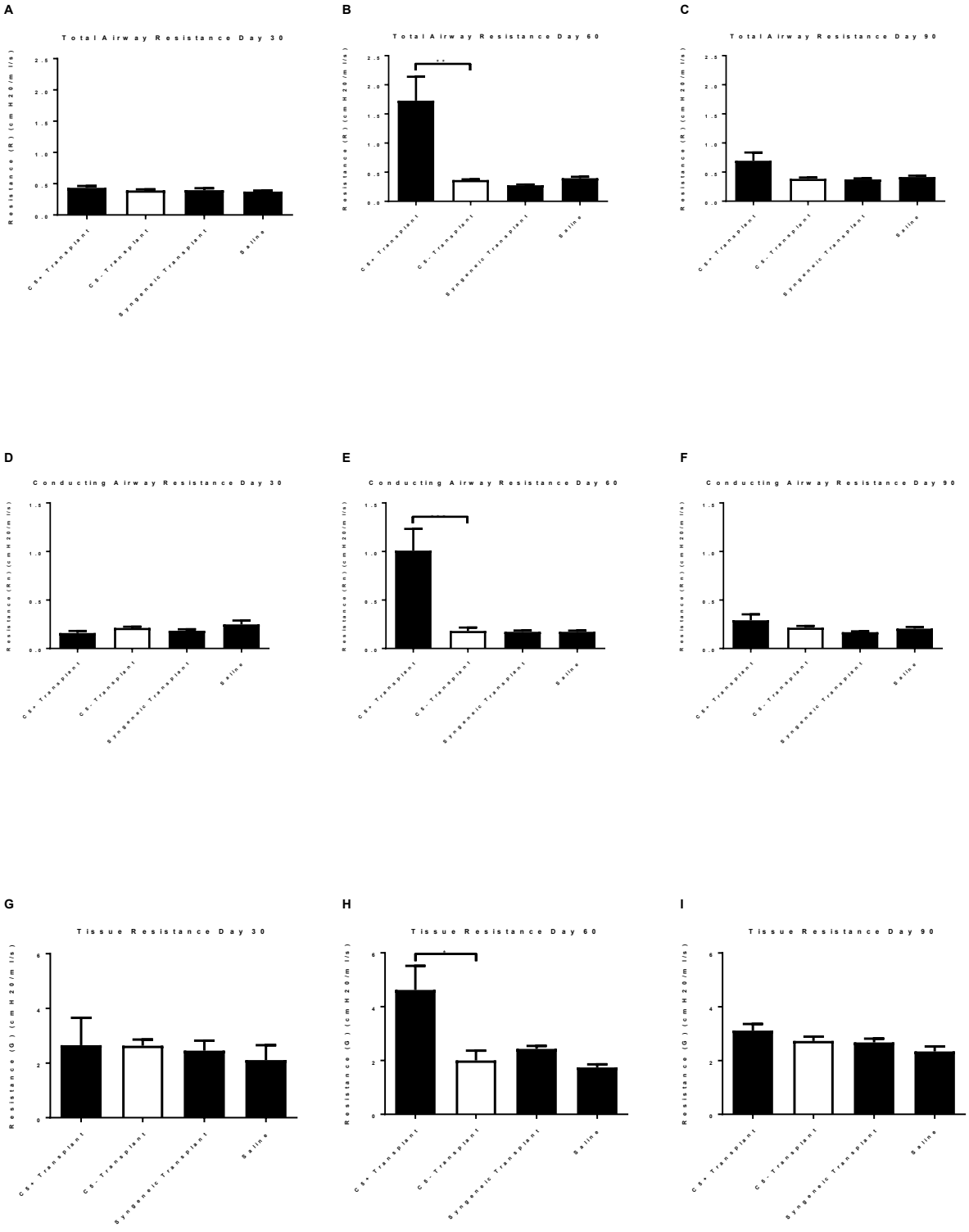
A
Total Airway Resistance Day 30
B
Total Airway Resistance Day 60
C
Total Airway Resistance Day 90
D
Conducting Airway Resistance Day 30
E
Conducting Airway Resistance Day 60
F
Conducting Airway Resistance Day 90
G
Tissue Resistance Day 30
H
Tissue Resistance Day 60
I
Tissue Resistance Day 90
Cs+ Transplant
Cs- Transplant
Syngeneic Transplant
Saline

Figure 7

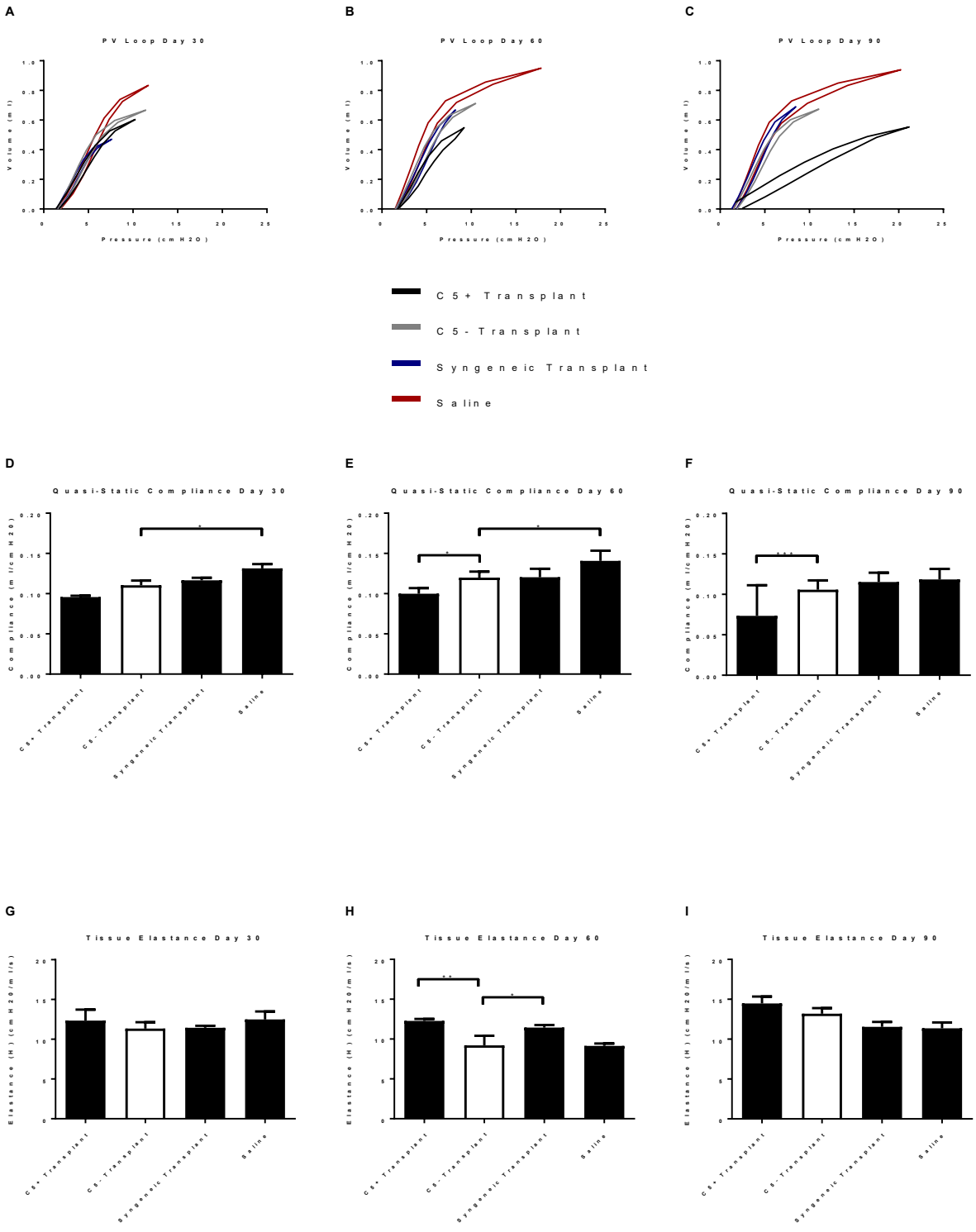
A
PV Loop Day 30
B
PV Loop Day 60
C
PV Loop Day 90
Volume (ml)
Pressure (cmH2O)
C5+ Transplant
C5- Transplant
Syngeneic Transplant
Saline
D
Quasi-Static Compliance Day 30
E
Quasi-Static Compliance Day 60
F
Quasi-Static Compliance Day 90
Compliance (ml/cmH20)
G
Tissue Elastance Day 30
H
Tissue Elastance Day 60
I
Tissue Elastance Day 90
Elastance (H) (cmH20/ml/s)

Supplemental Data

Methods

Sircol Assay

The soluble collagen content of the lungs was assessed using a sircol assay according to the manufactures instructions (Sircol^{TM} Soluble Collagen Assay, Biocolor, UK). Briefly, the right 4 lobes of each lung were homogenized in RIPA buffer, the supernatant was collected and stained with the sircol dye, washed with an acid-salt solution and alkali reagent and finally analyzed using a spectramax i3 plate reader (Molecular Devices) at 555nm.

Quantification of Lung and Airway Fibrosis

Collagen deposition was quantified from Masson's trichrome blue stained whole lung section images. Photoshop CC (Adobe) was used to select entire lung section and the background was painted black. The masked images were imported into ImageJ and a script was used to colour threshold the image to selectively highlight the blue stained areas (Hue 130-215, Saturation 20-255, Brightness 170-255). A second script was used to measure the area of the entire lung section. The blue stained area was divided by the total lung area to determine the total blue stained area of each lung. Peribronchiolar fibrosis was similarly analyzed by selectively masking out the lung parenchyma and lumen of

each airway and dividing the blue stained area by the total area of the peribronchiolar area.

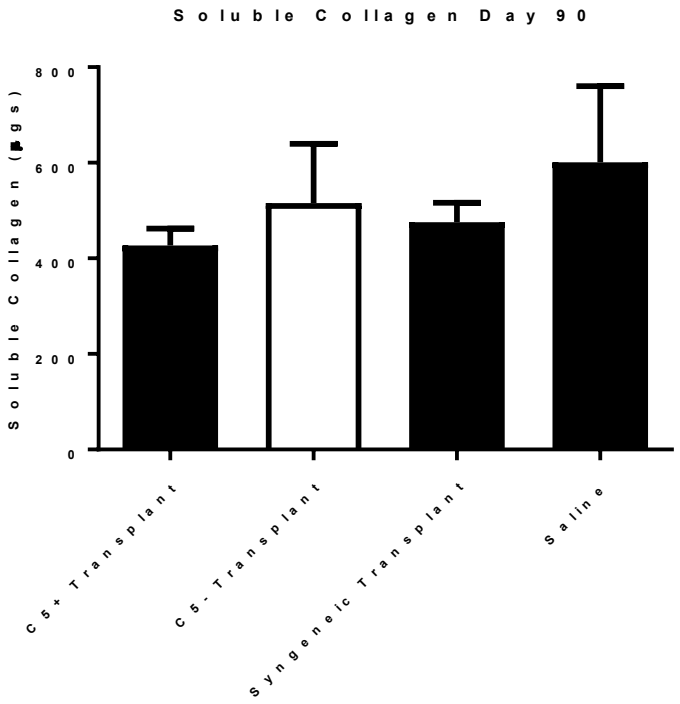

Supplemental Figure 1. No difference in late-stage right lung soluble sircol staining. Sub-lethally irradiated BALB/c(Qa2$^-$) mice reconstituted with 2x10^6 spleen and 1x10^6 bone marrow cells from C5+, C5-, syngeneic donor mice or saline. The right four lobes of each lung were stained with sircol and acid solubilized to quantify total soluble collagen. C5+ transplant group (n=10), C5- transplant group (n=10), syngeneic group (n=15) and saline (n=10). (A) No difference in total soluble collagen was observed between any of experimental groups at day 90. Data were analyzed using a one-way ANOVA with a Dunnett's multiple comparisons test to compare the means of each group against the mean of the C5- transplant group and represented as +/- SEM.

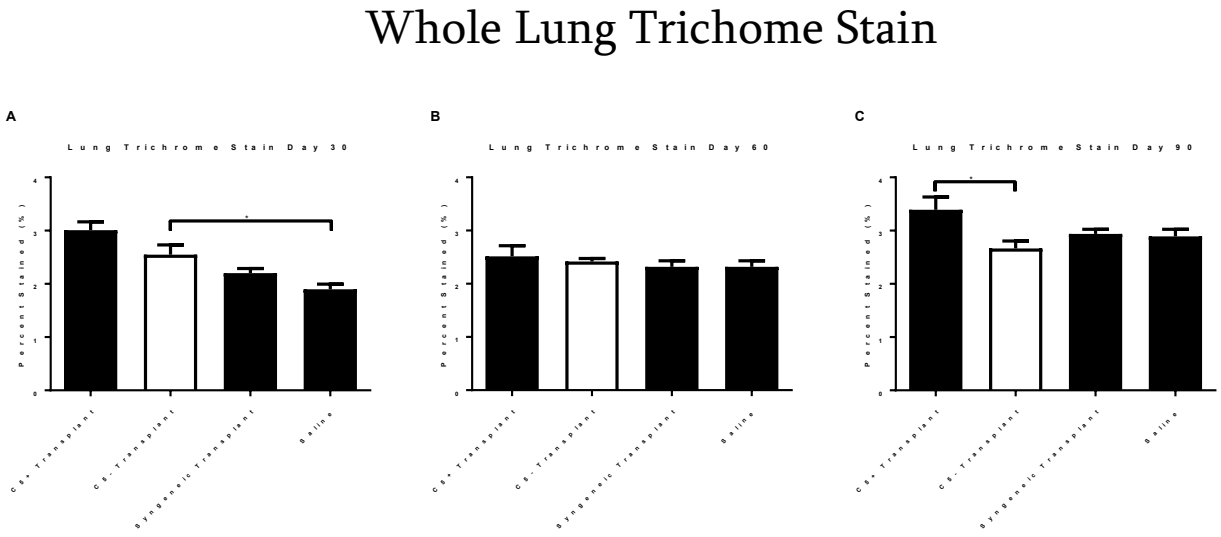

Supplemental Figure 2. Reduced late stage whole lung fibrosis in BALB/c mice transplanted with B10.D2 C5 deficient bone marrow and spleen cells. Sub-lethally irradiated BALB/c(Qa2$^-$) mice reconstituted with 2x10^6 spleen and 1x10^6 bone marrow cells from C5+, C5-, syngeneic donor mice or saline. Whole lung sections were stained with Masson's trichrome for collagen and quantified. C5+ transplant group (n=5, 7, 10), C5- transplant group (n=4, 5, 10), syngeneic group (n=10, 10, 15) and saline (n=5, 5, 10). There was no difference between the C5+, C5- and syngeneic groups at (A) day 30 and (B) day 60 post-BMT. (C) Mice transplanted with C5 sufficient cells had increased trichrome stained whole lung sections compared to the C5- transplant and control groups. Data were analyzed using a one-way ANOVA with a Dunnett's multiple comparisons test to compare the means of each group against the mean of the C5- transplant group and represented as +/- SEM; *p≤*0.05*.

ImageJ Scripts

The script used to calculate peribronchiolar, perivascular and whole tissue areas of masked images

```
run("Duplicate...", " ");
run("8-bit");
//run("Brightness/Contrast...");
setMinAndMax(19, 20);
run("Apply LUT");
setAutoThreshold("Default dark");
//run("Threshold...");
setThreshold(254, 255);
//setThreshold(254, 255);
setOption("BlackBackground", false);
run("Convert to Mask");
run("Create Selection");
run("Measure");
```

The script used to count the number of infiltrating cells in perivascular areas of masked images

```
run("16-bit");
setAutoThreshold("Default");
//run("Threshold...");
setThreshold(0, 180);
setOption("BlackBackground", false);
run("Convert to Mask");
run("Watershed");
run("Analyze Particles...", "size=20-Infinity circularity=0.65-1.00 clear summarize");
```

The script used to calculate blue stained areas of masked images

```
run("Duplicate...", " ");
run("Color Threshold...");
// Color Thresholder 2.0.0-rc-43/1.50g
// Autogenerated macro, single images only!
min=newArray(3);
max=newArray(3);
filter=newArray(3);
a=getTitle();
run("HSB Stack");
run("Convert Stack to Images");
selectWindow("Hue");
rename("0");
selectWindow("Saturation");
rename("1");
selectWindow("Brightness");
rename("2");
```

```
min[0]=110;
max[0]=220;
filter[0]="pass";
min[1]=20;
max[1]=255;
filter[1]="pass";
min[2]=0;
max[2]=255;
filter[2]="pass";
for (i=0;i<3;i++){
  selectWindow(""+i);
  setThreshold(min[i], max[i]);
  run("Convert to Mask");
  if (filter[i]=="stop")  run("Invert");
}
imageCalculator("AND create", "0","1");
imageCalculator("AND create", "Result of 0","2");
for (i=0;i<3;i++){
  selectWindow(""+i);
  close();
}
selectWindow("Result of 0");
close();
selectWindow("Result of Result of 0");
rename(a);
// Colour Thresholding----------
run("Create Selection");
run("Create Mask");
run("Create Selection");
run("Measure");
```

Chapter 3. Immune responses to HLA-A2 drive multiorgan pathology in a humanized murine model of Graft versus Host Disease

Immune responses to HLA-A2 drive multiorgan pathology in a humanized murine model of Graft versus Host Disease

Imani. J[1,2,3], Wattie. J[1,3], Inman. MD[1], Kolb. M[1], Margetts[4]. P, Ball, ST[5], Larché. M[1,2,3]

1. Department of Medicine, Division of Respirology & Firestone Institute for Respiratory Health, The Research Institute at St. Joe's, McMaster University, Hamilton, ON, Canada

2. McMaster Immunology Research Center, McMaster University, Hamilton, ON, Canada

3. Department of Medicine, Division of Clinical Immunology & Allergy, McMaster University, Hamilton On, Canada

4. Department of Medicine, Division of Nephrology, McMaster University, Hamilton On, Canada

5. Department of Renal Medicine, Queen Elizabeth Hospital Birmingham, Edgbaston, United Kingdom

Keywords: Transgenic, HLA-DR4, HLA-A2, Bone Marrow Transplant, Graft vs Host, Pulmonary Fibrosis, Skin, Liver, Inflammation, T cell

Corresponding author: Dr. Mark Larché, Department of Medicine, McMaster University and The Research Institute of St. Joe's Hamilton, Firestone Institute for Respiratory Health, Hamilton Health Sciences, Rm 4H20, 1280 Main street W, Hamilton Ontario L8S 4L8, Ph# (905) 525-9140 ext. 21284; Fax# (905) 521-4971, E-mail: larche@mcmaster.ca

Abstract

Graft vs host disease occurs following transplantation of allogeneic hematopoietic stem cells and lymphocytes. Donor lymphocytes recognize mismatched minor or major antigens on recipient tissues and initiate anti-host responses. This process starts a cascade of events which begins with tissue inflammation and concludes with end-stage fibrosis of the major organs. Mismatches within the MHC locus (HLA in humans) between donor: recipient transplant pairs are immunodominant compared to minor antigen mismatches and lead to severe GvHD. Analysis of GvHD patients has revealed that class I HLA mismatches are key drivers of disease and CD4+ donor T cells have been shown to respond to HLA-A2-derived peptides presented by donor class II HLA-DR. To study the relationship between anti-HLA-A2 responses and GvHD, we created a humanized mouse model of GvHD whereby donor HLA-DRB*0401^{+} cells were transplanted into irradiated HLA-A2.1^{+} recipients. Recipient mice developed significant inflammation and fibrosis within the lungs, skin, and liver as early as 60 days post-transplant. Measurement of airway physiology revealed increased total airway resistance and reduced compliance (indicative of fibrotic remodeling) in mice receiving allogeneic transplants. Increased collagen deposition and loss of subcutaneous fat were observed in skin tissue. Perivascular fibrosis was observed in liver tissues together with evidence of excess lipid deposition. We conclude that donor immune response to the HLA-A2 molecule alone is sufficient to induce multiorgan GvHD.

Introduction

Transplantation of allogeneic stem cells is used to treat bone marrow malignancies such as myeloid or lymphoid leukemia. Allogeneic lymphocytes within the donor cell population recognize cancer-associated and/or specific antigens in the recipient and cause the destruction of the cancer cells in a process known as the graft vs leukemia effect [1]. However, an unwanted side effect of this therapy is graft vs host disease (GvHD); whereby donor lymphocytes also recognize mismatched minor or major histocompatibility antigens [2,3] (MHC or miHC) on healthy recipient tissues and initiate inflammatory and fibrotic responses.

The processes that lead to the initiation of GvHD begin with the conditioning regiment. Total body irradiation and chemotherapy drugs are used to destroy rapidly dividing cancer cells but collateral damage to healthy tissue also occurs, activating the host immune system in the process. Tissue-resident macrophages and dendritic cells recognize these products [4,5] and release pro-inflammatory cytokines (IL-1, TNF-α, IFN-γ). As donor stem cells are infused into the patient, donor macrophages [6] and DC [7] are activated by the proinflammatory environment and migrate into peripheral tissues to acquire host antigens from host tissues. Concurrently, donor lymphocytes migrate into secondary lymphoid organs [8] where they are activated by host APCs through direct antigen presentation [7] and non-cognate pro-inflammatory cytokine stimulation [9], however as these APCs are replaced by donor APCs, indirect antigen presentation of recipient alloantigens occurs [10]. MHC or the human leukocyte antigens (HLA) are the dominant alloantigens in

transplantation; mismatches between donor and recipient leads to severe GvHD [3] such that these genes are matched first in both HSCT and solid organ transplantation [11]. The HLA locus contains three class I molecules (HLA-A/B/C) and three class II molecules (HLA-DR/DP/DQ) involved in antigen presentation. Each of these molecules has multiple alleles in the population with each individual containing a unique MHC haplotype [12]. In a retrospective study of 1298 bone marrow transplant recipients, development of cGvHD was linked to mismatches within class I HLA-A/B molecules [13]. Furthermore, Hanvesakul et al., [14] have shown that 15 amino acids peptides derived from class I HLA-A2 and restricted by HLA-DR, can stimulate CD4+ T cells. These peptides were also shown to have a strong binding affinity for multiple class II HLA-DR molecules (HLA-DR1-4) [14]. Subsequent analysis of 21 patients with cGvHD revealed 13 patients formed responses against HLA-A2 derived peptides [15] suggesting that anti-HLA-A2 responses may play a role in GvHD.

To study the relationship between anti-HLA-A2 responses and GvHD, herein we describe the creation of a novel humanized model of murine GvHD in which the HLA-A2 molecule constitutes a major histocompatibility mismatch. We transplanted donor mice expressing human class II HLA-DRB1*0401, but not endogenous mouse class II (HLA-DR4 mice), into recipient mice expressing human class I HLA-A2.1 (HLA-A2 mice) such that donor lymphocytes would be indirectly presented HLA-A2 derived peptides in the context of donor class II HLA-DR4^{+} APC. Examination of these mice at 60 days post-transplantation revealed significant lung inflammation and early stages of fibrosis within

the skin and liver tissues. In contrast, irradiated recipient mice reconstituted with syngeneic donor cells did not develop GvHD.

Methods

Humanized Model of GvHD

Six-eight week-old female C57BL/6-Tg(HLA-A2.1)1Enge/J mice [16] (Jackson Laboratory) (HLA-A2 mice) were irradiated with 750 RADs and reconstituted with $5x10^5$ red blood cell (RBC)-free spleen cells and $5x10^5$ RBC-free bone marrow (BM) cells from female B6.129S2-*H2-Ab1*^{tm1Gru} Tg(HLA-DRA/H2-Ea,HLA-DRB1*0401/H2-Eb)1Kito [17] (Taconic) (HLA-DR4 mice).

Spleen cells were prepared by rupturing the spleen in cold PBS and filtering the cells through a 40 μm cell strainer, while BM was recovered by crushing the femur and tibia bones in a mortar and pestle and then filtering the suspension through a 40 μm cell strainer. Red blood cells in the BM and spleens cells were lysed using Ammonium Chloride Potassium (ACK) lysis buffer. The BM and spleen cells were then washed twice with PBS, mixed to achieve desired cell concentrations and injected retro-orbitally (RO) into recipient mice under gaseous isoflurane anesthesia. The recipient mice were housed in ultraclean level 2 facilities at the Central Animal Facility (McMaster University). On day 60 (selected as an optimal time point to observe elements of inflammation and fibrosis based on a related model of GvHD we have studied; data not shown) post-transplant, mice were euthanized to assess airway physiological, and morphological

changes within the lungs, skin, kidney, and liver. HLA-A2 mice were injected with saline or C57BL/6 mice were reconstituted with syngeneic cells as controls.

Assessing Engraftment of donor cells.

On day 60 post-transplant, spleen cells were harvested from the recipient mice to assess donor cell engraftment. The spleen was physically ruptured to release lymphoid cells and washed twice with PBS. ACK buffer was used to lyse the red blood cells. Remaining cells were suspended in staining buffer (Biolegend Cat# 420201), blocked with rat anti-mouse CD16/CD32 (BD Pharmingen Cat# 553141) and stained with PE anti-mouse CD4 (BD Pharmingen Cat# 553049) and PerCP anti-mouse CD8a (BD Biosciences Cat# 553036), FITC anti-mouse CD19 (Biolegend Cat#115505), Alexa Flour 647 anti-human HLA-DR (Biolgened Cat#307622) and APC-Cy7 anti-mouse CD11b (BD Biosciences Cat# 557657). Stained cells were captured on a BD FACS Canto cell analyzer (BD Biosciences) and were analyzed using Flowjo 10 software (Flowjo. LLC)

Assessment of Airway physiology

On day 60 post-transplant, mice were intraperitoneally injected (IP) with xylazine hydrochloride (10 mg/kg) for sedation followed by an IP injection of sodium pentobarbital (30 mg/kg) for anesthesia. The mice were subsequently tracheotomized and cannulated with a 19-gauge blunted needle and IP injected with pancuronium bromide (20 mg/kg) to inhibit respiratory effort. Each mouse was attached to a rodent mechanical

ventilator (Flexivent, SCIREQ) and ventilated at a rate of 150 breaths per minute (10 ml/kg). Forced oscillation waveform maneuvers were applied and the changes in airflow, volume, and pressure within the airways were recorded. The raw data was fit to the single compartment model to assess total airway resistance (R), and the constant phase model to assess parameters associated with conducting airway resistance (Rn), tissue resistance (G) and tissue elastance (H), and the *Salazar-Knowles equation* to assess quasi-static compliance (CST) [18,19].

Histology

Ten percent formalin was used to inflate the left lung of each mouse at a pressure of 20 cmH_20 followed by 48 hours fixation in formalin. The dorsal skin was shaved and excised, the skin was then spread onto a piece of tissue paper to maintain shape and placed into formalin. The right kidney and one lobe of the liver were directly placed into formalin. All the tissues were fixed for 48 hours and then dissected. The lung and liver lobe were dissected into a superior, middle and inferior section, the kidney was cut into 2 halves and the skin was cut into rectangular strips. The processed tissues were embedded in paraffin wax and cut into 4 µm sections for staining with hematoxylin and eosin (H&E) and Masson's trichrome blue. Whole tissue sections images were then scanned at 200x resolution using an Olympus VSI 120 microscope system (Olympus).

Quantification of Fibrosis

Collagen deposition in the tissues sections was quantified from Masson's trichrome blue stained sections. Each entire tissue section from the corresponding organs was selected using Photoshop CC (Adobe) and the background was masked out in black. The masked images were then imported into Fiji ImageJ and a script was used to calculate the entire tissue area. A second script was then used to selectively highlight and measure the trichrome stained blue areas (Hue 110-220, Saturation 20-255, Brightness 0-255). The blue stained area was divided by the total lung area to determine the total blue stained area of each tissue section. To calculate perivascular fibrosis of the liver, the band of tissue from the inner lumen of the blood vessel to the tissue parenchyma was similarly selected in photoshop and the liver parenchyma and blood vessel lumen were masked out. To calculate collagen staining of the skin, a band of tissue encompassing the area between the epidermis-dermis border to the border between the subcutaneous and muscle layer was selected. The two scripts were then used to calculate the area and blue stained areas of the selected tissues.

Analysis of Perivascular Infiltration

To assess perivascular infiltration, H&E stained lung tissue images were loaded into Photoshop (Adobe) and each blood vessel and surrounding perivascular area was selected. The parenchyma and blood vessel were masked out. Two Fiji ImageJ scripts were then used to calculate the area and dark staining nuclei within the selected

perivascular areas. Endothelial cells were excluded by setting a circularity threshold of 0.5. The total cell count was then divided by the area of the perivascular to assess the number of cells/um^2 of perivascular tissue.

Statistics

To analyze the data, a one-way ANOVA with a Dunnett's multiple comparisons test was used to compare the means of syngeneic and saline groups against the mean of the allogeneic transplant group. Each bar in the graphs is represented as ± SEM; A p-value of less than or equal to 0.05 was considered significant.

Study approval

The study and associated procedures were approved by the McMaster University animal research ethics board (AREB). Mice were housed in ultraclean level 2 facilities at McMaster University central animal facility, Hamilton Ontario Canada.

Results

HLA-DR4$^+$ donor cells engraft into the spleens of irradiated HLA-A2$^+$ recipient mice

To assess donor cell engraftment into recipient host tissues, HLA-A2 recipient mice were euthanized on day 60 post-transplant and the spleens were harvested for analysis of donor cells. The spleens were prepared into a single cell suspension and stained with anti-mouse CD4, CD8, CD19, CD11b, and anti-human HLA-DR. HLA-DR+ CD4, CD8, CD19 and CD11b+ donor cells **(Figure 1A)** were detectable in spleen at study endpoint. More than 60% of all CD4+ cells **(Figure 1B)**, 50% of CD8+ **(Figure 1C)**, 85% of CD19+ **(Figure 1D)** and 20% of CD11b+ **(Figure 1E)** cells stained positive for HLA-DR**.** In contrast, cells from mice reconstituted with HLA-DR4$^-$ syngeneic donor cells or saline did not stain positive for HLA-DR. These data confirm that allogeneic HLA-DR4$^+$ donor cells successfully engrafted into the recipient HLA-A2$^+$, HLA-DR4$^-$ mice.

Increased inflammation in the lungs of irradiated HLA-A2$^+$ mice reconstituted with allogeneic HLA-DR4$^+$ donor Cells

Mice reconstituted with allogeneic HLA-DR4$^+$ donor cells had increased recruitment of inflammatory cells into the perivascular areas of the lungs and parenchymal tissue. Whole H&E stained lung tissue sections from day 60 post-transplant recipient mice were captured on a slide scanning microscope (Olympus VS120). Irradiated HLA-A2$^+$ recipient mice reconstituted with allogeneic HLA-DR4$^+$ donor cells had significantly

increased recruitment of inflammatory cells into the perivascular areas of the lung **(Figure 2A)** compared to mice reconstituted syngeneic cells (**Figure 2B**), or mice administered saline only **(Figure 2C)**. The number of recruited inflammatory cells in the perivascular area from each blood vessel was enumerated using Fiji ImageJ and represented as the number of cells/area (um^2) of perivascular tissue **(Figure 2D).** Mice reconstituted with allogeneic cells had significantly increased perivascular inflammation compared to the control groups, whereas there was no difference between the syngeneic transplant and saline control groups.

Histological analysis of the whole lung tissue sections revealed that mice reconstituted with allogeneic HLA-DR4$^+$ donor cells also had substantial inflammation within the lung parenchyma **(Figure 3A**) whereas there was no inflammation in mice reconstituted with syngeneic donor cells (**Figure 3B**) or saline (**Figure 3C**). The left lung lobe from each mouse was fixed and cut into 3 sections (superior, middle & inferior). Six of nine mice reconstituted with allogeneic donor cells had parenchymal inflammation in at least one of the three lung sections whereas no mice from either control group displayed parenchymal inflammation (**Figure 3D**). Together, these data indicate that the observed phenotype of perivascular and parenchymal inflammation in this model was restricted to recipients that received allogeneic HLA-DR4 expressing donor cells.

Irradiated HLA-A2$^+$ mice reconstituted with allogeneic HLA-DR4$^+$ donor cells display increased tissue resistance

Irradiated HLA-A2$^+$ mice reconstituted with allogeneic HLA-DR4$^+$ donor cells displayed increased tissue resistance compared to mice reconstituted with syngeneic donor cells or saline. To determine the physiological impact on lung mechanics following transplant of bone marrow and spleen cells, we used a rodent mechanical ventilator on day 60 post-transplant to assess lung function. The ventilator applied forced oscillation waveforms and recorded the subsequent changes in flow, volume, and pressure within the lungs. There was no difference in total airway resistance, tissue resistance, or conducting airway resistance between the mice reconstituted with syngeneic donor cells and saline. There was, however, a significant difference in total airway resistance between mice reconstituted with allogeneic donor cells and the two control groups (**Figure 4A**). Segmentation of the data revealed this was localized to changes in the tissue parenchyma as there was a difference in tissue resistance between the allogeneic and syngeneic transplant groups **(Figure 4 B),** but there was no significant difference in the resistance within the conducting airways of any experimental group **(Figure 4C)**.

Irradiated HLA-A2$^+$ mice reconstituted with allogeneic HLA-DR4$^+$ cells display decreased lung compliance

Lung compliance was assessed using mechanical ventilation. Lungs were inflated in 8 consecutive steps of increasing pressure to a maximum of 30 cm of H_2O. At each step, the corresponding volume of inflated air was recorded. Pressure-volume data was plotted as a Pressure-Volume (PV) loop. A relatively small increase in the volume of inflated air for

each step of applied pressure indicates that the lung is stiffer and more "fibrotic" and has a corresponding low lung compliance. This can be observed as a downward shift in the PV loop. The PV loop for the syngeneic and saline groups was similar, while the loop for the allogeneic transplant group was shifted markedly downward **(Figure 4D)**. The expiratory branch of the PV loop was fitted to the *Salazar-Knowles equation* [18] *to determine the quasi-static compliance. Analysis of the quasi-static compliance data revealed no difference between the control groups, but a significant difference between the groups reconstituted with allogeneic donor cells and syngeneic cells* ***(Figure 4E)****. Thus, mice receiving allogeneic transplants had significantly stiffer lungs than controls. We next examined tissue elastance using the constant phase model* [18], we observed a non-significant increase in tissue elastance in mice reconstituted with allogeneic cells compared to the control groups **(Figure 4F)**.

Irradiated HLA-A2$^+$ mice reconstituted with HLA-DR4$^+$ allogeneic donor cells display increased skin and liver fibrosis

Irradiated HLA-A2$^+$ mice reconstituted with allogeneic HLA-DR4$^+$ donor cells display increased deposition of collagen in the skin dermis and perivascular areas of the liver. To assess the impact of allogeneic stem cell transplant on tissue fibrosis in our model, we analyzed Masson's trichrome staining of collagen in the lung, kidney, skin, and liver. We did not observe any difference in trichrome staining within lung or kidney tissues between any of the groups (data not shown). Within the skin, we analyzed collagen content in the band of tissue stretching from the epidermis to the skeletal muscle. In mice

reconstituted with allogeneic HLA-DR4^{+} donor cells, the subcutaneous layer was absent and replaced with collagen **(Figure 5A)**. In contrast, the subcutaneous layer in the syngeneic transplant **(Figure 5B)** and saline groups **(Figure 5C)** remained intact. Furthermore, the intensity of Masson's trichrome staining in mice reconstituted with allogeneic HLA-DR4^{+} donor cells was increased; quantification of the staining revealed that skin collagen content in these mice was significantly greater than mice reconstituted with syngeneic donor cells, or saline, while there was no difference between the two control groups **(Figure 5D)**.

Analysis of trichrome staining in the liver revealed no difference in total collagen content between mice reconstituted with allogeneic donor cells and mice reconstituted with syngeneic donor cells or saline (data not shown). However, high-resolution analysis of liver revealed collagen staining was primarily localized around the blood vessels in the perivascular areas **(Figure 6A-C)**. Quantification trichrome staining in the perivascular areas revealed significantly increased collagen content in mice reconstituted with allogeneic HLA-DR4^{+} compared to mice reconstituted with syngeneic donor cells, or saline **(Figure 6D)**

Discussion

We have previously reported that bone marrow transplant patients with cGvHD generated T-cell responses to HLA-A2 derived peptides [15] and T-cell responses to these peptides are HLA-DR restricted [14], suggesting that HLA-A2 may be playing a dominant role as an antigen in GvHD. To the study the impact of anti-HLA-A2 immune responses on the initiation of GvHD, we reconstituted irradiated HLA-$A2^+$ mice with donor HLA-$DR4^+$ cells.

Donor mice expressing human class II HLA-$DRB1^*$0401 were generated by others by ligating the binding domains of human HLA-DRA and HLA-DRB1*0401 to the membrane proximal domains of mouse H2-E. The hybrid construct was injected into fertilized C57BL/6 eggs and the resulting offspring were bred with MHC class II-deficient mice (Abb knockout on B6 background) to produce mice which only express the hybrid HLA-H2-E molecule while retaining the same peptide binding specificity as native HLA-DRB1*0401 molecule [17,20]. Recipient mice expressing human class I HLA-A2.1 were created by others by injecting the class I molecule into fertilized C57BL/6 oocytes. Mice homozygous for HLA-A2.1 express similar levels of the human class I molecules to the endogenous mouse H-2D class I molecule [21].

We anticipated that transplantation of HLA-$DR4^+$ donor cells into irradiated HLA-$A2^+$ mice would result in anti-HLA-A2 T cell responses restricted by HLA-DR4, leading to the development of GvHD in recipient mice. However, the use of total body irradiation

can also cause significant damage to the recipient mice. Within the lungs, radiation causes DNA, alveolar and blood vessel damage, additional damage is also caused by reactive oxygen/nitrogen species and pro-inflammatory cytokines TNF-α and IL-1 released from tissue-resident macrophages and damaged cells. Together these processes lead to pulmonary edema [22] and inflammation [23]. The release of chemotactic factors (TGF- β, PDGF- β, IGF-1, and MCP-1) from macrophages recruits fibroblasts which are subsequently converted into collagen-secreting myofibroblasts culminating in lung fibrosis [24]. A similar process of DNA damage, reactive oxygen/nitrogen species, inflammation, and fibrosis also occur in the skin, liver, and kidney [25]. To control for this aspect of tissue damage we used irradiated mice reconstituted with syngeneic donor cells as a control. We additionally employed a second control group of mice administered saline only, to account for natural structural changes within the mice as they aged from 0-60 days post-transplant.

Following reconstitution of donor cells into irradiated mice, engraftment has been reported to occur between day 7 and 21 post-transplant[5]. We examined the transplanted mice at 60 days post-transplant (based on observations we have made in a related model of GvHD, data not shown) for signs of inflammation, and fibrosis. Indeed, examination of the spleens from recipient mice reconstituted with allogeneic HLA-DR4^{+} donor cells at 60 days post-transplant, revealed that DR+ CD4, CD8, CD19, and CD11b cells were all present and engrafted.

Within the lung tissue, we observed significant recruitment of inflammatory cells into the perivascular areas, as well inflammation within the parenchymal tissue in six of nine mice. Importantly, only three slices of lung tissue were sampled per mouse, therefore we cannot rule out the possibility of inflammatory foci within the unsampled areas from the three "unaffected" mice reconstituted with allogeneic HLA-DR4+ donor cells. In comparison to the allogeneic transplant group, we observed less perivascular inflammation in mice reconstituted with syngeneic donor cells or administered saline. Furthermore, there was no parenchymal inflammation within these control groups, indicating that post-transplant inflammation was caused by the allogeneic HLA-DR4^{+} donor cells and not post radiation inflammation. We next assessed the development of fibrosis within the lungs. Masson's trichrome stained whole lung sections were quantified with Fiji ImageJ software for blue-staining collagen. We did not observe any difference in collagen staining between mice reconstituted with allogeneic or syngeneic donor cells, or saline. Fibrosis is most frequently detected in the aftermath of inflammatory responses. Therefore, the observed increase in perivascular inflammatory infiltrates in allogeneic transplants may indicate that the day 60 observation point in this cross-sectional study was too early to detect fibrosis in the lung.

We next assessed the impact of allogeneic bone marrow and spleen transplant on the functional status of the lung. Using a rodent ventilator, we assessed total airway resistance (R) using the single compartment model [18]. We observed increased lung resistance within the mice reconstituted with allogeneic donor cells, but not those mice reconstituted with syngeneic donor cells or administered saline. To delineate the source of

increased resistance, the constant phase model was utilized to determine the resistance in the conducting airways (Rn) vs tissue resistance (H). While we did not observe any differences in conducting airway resistance between any of the experimental groups, we did observe a difference in tissue resistance between the allogeneic and syngeneic transplant groups. Increases in tissue resistance can be caused by interstitial fibrosis or liquid bridging from inflammation-induced pulmonary edema [19,26]. As there was no evidence of fibrosis, we hypothesize that differences in resistance were likely due to inflammation, and not lung fibrosis. As inflammation induced liquid bridging can also influence tissue elastance (H), the observed non-significant increase in tissue elastance within the allogeneic transplant group may also have been related to pulmonary edema, and not lung fibrosis. It is of note that collection of pulmonary function tests was conducted on the ventilator while the thoracic cavity remained closed and intact, such that the value collected for the quasi-static compliance would be influenced by the elastic recoil forces of both the alveoli and the elastic recoil forces of the chest wall [27] including the skin. As we observed increased staining of collagen within the skin of mice reconstituted with allogeneic donor cells, compared to mice reconstituted with syngeneic donor cells, or mice administered saline, it is possible that skin fibrosis contributed to the observed increase in quasi-static compliance within the allogeneic transplant group, particularly as there was no indication of lung fibrosis.

Looking at the kidney we did not observe any indications of inflammation or differences in collagen deposition between the three experimental groups (data not shown). We did,

however, observe increased perivascular collagen staining within the liver tissues of mice reconstituted with allogeneic donor cells.

Following transplantation, we hypothesis that donor CD8+ T cell would generate responses against miHC antigen peptides, and HLA-A2 derived peptides, presented to CD8+ T cells in the context of HLA-A2. Furthermore, we anticipate that CD4+ T cells would generate responses against HLA-A2-derived peptides presented to CD4+ T cells in the context of HLA-DR4. However, as we did not observe the full reconstitution of donor cells, the presence of recipient APCs may have increased the number of possible donor T-cell: peptide: HLA/MHC interactions. As recipient APCs primarily activate donor lymphocytes in the early stages of disease [28], donor CD8+ T cells may also have generated responses against mouse class II peptides (present in recipients) in the context of mouse class I H2-D and human class I HLA-A2 on recipient APCs. Additionally, donor CD4+ T cells may have generated responses against miHC, HLA-A2, and mouse MHC II-derived peptides in the context of mouse class II I-A^{b} on recipient APCs.

In conclusion, transplantation of HLA-DR4+ hematopoietic cells into irradiated HLA-A2.1+ recipient mice led to the development of GvHD. At day 60 post-allogeneic transplant, we observed perivascular and parenchymal inflammatory changes in the lung that were associated with detrimental changes in airway physiology. Perivascular fibrosis with little inflammation was observed in the liver and marked fibrosis and loss of subcutaneous tissue were observed in the skin. Due to the presence of murine MHC class II in recipient (but not donor) mice in addition to HLA-A2, we cannot yet be certain of the relative contributions of HLA-A2 and H2 to the observed disease outcomes.

Acknowledgments.

We thank the central animal facility (McMaster University, ON, Canada) for their exceptional care and monitoring of the mice and the core histology facility for their staining services. We thank Dr. Kjetil Ask for use of the VSI 120 microscope system. We thank the members of the Larché lab for their continued guidance and support. This work was performed and funded by the generous support of the Scleroderma Society of Ontario

Authorship Contributions: Conception and design of study: JI, MI, MK, PM, STB and ML; Conducted experiments: JI, JW; Analysis and interpretations of Data: JI, JW, MI, MK, PM, STB and ML; Drafting the manuscript: JI; Edited and revised manuscript: JI, MI, MK, PM, STB and ML. All authors read and approved the final version.

Conflicts of interest: No conflicts of interests are declared

References

1. Kolb HJ. Graft-versus-leukemia effects of transplantation and donor lymphocytes. *Blood*. 2008;112(12):4371-4383.
2. Spierings E. Minor histocompatibility antigens: past, present, and future. *Tissue Antigens*. 2014;84(4):374-360.
3. Warren EH, Zhang XC, Li S, et al. Effect of MHC and non-MHC donor/recipient genetic disparity on the outcome of allogeneic HCT. *Blood*. 2012;120(14):2796-2806.
4. Doe WF. The intestinal immune system. *Gut*. 1989;30(12):1679-1685.
5. Duran-Struuck R, Dysko RC. Principles of bone marrow transplantation (BMT): providing optimal veterinary and husbandry care to irradiated mice in BMT studies. *J Am Assoc Lab Anim Sci*. 2009;48(1):11-22.
6. Alexander KA, Flynn R, Lineburg KE, et al. CSF-1-dependant donor-derived macrophages mediate chronic graft-versus-host disease. *J Clin Invest*. 2014;124(10):4266-4280.
7. Markey KA, Banovic T, Kuns RD, et al. Conventional dendritic cells are the critical donor APC presenting alloantigen after experimental bone marrow transplantation. *Blood*. 2009;113(22):5644-5649.
8. Wysocki CA, Panoskaltsis-Mortari A, Blazar BR, Serody JS. Leukocyte migration and graft-versus-host disease. *Blood*. 2005;105(11):4191-4199.
9. Ferrara JL, Abhyankar S, Gilliland DG. Cytokine storm of graft-versus-host disease: a critical effector role for interleukin-1. *Transplant Proc*. 1993;25(1 Pt 2):1216-1217.
10. Wang X, Li H, Matte-Martone C, et al. Mechanisms of antigen presentation to T cells in murine graft-versus-host disease: cross-presentation and the appearance of cross-presentation. *Blood*. 2011;118(24):6426-6437.
11. Lennard AL, Jackson GH. Stem cell transplantation. *Bmj*. 2000;321(7258):433-437.
12. Choo SY. The HLA system: genetics, immunology, clinical testing, and clinical implications. *Yonsei Med J*. 2007;48(1):11-23.
13. Morishima Y, Sasazuki T, Inoko H, et al. The clinical significance of human leukocyte antigen (HLA) allele compatibility in patients receiving a marrow transplant from serologically HLA-A, HLA-B, and HLA-DR matched unrelated donors. *Blood*. 2002;99(11):4200-4206.
14. Hanvesakul R, Maillere B, Briggs D, Baker R, Larche M, Ball S. Indirect recognition of T-cell epitopes derived from the alpha 3 and transmembrane domain of HLA-A2. *Am J Transplant*. 2007;7(5):1148-1157.
15. Smith HJ, Hanvesakul R, Morgan MD, et al. Chronic graft versus host disease is associated with an immune response to autologous human leukocyte antigen-derived peptides. *Transplantation*. 2010;90(5):555-563.
16. Kaplan DH, Anderson BE, McNiff JM, Jain D, Shlomchik MJ, Shlomchik WD. Target antigens determine graft-versus-host disease phenotype. *J Immunol*. 2004;173(9):5467-5475.
17. Ito K, Bian HJ, Molina M, et al. HLA-DR4-IE chimeric class II transgenic, murine class II-deficient mice are susceptible to experimental allergic encephalomyelitis. *J Exp Med*. 1996;183(6):2635-2644.
18. Irvin CG, Bates JHT. Measuring the lung function in the mouse: the challenge of size. *Respiratory Research*. 2003;4(1):4-4.
19. Hantos Z, Daroczy B, Suki B, Nagy S, Fredberg JJ. Input impedance and peripheral inhomogeneity of dog lungs. *J Appl Physiol (1985)*. 1992;72(1):168-178.

20. Grusby MJ, Johnson RS, Papaioannou VE, Glimcher LH. Depletion of CD4+ T cells in major histocompatibility complex class II-deficient mice. *Science*. 1991;253(5026):1417-1420.
21. Le AX, Bernhard EJ, Holterman MJ, et al. Cytotoxic T cell responses in HLA-A2.1 transgenic mice. Recognition of HLA alloantigens and utilization of HLA-A2.1 as a restriction element. *J Immunol*. 1989;142(4):1366-1371.
22. Ghafoori P, Marks LB, Vujaskovic Z, Kelsey CR. Radiation-induced lung injury. Assessment, management, and prevention. *Oncology (Williston Park)*. 2008;22(1):37-47; discussion 52-33.
23. Giridhar P, Mallick S, Rath GK, Julka PK. Radiation induced lung injury: prediction, assessment and management. *Asian Pac J Cancer Prev*. 2015;16(7):2613-2617.
24. Morgan GW, Breit SN. Radiation and the lung: a reevaluation of the mechanisms mediating pulmonary injury. *Int J Radiat Oncol Biol Phys*. 1995;31(2):361-369.
25. Straub JM, New J, Hamilton CD, Lominska C, Shnayder Y, Thomas SM. Radiation-induced fibrosis: mechanisms and implications for therapy. *Journal of cancer research and clinical oncology*. 2015;141(11):1985-1994.
26. Wagers S, Lundblad LK, Ekman M, Irvin CG, Bates JH. The allergic mouse model of asthma: normal smooth muscle in an abnormal lung? *J Appl Physiol (1985)*. 2004;96(6):2019-2027.
27. Mitzner W. MECHANICS OF THE LUNG IN THE 20(TH) CENTURY. *Comprehensive Physiology*. 2011;1(4):2009-2027.
28. Matte CC, Liu J, Cormier J, et al. Donor APCs are required for maximal GVHD but not for GVL. *Nat Med*. 2004;10(9):987-992.

Figure Legends

Figure 1. HLA-DR4 donor cells engraft into the spleens of irradiated HLA-A2

Allogeneic transplant: Irradiated C57BL/6(HLA-A2.1) mice were reconstituted with $5x10^5$ spleen and $5x10^5$ bone marrow cells from allogeneic B6.129S2-*H2-Ab1*^{tm1Gru} Tg(HLA-DRA/H2-Ea, HLA-DRB1*0401/H2-Eb)1Kito mice. Syngeneic transplant: Irradiated C57BL/6 mice were reconstituted with the same numbers of syngeneic donor cells. Saline controls: C57BL/6 mice were administered saline without prior irradiation. The spleens of the recipient HLA-DR4$^-$ mice were collected at 60 days post-transplant and stained with anti-CD4, CD8, CD19, CD11b, and HLA-DR antibodies. **(A)** Representative flowjo gating strategy for assessing HLA-DR staining within the CD4+, CD8+, CD19+, and CD11b+. Percentage of HLA-DR+ stained CD4+**(B)**, CD8+**(C)**, CD19+**(D)** and CD11b+**(E)** spleen cells from HLA-DR4$^-$ mice reconstituted with allogeneic HLA-A2$^+$ donor cells (allogeneic transplant; n=4), syngeneic donor cells (syngeneic transplant; n=5) and mice administered saline only (saline control; n=5).

Figure 2. Increased perivascular inflammation in the lungs of irradiated HLA-A2 mice reconstituted with allogeneic HLA-DR4$^+$ donor cells

Allogeneic transplant: Irradiated C57BL/6(HLA-A2.1) mice were reconstituted with $5x10^5$ spleen and $5x10^5$ bone marrow cells from allogeneic B6.129S2-*H2-Ab1*^{tm1Gru} Tg(HLA-DRA/H2-Ea, HLA-DRB1*0401/H2-Eb)1Kito mice. Syngeneic transplant: Irradiated C57BL/6 mice were reconstituted with the same numbers of syngeneic donor

cells. Saline controls: C57BL/6 mice were administered saline without prior irradiation. Whole lung tissue sections were stained with H&E; each blood vessel area was cropped out and the number of recruited inflammatory cells within the perivascular areas was quantified using Fiji ImageJ. Each experiment was conducted twice and data were pooled together. Allogeneic transplant group (n=9), syngeneic transplant group (n=9), saline group (n=5). Representative blood vessels from mice reconstituted with **(A)** HLA-DR4^{+} donor cells, **(B)** HLA-DR4^{-} syngeneic donor cells and **(C)** mice administered saline. **(D)** Significant perivascular infiltration (cells/perivascular area μm^2) was observed within the allogeneic transplant group compared to the syngeneic transplant and saline groups. Data were analyzed using a one-way ANOVA with a Dunnett's multiple comparisons test to compare the means of each group against the mean of the allogeneic transplant group and represented as +/- SEM; ***p≤*0.0005.*

Figure 3. Lung parenchymal inflammation is only present in the lungs of irradiated recipient mice reconstituted with allogeneic HLA-DR4^{+} donor cells

Allogeneic transplant: Irradiated C57BL/6(HLA-A2.1) mice were reconstituted with 5x10^5 spleen and 5x10^5 bone marrow cells from allogeneic B6.129S2-*H2-Ab1^{tm1Gru}* Tg(HLA-DRA/H2-Ea, HLA-DRB1*0401/H2-Eb)1Kito mice. Syngeneic transplant: Irradiated C57BL/6 mice were reconstituted with the same numbers of syngeneic donor cells. Saline controls: C57BL/6 mice were administered saline without prior irradiation. Whole lung section tissues were stained with H&E and captured at 100x resolution using

an Olympus VS120 slide scanner. Each lung was visually examined for signs of parenchymal inflammation. Each experiment was conducted twice and data were pooled together. Allogeneic transplant group (n=9), syngeneic transplant group (n=9), saline group (n=5). Representative whole lung sections and three 1000x1000 pixel 100x resolution sections from mice reconstituted with **(A)** HLA-DR4^{+} donor cells, **(B)** HLA-DR4^{-} syngeneic donor cells and **(C)** mice administered saline. **(D)** six of nine mice reconstituted with allogeneic donor cells had parenchymal inflammation, whereas there was no inflammation in the two control groups.

Figure 4. Irradiated HLA-A2 Mice reconstituted with allogeneic HLA-DR4 donor cells have increased tissue resistance and decreased lung compliance

Allogeneic transplant: Irradiated C57BL/6(HLA-A2.1) mice were reconstituted with 5x10^{5} spleen and 5x10^{5} bone marrow cells from allogeneic B6.129S2-*H2-Ab1*^{tm1Gru} Tg(HLA-DRA/H2-Ea, HLA-DRB1*0401/H2-Eb)1Kito mice. Syngeneic transplant: Irradiated C57BL/6 mice were reconstituted with the same numbers of syngeneic donor cells. Saline controls: C57BL/6 mice were administered saline without prior irradiation. On day 60 post-transplant, a mechanical ventilator was used to assess pulmonary function from mice reconstituted with allogeneic HLA-DR4^{+} donor cells, syngeneic donor cells, and mice administered saline. Resistance measurements were collected from 9, 9 and 5 mice from each respective group, whereas compliance data was collected from 5,5 and 5 mice from each respective group. Mice reconstituted with allogeneic HLA-DR4^{+} donor cells displayed increased **(A)** total airway resistance compared to mice reconstituted with

syngeneic donor cells or saline. Mice reconstituted with allogeneic cells also displayed increased **(B)** tissue resistance compared to the syngeneic control, but not the saline group. Within the **(C)** conducting airways, there was no significant difference in resistance between any experimental group. **(D)** Pressure/volume (PV) loops were plotted from averaged values from each mouse in the group. A shift downward in the loop indicates a lung with decreased compliance. Plotting the **(E)** quasi-static compliance revealed that mice reconstituted with allogeneic donor cells displayed decreased lung compliance compared to the two control groups, however, this was not attributed to morphological changes into the parenchyma has there was no difference in **(F)** tissue elastance between any of the experimental groups. Data were analyzed using a one-way ANOVA with a Dunnett's multiple comparisons test to compare the means of each group against the mean of the allogeneic transplant group and represented as SEM; *p≤*0.05;* **p≤*0.005.*

Figure 5. Mice reconstituted with HLA-DR4^{+} allogeneic donor cells have increased skin fibrosis

Allogeneic transplant: Irradiated C57BL/6(HLA-A2.1) mice were reconstituted with $5x10^5$ spleen and $5x10^5$ bone marrow cells from allogeneic B6.129S2-*H2-Ab1*^{tm1Gru} Tg(HLA-DRA/H2-Ea, HLA-DRB1*0401/H2-Eb)1Kito mice. Syngeneic transplant: Irradiated C57BL/6 mice were reconstituted with the same numbers of syngeneic donor cells. Saline controls: C57BL/6 mice were administered saline without prior irradiation. Strips of dorsal neck skin were stained with Masson's trichrome; A band of tissue

encompassing space between the dermis and skeletal muscle (double-ended arrows) was selected for trichome analysis using Fiji ImageJ. Each experiment was conducted twice and data were pooled together. Allogeneic transplant group (n=9), syngeneic transplant group (n=9), saline group (n=5). Representative cross sections of skin tissue from mice reconstituted with **(A)** HLA-DR4^{+} donor cells, **(B)** HLA-DR4^{-} syngeneic donor cells and **(C)** mice administered saline. Double-ended black arrows denote the area of tissue analyzed. **(D)** Quantification of collagen staining revealed significant skin fibrosis within the allogeneic transplant group compared to the syngeneic transplant and saline groups. Data were analyzed using a one-way ANOVA with a Dunnett's multiple comparisons test to compare the means of each group against the mean of the allogeneic transplant group and represented as +/- SEM; **p≤*0.005*.

Figure 6. Mice reconstituted with HLA-DR4^{+} allogeneic donor cells have increased skin fibrosis

Allogeneic transplant: Irradiated C57BL/6(HLA-A2.1) mice were reconstituted with 5x10^{5} spleen and 5x10^{5} bone marrow cells from allogeneic B6.129S2-*H2-Ab1^{tm1Gru}* Tg(HLA-DRA/H2-Ea, HLA-DRB1*0401/H2-Eb)1Kito mice. Syngeneic transplant: Irradiated C57BL/6 mice were reconstituted with the same numbers of syngeneic donor cells. Saline controls: C57BL/6 mice were administered saline without prior irradiation. Whole liver tissue sections were stained with Masson's trichrome; each blood vessel area was cropped out and collagen staining within the perivascular areas was quantified using Fiji ImageJ. Each experiment was conducted twice and data were pooled together.

Allogeneic transplant group (n=9), syngeneic transplant group (n=9), saline group (n=5). Representative blood vessels from mice reconstituted with **(A)** HLA-DR4^{+} donor cells, **(B)** HLA-DR4^{-} syngeneic donor cells and **(C)** mice administered saline. **(D)** There is significant perivascular fibrosis within the allogeneic transplant group compared to the syngeneic transplant and saline groups. Data were analyzed using a one-way ANOVA with a Dunnett's multiple comparisons test to compare the means of each group against the mean of the allogeneic transplant group and represented as +/- SEM; **$p \leq 0.005$.

Figure 1

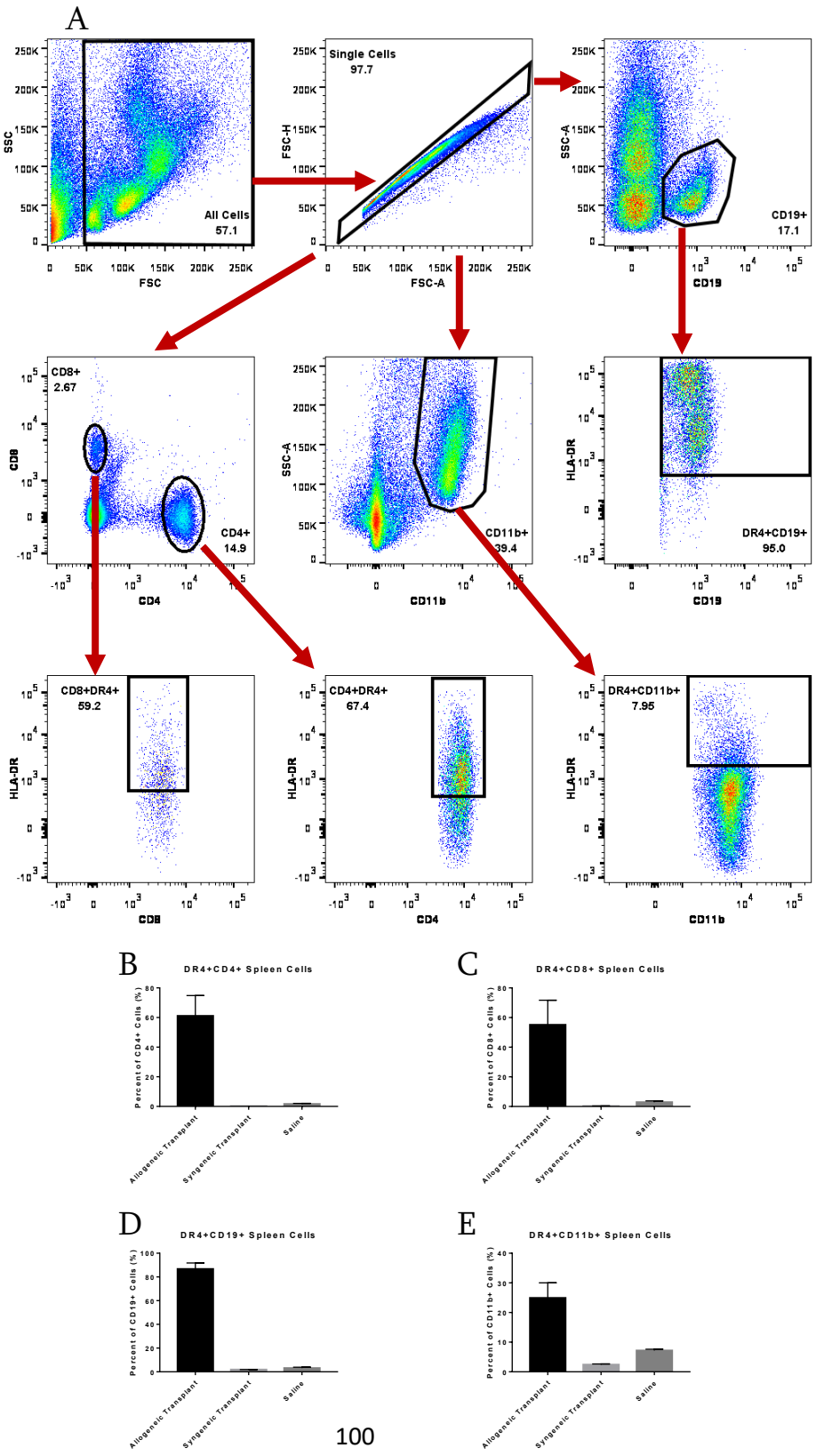
A
All Cells
57.1
Single Cells
97.7
CD19+
17.1
CD8+
2.67
CD4+
14.9
CD11b+
39.4
DR4+CD19+
95.0
CD8+DR4+
59.2
CD4+DR4+
67.4
DR4+CD11b+
7.95
B
DR4+CD4+ Spleen Cells
C
DR4+CD8+ Spleen Cells
D
DR4+CD19+ Spleen Cells
E
DR4+CD11b+ Spleen Cells
Allogeneic Transplant
Syngeneic Transplant
Saline

Figure 2

A

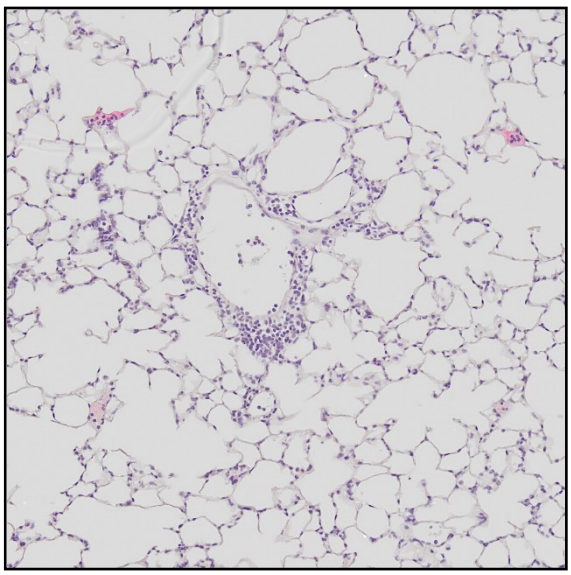

B

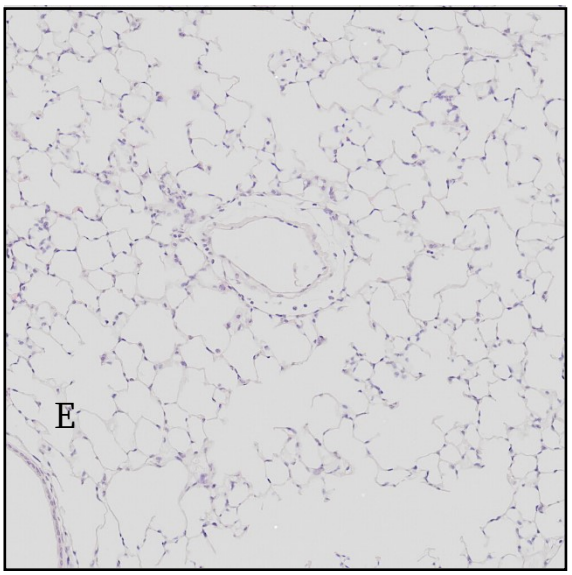

C

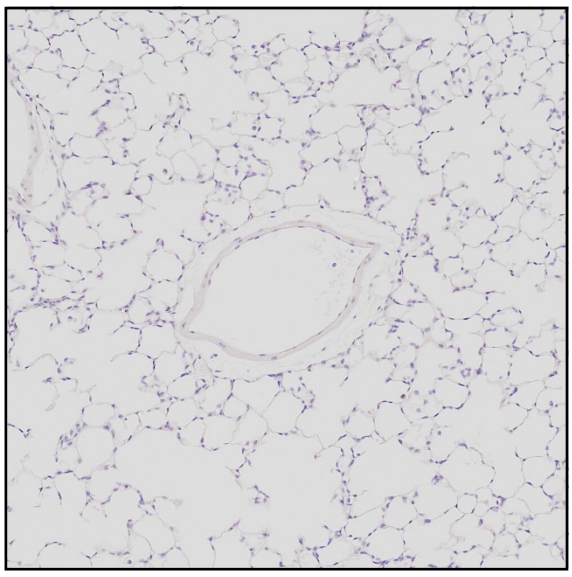

D

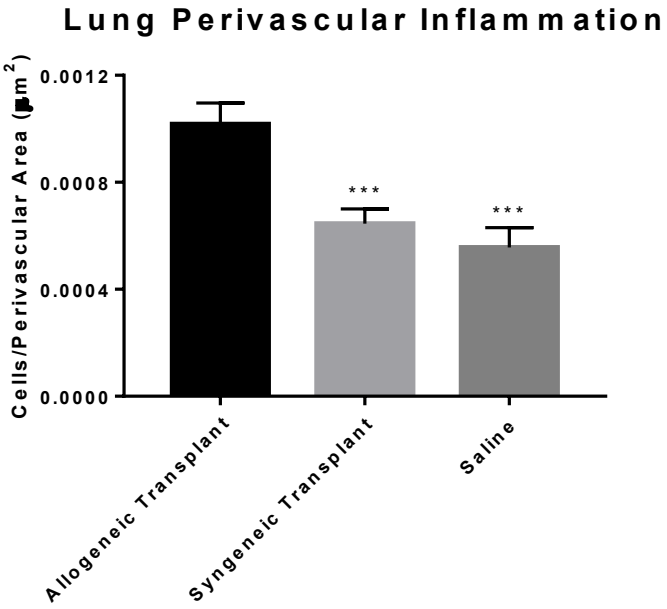

Figure 3

A

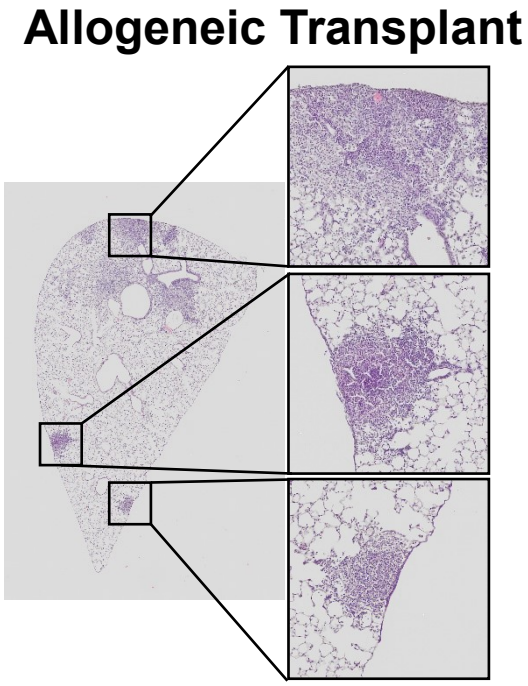

B

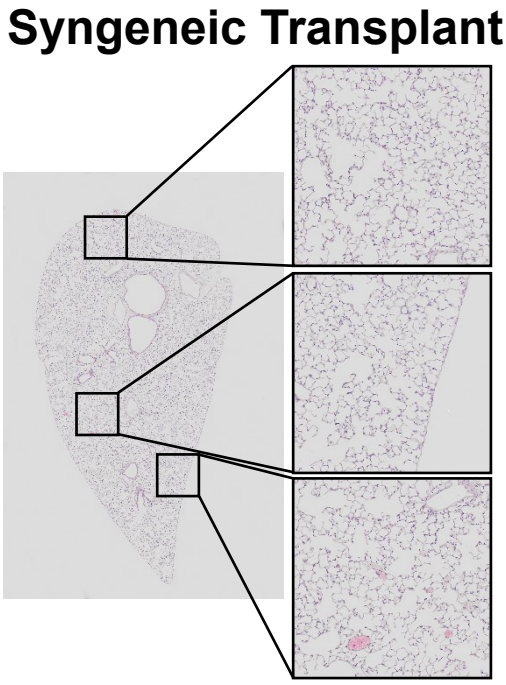

C

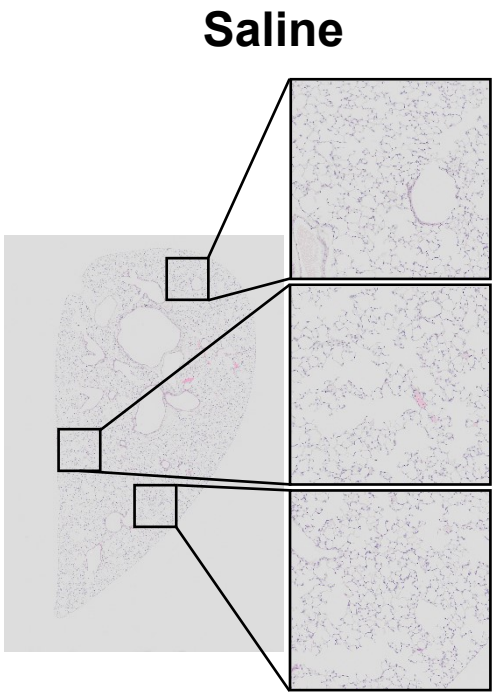

D

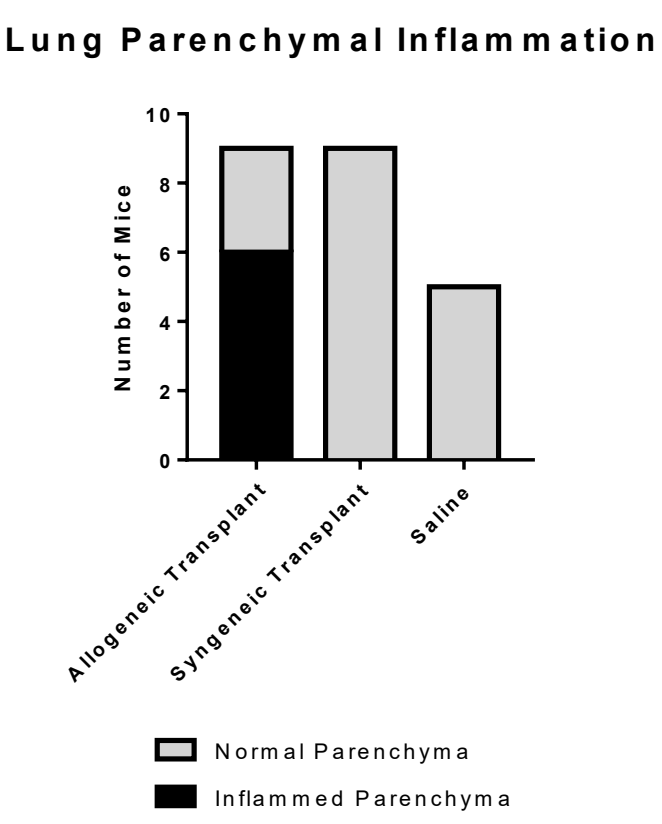

Figure 4

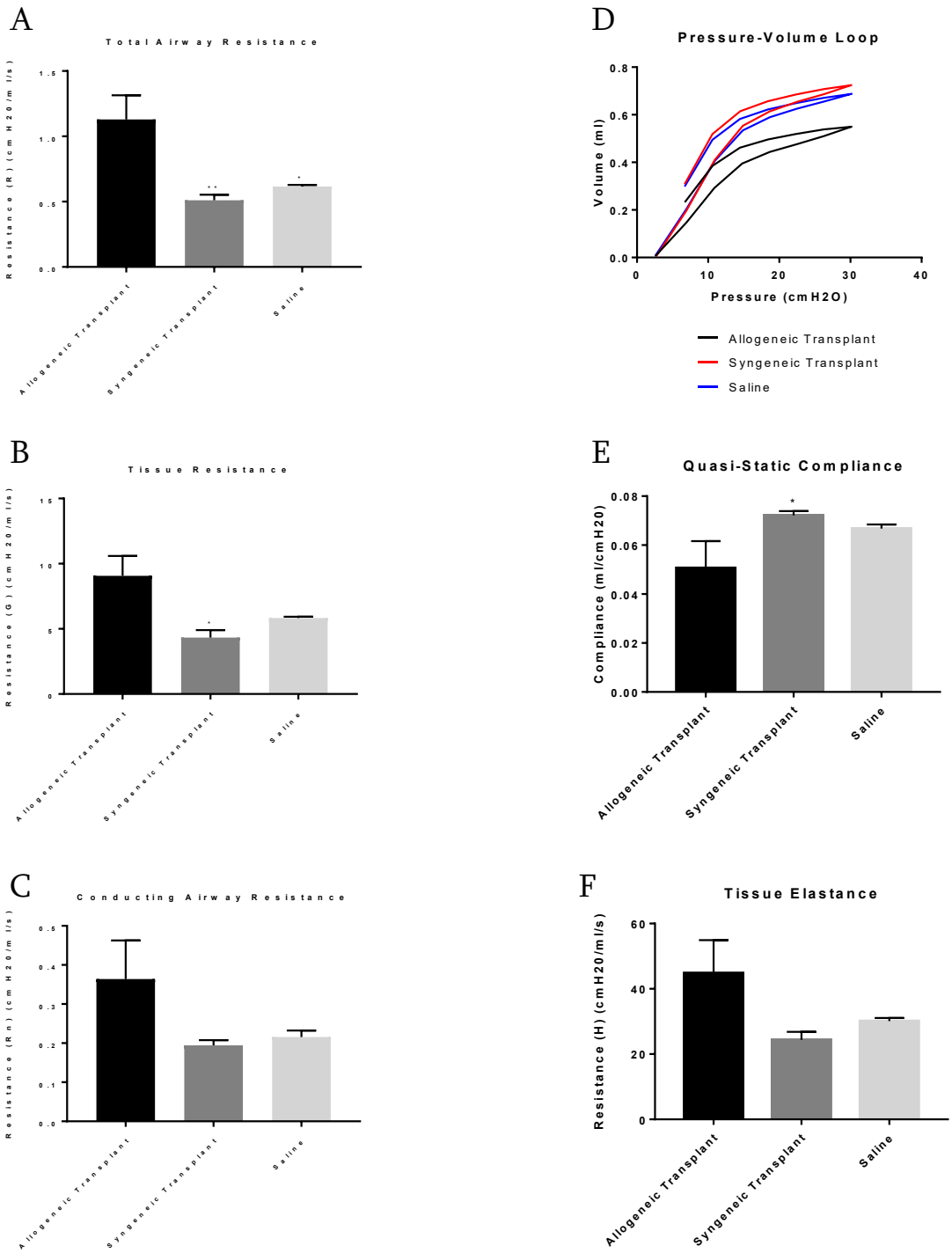
A
Total Airway Resistance
Resistance (R) (cmH20/ml/s)
1.5
1.0
0.5
0.0
**
*
Allogeneic Transplant
Syngeneic Transplant
Saline
B
Tissue Resistance
Resistance (G) (cmH20/ml/s)
15
10
5
0
*
Allogeneic Transplant
Syngeneic Transplant
Saline
C
Conducting Airway Resistance
Resistance (Rn) (cmH20/ml/s)
0.5
0.4
0.3
0.2
0.1
0.0
Allogeneic Transplant
Syngeneic Transplant
Saline
D
Pressure-Volume Loop
Volume (ml)
0.8
0.6
0.4
0.2
0.0
0
10
20
30
40
Pressure (cmH2O)
Allogeneic Transplant
Syngeneic Transplant
Saline
E
Quasi-Static Compliance
Compliance (ml/cmH20)
0.08
0.06
0.04
0.02
0.00
*
Allogeneic Transplant
Syngeneic Transplant
Saline
F
Tissue Elastance
Resistance (H) (cmH20/ml/s)
60
40
20
0
Allogeneic Transplant
Syngeneic Transplant
Saline

Figure 5

A

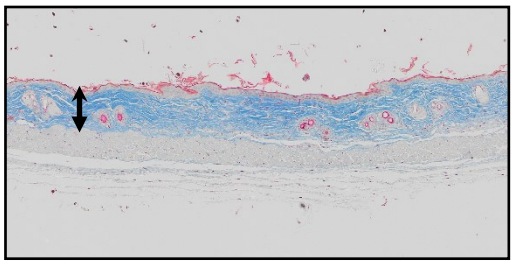

B

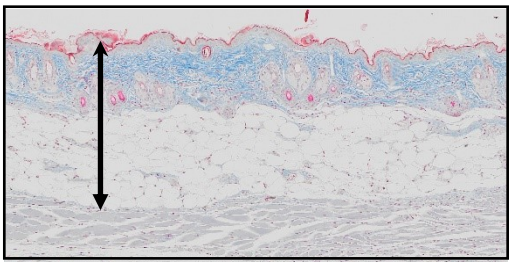

C

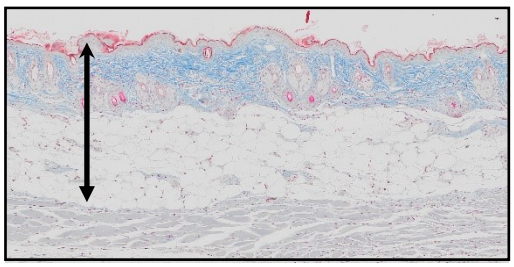

D

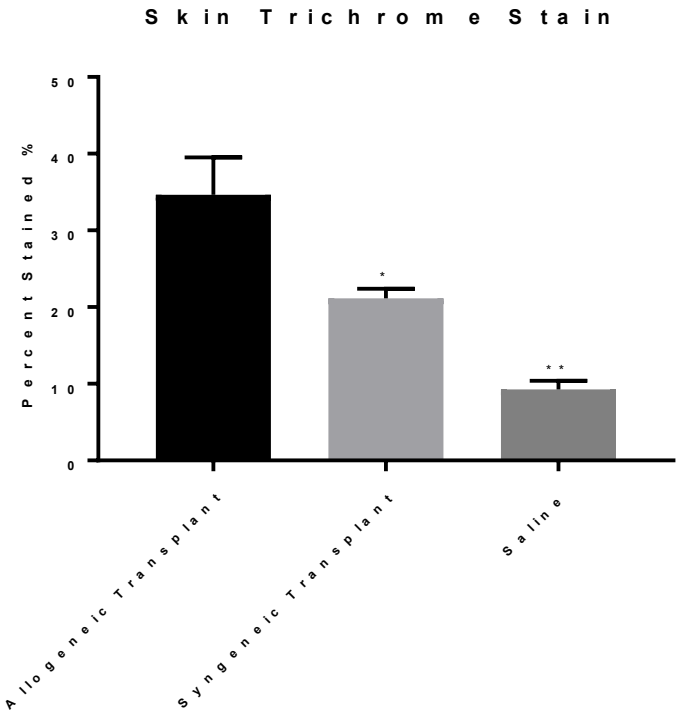

Figure 6

A

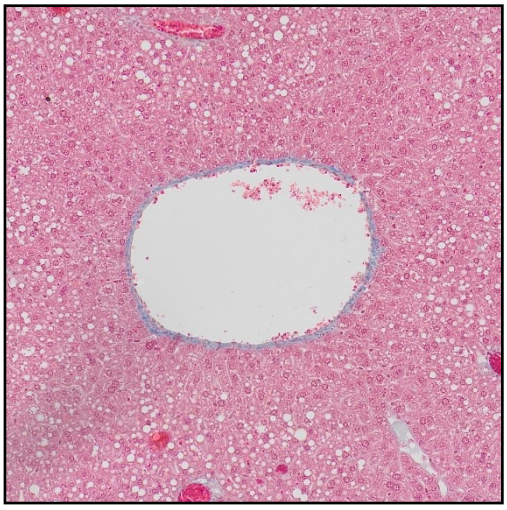

B

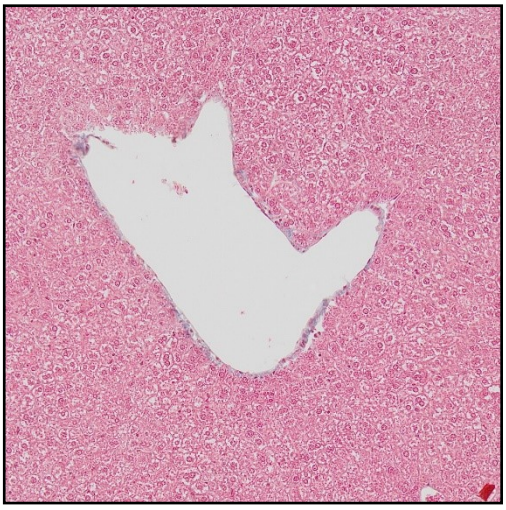

C

D

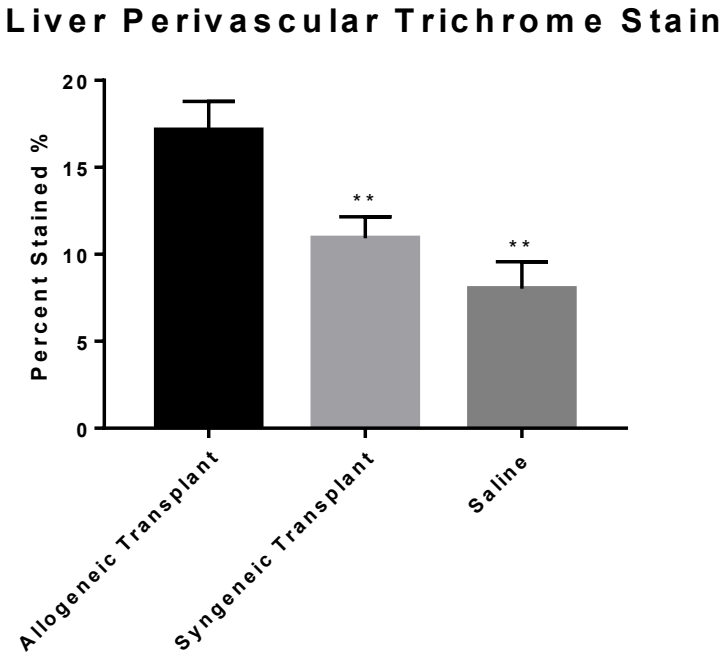

Chapter 4. Examining the efficacy of peptide therapy in a humanized model of Graft vs Host Disease

Examining the efficacy of peptide therapy in a humanized model of Graft vs Host Disease

Imani. J[1,2,3], Inman. MD[1], Kolb. M[1], Margetts[4]. P, Ball, ST[5], Larché. M[1,2,3]

1. Department of Medicine, Division of Respirology & Firestone Institute for Respiratory Health, The Research Institute at St. Joe's, McMaster University, Hamilton, ON, Canada

2. McMaster Immunology Research Center, McMaster University, Hamilton, ON, Canada

3. Department of Medicine, Division of Clinical Immunology & Allergy, McMaster University, Hamilton On, Canada

4. Department of Medicine, Division of Nephrology, McMaster University, Hamilton On, Canada

5. Department of Renal Medicine, Queen Elizabeth Hospital Birmingham, Edgbaston, United Kingdom

Keywords: Transgenic, HLA-DR4, HLA-A2, Bone Marrow Transplant, Graft vs Host, Pulmonary Fibrosis, Skin, Inflammation, T cell, Peptide Therapy, Transplant Tolerance.

Corresponding author: Dr. Mark Larché, Department of Medicine, McMaster University and The Research Institute of St. Joe's Hamilton, Firestone Institute for Respiratory Health, Hamilton Health Sciences, Rm 4H20, 1200 Main street W, Hamilton Ontario L8N 3Z5, Ph# (905) 525-9140 ext. 21284; Fax# (905) 521-4971, E-mail: larche@mcmaster.ca

Abstract

Graft vs Host Disease is an unwanted side of allogeneic hematopoietic stem cell transplant.

The disease begins with donor lymphocytes recognizing mismatched host antigens in the context of self-class II MHC through indirect antigen presentation and ends with fibrosis of major organs. Mismatches within class I HLA-A between donor and recipient pairs have been linked to the development of severe GvHD. Current treatments for GvHD suppress the immune system non-specifically and only delay the onset of disease. New strategies aimed at inducing transplant tolerance may overcome the limitations of current therapies. Analysis of GvHD patients has revealed the presence of CD4+ T cells that form responses against HLA-A2 derived peptides that have also been shown to have strong binding affinities for class II HLA-DRB1*0401. Herein we assess the efficacy of peptide-based therapies to induce transplant tolerance in a previously established humanized mouse model of GvHD. Four candidate peptides derived from regions of low polymorphisms in the α-3 domain of class I HLA-A2.1 were used to treat class I HLA-A2.1 expressing mice reconstituted with allogeneic donor cells expressing HLA-DRB1*0401. Our observations suggest that the chosen protocol used to treat mice was ineffective at conferring protection from GvHD and further optimizations are likely required before transplant tolerance can be induced.

Introduction

Graft vs Host disease (GvHD) is an unwanted side effect of mismatched hematopoietic stem cell transplant (HSCT). HSCT is traditionally used to treat lymphomas and myelomas; whereby allogeneic donor lymphocytes recognize cancer antigens in the recipient and induce apoptosis of the cancer cells in a process known as the graft vs leukemia effect[1]. However, donor T cells also recognize antigens on healthy host tissues derived from mismatched minor or major histocompatibility proteins[2,3] (miHC or MHC) and then induce anti-host immune responses.

The etiology of GvHD is poorly understood, however, studies in human and animal models have implicated specific pathways in initiation and progression[4]. The disease begins when patients are first prepared for transplant, total body irradiation and chemotherapy drugs are used to destroy the cancer cells but this conditioning regiment also kills healthy tissues and induces systemic inflammation[5] through release of release proinflammatory cytokines (IL-1, TNF-α, IFN-γ) by activated recipient macrophages and dendritic cells (DC)[6,7]. As donor cells are infused into the patient, donor macrophages[8] and DCs[9] are acquire antigens from host tissues and migrate to secondary lymphoid tissues where donor lymphocytes [10] are activated by non-cognate inflammatory cytokines[11] and through direct and indirect antigen presentation by the recipient and donor APCs respectively[9]. Clonally expanded CD8+ T cells attack host cells while donor CD4+ T cells are differentiated into proinflammatory Th1 cells[12] and IL-4, IL-5, and IL-13 producing Th2 cells; B cells are activated and differentiate into autoantibody-producing plasma cells[13,14]. These B and T cells then migrate into peripheral tissues and

activate macrophages. In the final stages, fibroblasts are activated by dysregulated immune responses into collagen-secreting myofibroblasts[15].

Current treatments for GvHD include prophylactic prednisone with or without calcineurin inhibitors to suppress the immune system but secondary treatments are used as the disease progresses[16]. Commonly used secondary therapies include mycophenolate mofetil, rituximab, sirolimus or imatinib[17] to down-regulate immune responses as well. However, these therapies can also cause unwanted side effects from prolonged use, and in time, patients may become refractory to treatment. Additionally, immunosuppressed patients are also susceptible to secondary bacterial or viral infections[17]. While these standard treatments suppress the immune system and delay the onset of GvHD, they fail to address the root cause of the disease; the rejection of recipient tissues which express allogeneic proteins. MHC derived peptides are the dominant alloantigens in transplantation; with major mismatches between donor and recipient leading to severe GvHD[3]. Interrupting the indirect antigen presentation pathway and targeting the interaction between the donor antigen presenting cell (APC) and donor lymphocyte may prevent the cascade of events that leads to organ fibrosis.

Induction of transplant tolerance was first observed in 1953, where donor skin grafts from CBA mice were tolerated in recipient A strain mice following in utero injection of donor-derived adults cells [18]. Further research has shown that tolerance in allograft transplants also occurs in mature animals following treatment of recipient animals with donor

antigens including pre-operative blood transfusions in kidney and heart allograft transplants[19]. Tolerance in these transfusions is thought to be established through induction of CD4+CD25+ T regulatory cells following the presentation of donor peptides in the context of self-class II HLA[20] through the indirect antigen presentation pathway[4]. The T regulatory cells are thought to ether clonally delete or clonally anergize alloreactive T cells[21]. Furthermore, this also induces hyporesponsiveness to all other peptides presented by the same class II HLA on the APC through linked suppression[22].

In a mismatched hematopoietic stem cell transplant setting, we hypothesize that use of recipient-derived peptides to treat reconstituted mice will also induce tolerance towards recipient antigens and thereby prevent GvHD. Like the processes that govern blood transfusion-induced transplant tolerance, peptide-based therapy is a process by which treatment with synthetic peptides derived from a protein antigen induces tolerance towards that antigen. This tolerance is also thought to develop from the induction of CD4+CD25+FOXP3+ T regulatory cells[23]. Upon treatment, peptides rapidly enter the circulation and bind to MHC class II molecules on the surface of APCs; upon presentation to naïve T cells by the APC[21] in the absence of inflammation, a tolerance response is generated by the T cells through the generation of antigen-specific CD4+CD25+ T regulatory cells and the expansion of existing T regulatory populations. Peptide-based therapies have evolved from whole allergen therapeutic strategies to treat allergic diseases but have also been used to treat autoimmune diseases including diabetes, rheumatoid arthritis, multiple sclerosis[23], and systemic lupus erythematosus[20].

As current models of GvHD employ transplantation of murine bone marrow and/or spleen cells across MHC mismatched strains of mice[4], generating peptide-based therapies targeting mouse MHC molecules is irrelevant for a clinical setting, as such, we have previously created a mouse model of GvHD whereby donor mice expressing human class II HLA-DRB1*0401 (HLA-DR4 mice) are used to reconstitute mice expressing human class I HLA-A2.1 (HLA-A2 mice). At 60-days post-transplant, these mice develop transplant-induced lung inflammation and skin and liver fibrosis. Herein, we assess the efficacy of using synthetic peptides derived from class I HLA-A2.1 to tolerize donor HLA-DR4^{+} cells in a pre-transplant and post-transplant setting using our humanized GvHD model. Our results suggest further optimization of the therapy protocol is required prior to observing downregulation of GvHD responses.

Methods

Humanized Model of GvHD

Female C57BL/6-Tg(HLA-A2.1)1Enge/J mice[24] (Jackson Laboratory) (HLA-A2 mice) were irradiated with 750 RADs and reconstituted with 5x10^{5} red blood cell (RBC)-free spleen cells and 5x10^{5} RBC-free bone marrow (BM) cells from female B6.129S2-*H2-Ab1^{tm1Gru}* Tg(HLA-DRA/H2-Ea,HLA-DRB1*0401/H2-Eb)1Kito[25] (Taconic) (HLA-DR4 mice).

Donor spleens were excised and physically ruptured in cold phosphate buffered saline (PBS) using a 1 ml syringe and then filtered through a 40 µm cell strainer (Corning Cat#

431750). The cells were treated with Ammonium Chloride Potassium (ACK) to lysis red blood cells (RBCs) and then washed twice with cold PBS. BM cells were prepared by collecting the femur and tibia bones and crushing them in a mortar; the cell suspension was filtered through a 40 μm cell strainer. The BM cells were then treated with ACK and washed twice with PBS. The spleen cells and BM cells were mixed together in saline and retro-orbitally (RO) injected into the recipient mice. The recipient mice were housed in ultraclean level 2 facilities at the Central Animal Facility (McMaster University). On day 60 post-transplant, the mice were euthanized to assess gross skin and airway physiological changes.

Mixed Lymphocyte Reactions

Spleens from HLA-DR4^{+} and HLA-A2^{+} mice were excised, and a single cell suspension was created as previously described. The HLA-A2^{+} cells were irradiated with 3000 RADs (Gammacell 3000, Best Theratronics) and washed twice with complete media (RPMI 1640, 10% FBS, 1% Penicillin-Streptomycin). Two million irradiated HLA-A2^{+} cells were mixed with 5x10^{5} HLA-DR4^{+} cells at 37^{0} Celsius cells in a 96-well microplate. HLA-DR4^{+} cells were treated with 10 ng/ml Phorbol 12-Myristate 13-Acetate (PMA) and 0.5 μM Ionomycin as a positive control [26]. After 4 days, each well was pulsed with 10 μl of 50 μCi 3H-Thymidine (General Electric Healthcare) and then harvested (FilterMate Universal Harvester; Perkin Elmer) after 16 hours onto glass-fibre filter mats (Wallac; Turku, Finland). The filter mats were dried overnight and then submerged in scintillation

solution (BetaPlate Scint; Perkin Elmer). The radioactivity of each well was then measured and quantified using a microBeta trilux machine (Perkin Elmer)

Peptide Formulation

The four synthetic peptides (Table 1) derived from HLA-A2 (Genscript) were dissolved in ddH_2O (peptide 1, 3, 4) or in 10^{-4} M HCl (peptide 2) and mixed together at a concentration of 1000 μg/ml. The stock was then serially diluted with ddH_2O to create stock concentrations of 100 μg/ml, 10 μg/ml, 1 μg/ml and 0.1μg/ml. 100 μl of peptide mix from each stock was then used for the respective assays.

Prophylactic Peptide Treatment

Groups of three HLA-$DR4^+$ mice were injected intraperitoneally (IP) or retro-orbitally (RO) with 0.01 μg, 0.1 μg, 1 μg or 10 μg of synthetic HLA-A2.1 derived peptides once a week for 3 weeks. Control HLA-$DR4^+$ mice were injected with saline (vehicle group). Spleen cells from peptide-treated or vehicle HLA-$DR4^+$ mice were collected and used as responder cells against irradiated HLA-$A2^+$ stimulator cells in a mixed lymphocyte reaction.

Post-Transplant Peptide Treatment

HLA-$A2^+$ mice were reconstituted with HLA-$DR4^+$ cells as described, on days 9, 13 and 23 post-transplant the mice were IP or RO injected with 0.01 μg, 0.1 μg, 1 μg or 10 μg of synthetic HLA-A2.1 derived peptides. HLA-$A2^+$ mice reconstituted with HLA-$DR4^+$

cells were also injected with saline as a vehicle control group. At 60 days post-transplant, all the mice were euthanized to assess gross skin changes and airway physiological changes.

Assessing Engraftment of donor cells.

Engraftment of donor HLA-DR4^{+} cells into recipient mice was assessed on day 60 post-transplant. A single-cell suspension of spleen cells was prepared as previously described. The cells were suspended in staining buffer (Biolegend Cat# 420201), blocked with Rat Anti-Mouse CD16/CD32 (BD Pharmingen Cat# 553141) and stained with PE-Cy5 anti-mouse CD3 (BD Pharmingen Cat#555276), Alexa Fluor 700 anti-mouse CD4 (BD Pharmingen Cat#557956), APC-H7 anti-mouse CD8a (BD Pharmingen Cat#560182), BV650 anti-mouse CD19 (Biolegend Cat#115541), PerCp Cy5.5 anti-mouse CD11b (BD Pharmingen Cat#550993), BV421 anti-mouse MHC II (Biolegend Cat#107631), FITC anti-human HLA-A2 (Biolegend Cat#343304), and Alexa Fluor 647 anti-human HLA-DR (Biolegend Cat#307622). Stained cells were captured on a BD LSR Fortessa cell analyzer (BD Biosciences) and were analyzed using Flowjo 10 software (Flowjo. LLC)

Assessment of Skin

At 60 days post-transplant, recipient mice were euthanized, and the dorsal surface of each mouse was imaged using a Canon 6D DSLR camera to observe gross changes within the skin.

Assessment of Airway physiology

Airway physiology was assessed on day 60 post-transplant; recipient mice were IP injected with xylazine hydrochloride (10 mg/kg) and sodium pentobarbital (30 mg/kg). The mice were tracheotomized and a 19-gauge blunted needle was inserted into the trachea and then pancuronium bromide (20 mg/kg) was IP injected prior to attaching the mouse to the ventilator (Flexivent, SCIREQ). Each mouse was ventilated at 150 breaths per minute (10 ml/kg). Forced oscillation waveform maneuvers were applied and the changes in airflow, volume, and pressure within the airways were recorded. The single compartment model was used to assess total airway resistance (R). Conducting airway resistance (Rn), tissue resistance (G) and tissue elastance (H) were calculated from the constant phase model and the *Salazar-Knowles* equation was used to assess quasi-static compliance (CST)[27,28].

Statistics

To analyze the data, an unpaired t-test was used to compare the MLR response between peptide treated HLA-DR4^{+} cells and vehicle HLA-DR4^{+} cells. To compare the different doses of peptide treatment a one-way ANOVA with a Dunnett's multiple comparisons test was used to compare the peptide treated groups against the vehicle group. Each bar graph is represented as ± SEM; a P-value of less than 0.05 was considered significantly different.

Study approval

The protocols described herein were developed and approved by the McMaster Animal Research Ethics Board. Mice were housed in ultraclean level 2 facilities at St. Joseph's Healthcare Hamilton and McMaster University central animal facility, Hamilton Ontario Canada.

Results

HLA-DR4$^+$ T cells react against irradiated HLA-A2$^+$ stimulator cells

HLA-DR4$^+$ spleen cells react strongly against irradiated HLA-A2$^+$ spleen cells. To determine if HLA-DR4$^+$ cells can directly respond against HLA-A2$^+$ cells; we first tested the reactivity of spleen cells from naïve HLA-DR4$^+$ mice against spleen cells derived from HLA-A2$^+$ mice. The HLA-DR4+ cells were used as responder cells and irradiated HLA-A2$^+$ cells as stimulator cells in an *in vitro* mixed lymphocyte reaction (MLR). The number and ratio of stimulator-to-responder cells were titrated (data not shown) to yield the greatest stimulation index. Incubation of $5x10^5$ HLA-DR4$^+$ spleen cells with $2x10^6$ irradiated HLA-A2$^+$ spleens cells yielded >9x more stimulation of the responder cells compared to HLA-DR4$^+$ cells incubated in complete media only **(Figure 1)**. Furthermore, as the stimulation index of irradiated HLA-A2$^+$ cells treated with PMA and Ionomycin (**far right bar**) was less than untreated HLA-A2$^+$ cells (**second bar from right**), this suggests that irradiated HLA-A2+ spleen cells are unresponsive to stimulation and likely

not generating responses towards HLA-DR4$^+$ spleen cells in the main MLR assay **(Third bar from left)**.

Peptide-treated HLA-DR4$^+$ mice react strongly against irradiated HLA-A2$^+$ stimulator cells

Spleen cells from HLA-DR4$^+$ mice treated with synthetic peptides derived from class I HLA-A2.1 have an exacerbated response to irradiated spleen cells from HLA-A2$^+$ mice. To measure the efficacy of peptide therapy on the ability of HLA-DR4+ cells to respond to irradiated HLA-A2$^+$ cells. HLA-DR4$^+$ mice were IP or RO injected with HLA-A2.1 derived peptides **(Table 1)**. Groups of three HLA-DR4$^+$ mice were injected with saline, 0.01 μg, 0.1 μg, 1 μg, or 10 μg of HLA-A2.1 peptides once a week for three weeks. Spleen cells were then harvested from peptide-treated and vehicle mice and stimulated with irradiated HLA-A2$^+$ spleen cells or PMA/Ionomycin. Compared to vehicle HLA-DR4$^+$ spleen cells, spleens cells treated with 0.01 μg of HLA-A2.1 peptides, injected IP **(Figure 2A)** and RO **(Figure 2B)** had significantly increased stimulation indices. Within the groups treated with the 0.1 μg, 1 μg, and 10 μg of IP **(Figure 2C, E, G)** and RO peptide **(Figure 2D, F, H)**, there was no difference in the stimulation index compared to vehicle HLA-DR4$^+$ mice. However, there was a general trend of increased response to irradiated HLA-A2$^+$ cells in these groups. This data suggests that treating HLA-DR4$^+$ mice with low does of synthetic HLA-A2.1 derived peptides increased the sensitivity of donor T cells towards HLA-A2$^+$.

Peptide-treated HLA-DR4$^+$ Cells engraft into irradiated HLA-A2$^+$ mice

Peptide treatment of reconstituted HLA-A2$^+$ mice does not affect the ability of donor HLA-DR4$^+$ BM and spleen cells to engraft into the recipient HLA-A2$^+$ mice. To test the efficacy of peptide-based therapy in a humanized mouse model of GvHD. We transplanted $5x10^5$ spleen and $5x10^5$ BM cells from transgenic C57BL/6 mice expressing human class II HLA-DRB1*0401 into irradiated transgenic C57BL/6 mice expressing human class I HLA-A2.1. On days 9, 13 and 23 post-transplant, groups of three reconstituted mice were IP or RO injected with vehicle, 0.01 μg, 0.1 μg, 1 μg, or 10 μg of synthetic peptides derived from class I HLA-A2.1. On day 56 post-transplant, the recipient mice were facial bled to assess engraftment of donor cells. We assessed HLA-DR vs HLA-A2 expression within the CD4+ and CD8+ populations of peripheral blood mononuclear cells (PBMC) and HLA-DR vs MHC II expression within the CD11b+ and CD19+ cell populations (**Figure 3**). In HLA-A2$^+$ mice reconstituted with saline only **(Figure 3, far right bar in all graphs**), class I HLA-A2.1 is expressed on 40% of the CD4+ cells and 70% of CD8+ cells. When reconstituted with HLA-DR4+ donor cells, however, the number of HLA-DR+ donor cells as a proportion of all the CD4+ and CD8+ cells were 10% and 3%, while the proportion of recipient-specific HLA-A2+ CD4+ and CD8+ cells dropped to 15% and 25% respectively **(Figure 3B-E)**. When the reconstituted HLA-A2$^+$ mice were treated with the HLA-A2.1 peptides, there was no difference in the proportion of donor-specific CD4+ **(Figure 3B, C)** and CD8+ **(Figure 3D, E)** cells between the vehicle group and any of the IP and RO peptide treated groups. In the

CD11b+ and CD19+ population of PBMCs, naïve HLA-A2$^+$ mice express MHC class II on 13% and 98% of each respective cell type and following transplantation of donor HLA-DR4$^+$ cells, the number of CD11b+ and CD19+ PBMCs expressing recipient-specific MHC II dropped to near zero while donor-specific HLA-DR4 was expressed on 9% and 88% of all CD11b+ and CD19+ cells respectively. Treatment of the reconstituted HLA-A2$^+$ mice with HLA-A2.1 peptides did not significantly alter the expression of donor HLA-DR4 on CD11b+ **(Figure 3F, G)** and CD19+ **(Figure 3H, I)** cells. This data shows that peptide treatment did not significantly alter the engraftment or proportion of donor-specific CD4+, CD8+, CD11b+, and CD19+ cells in the recipient mice.

HLA-A2$^+$ mice reconstituted with HLA-DR4$^+$ cells and treated with HLA-A2.1 derived peptides are protected from skin manifestations of GVHD

HLA-A2$^+$ mice reconstituted with HLA-DR4$^+$ cells and then treated with high dose of IP or low dose of RO HLA-A2.1 derived peptides were protected from skin manifestations of GvHD, while high dose RO peptide exacerbated skin manifestations of GvHD. To assess the impact of peptide therapy on the development of GvHD, we first examined gross morphological changes within the skin. Recipient mice were euthanized on day 60 post-transplant and the dorsal surface was imaged. In reconstituted vehicle mice, one of three mice **(Red Box)** displayed crusted skin lesions in the upper dorsal area **(Figure 4, top left row).** Mice treated with 0.01 μg, and 0.1 μg of IP peptides also had one of three mice display some degree of crusted skin lesions **(Red Boxes)**, however, it did not appear as severe as the vehicle group. In the group treated with 1 μg of IP peptides, there were no

signs of crusted skin lesions, however, one mouse had severe necrosis in the tail that required amputation **(Mouse 3)**. Mice treated with 10 μg of IP peptides did not display any skin manifestations of GvHD. In the groups treated with RO peptide, mice treated with 0.01 μg of peptide were protected from skin lesions but the other three groups were not. One of three mice treated with 1 μg and 10 μg of RO peptide had crusted skin lesions while one of three mice within the 0.1 μg and 10 μg RO peptide treated groups died prematurely. This data suggests that treatment with IP peptides confers some protection against skin lesions in a dose-dependent manner. In contrast, mice treated with the lowest dose of RO peptide are protected from skin damage while higher doses of RO peptide did not protect the mice from skin damage; suggesting increasing doses and/or routes of peptide injection can be ineffective at conferring protection.

HLA-A2$^+$ mice reconstituted with HLA-DR4$^+$ cells and treated with HLA-A2.1 derived peptides are not protected from changes in lung respiratory mechanics

HLA-A2$^+$ mice reconstituted with HLA-DR4$^+$ cells and then treated with synthetic HLA-A2.1 derived peptides had exacerbated GvHD associated changes in respiratory mechanics. At study endpoint, the mice were attached to a mechanical ventilator to assess lung function. The ventilator applied forced oscillation waveforms and recorded the subsequent changes in flow, volume, and pressure within the lungs. The data was then used to calculate the total airway resistance (R), conducting airway resistance (Rn), tissue resistance (G) and tissue elastance (H), and quasi-static compliance (CST). We have

previously established the baseline measurements for these parameters in HLA-$A2^+$ mice reconstituted with HLA-$DR4^+$ cells. Total lung resistance is increased, which was attributed to increases in tissue resistance in the parenchyma. Lung compliance in these mice was also decreased and was attributed to an increase in tissue elastance in the parenchyma. Mice treated with 0.01 μg of IP peptide had significantly increased total lung resistance compared to the vehicle group, but there was no difference in the other three IP treated groups **(Figure 5A)**. Segmentation of the data revealed that this difference was attributed to a significant increase in the tissue resistance **(Figure 5C)** as there was no difference in conducting airway resistance between any of the IP peptide-treated groups and the vehicle group **(Figure 5E)**. Within the RO peptide-treated mice, there was no difference in the total lung, conducting airway or tissue resistance between any of the groups. However, there was a general trend of dose-dependent increase in total lung resistance **(Figure 5B)** which was also mirrored in the tissue resistance measurement **(Figure 5D)** and an inverse trend in the conducting airway resistance **(Figure 5F)**. This indicates that like the vehicle group, changes in lung resistance within the peptide-treated mice is also confined to the lung parenchyma.

Lastly, we examined lung compliance. Each lung was inflated to a maximum pressure of 30 cm of H_2O, and the associated volume of inflated air was recorded. The pressure-volume data was plotted as a loop (PV loop). A downward shift in a PV loop indicates a lung that is stiffer or more fibrotic than a lung with a PV loop that is shifted higher. Mice treated with IP peptide had loops lower than vehicle group **(Figure 6A)** and only mice treated with 10 μg of RO peptide had a loop above the vehicle group **(Figure 6B)**. Using

the *Salazar-Knowles* equation, the quasi-static compliance was calculated from the expiratory branch of the PV loops. Mice treated with 0.01 μg and 0.1 μg of IP peptide had significantly decreased quasi-static compliance compared to the vehicle group while quasi-static compliance for the 1 μg and 10 μg IP treated mice were not different **(Figure 6C)**. Mice treated with RO peptides had decreased quasi-static compliance across all doses, however, significance was not achieved **(Figure 6D)**. Within the lung parenchyma, tissue elastance was significantly increased in mice treated with 0.01 μg of IP peptide **(Figure 6E)** 0.01 μg and 0.1 μg of RO peptide **(Figure 6F)**. In contrast, there was no difference in tissue elastance between the vehicle group and the mice treated with 0.1 μg, 1 μg, or 10 μg of IP peptide and mice treated with 1 μg, or 10 μg of RO peptide. These data suggest that lower doses of either IP or RO peptide exacerbate GvHD-associated changes in respiratory mechanics, while the higher doses are ineffective at preventing GvHD.

Discussion

Graft vs Host disease occurs following transplantation of allogeneic lymphocytes into mismatched recipients. The donor lymphocytes are presented recipient antigen peptides in the context of self-class II HLA on donor APCs through the indirect antigen presentation pathway[9]. These peptides are derived from both miHC and MHC molecules[2,3], however, mismatches within the MHC locus are immunodominant and leads to severe GvHD. Current treatments for GvHD include immunosuppressants that only delay the onset of

disease but do not stop the initiation of the disease. New strategies designed to induce transplant tolerance may represent a new approach to treating GvHD.

Use of pre-operative blood transfusions to tolerize patients prior to kidney allograft transplantations has been shown to be efficacious and this is thought to occur through up-regulation of CD4+CD25+ T regulatory cells and a similar approach of using recipient-derived peptides to tolerize donor cells may result in transplant tolerance in an HSCT setting.

Development of chronic GvHD in humans is linked to mismatches within the class I HLA-A/B locus[29], and HLA-DR4 restricted[30] peptides derived from regions of low polymorphisms in the α-3 transmembrane domain of class I HLA-A2.1 have been shown to activate CD4+ T cells[30] from HSCT patients with GVHD[31]. Therefore, we tested the efficacy of peptide-based therapies using a previously established humanized model of GvHD. These mice develop GvHD associated lung inflammation at 60 days post-transplant and have increased lung resistance and decreased lung compliance. We chose four candidate peptides shown to have a high binding affinity for class II HLA-DRB1*0401 and derived from regions of low polymorphisms within the α-3 transmembrane domain of human class I HLA-A2.

We first examined the ability of peptide therapy to downregulate anti-HLA-A2 responses in an MLR. Naïve HLA-DR4^{+} mice were injected through IP and RO routes at a dose of 0.01 μg, 0.1 μg, 1 μg or 10 μg of each peptide once a week for 3 weeks to “tolerize” the mice. Spleen cells were then used as responder cells against irradiated HLA-A2^{+} cells.

Surprisingly, mice treated with IP and RO peptides had increased or similar stimulation index compared to vehicle control mice. This suggests that treatment of peptide through IP or RO routes at the given doses is either ineffective at inducing tolerance or sensitizes the HLA-DR4^{+} mice to HLA-A2.1.

We next examined if peptide treatment would be effective if administered post-transplant. HLA-A2^{+} mice reconstituted with HLA-DR4^{+} cells were treated with 0.01 μg, 0.1 μg, 1 μg or 10 μg of each candidate peptide on days 9, 16, and 23 post-transplant. Examination of the PBMCs on day 56 post-transplant revealed that donor CD4, CD8, CD11b and CD19 cells all engrafted into the recipient mice to a similar degree, indicating that peptide treatment did not alter engraftment of donor cells. Furthermore, most class II expressing CD11b+ and CD119+ cells were of donor HLA-DR4+ origin and not recipient MHC II+ origin indicating that most antigen presentation to donor lymphocytes will be through the indirect antigen presentation pathway.

At study endpoint, we first examined changes in the skin, in the vehicle control group, one of three mice had crusted skin lesions. In the IP peptide-treated mice, only the mice treated with high dose 10 μg of peptide were protected from skin lesions, conversely only the low dose 0.01 μg of RO peptide protected mice from skin lesions, while low dose IP peptide and high dose RO peptide exacerbated skin changes. While further histological analysis is required for proper diagnosis, the data suggest that effective tolerance protocols are dependant on the route of injection in addition to the correct peptide dose.

Next, we looked at changes in respiratory mechanics. We observed changes in peptide-treated mice that were mirrored to the pathology observed in the skin; the lowest dose of IP peptide increased lung resistance and decreased compliance compared to the vehicle mice. The higher doses of IP peptide did not reduce resistance or increase compliance compared to the vehicle mice. Similarly, in the RO peptide-treated mice, there was a dose-dependent increase in lung resistance; while lung compliance was decreased or statistically the same as the vehicle group.

We have previously reported that HLA-A2$^+$ mice reconstituted with donor HLA-DR4$^+$ cells have lung inflammation but not fibrosis at day 60 post-transplant. Histological analysis of the lungs from peptide-treated much is required to decipher if the exacerbated respiratory mechanic measurements are associated with increased inflammation or fibrosis. Regardless of the outcome, use of synthetic peptides derived from human class I HLA-A2.1 to "tolerize" HLA-DR4$^+$ mice or HLA-A2$^+$ mice reconstituted with HLA-DR4$^+$ donor cells either exacerbated the response observed in the vehicle group or was ineffective. This suggests that incorrect doses of peptide treatment may sensitize HLA-DR4$^+$ cells towards HLA-A2.1.

While the principles of peptide therapy to treat T-cell based diseases is simple in concept, practically, the optimization of the protocol can be quite nuanced. A caveat of peptide therapy is the highly variable nature of the treatment protocol; depending on the disease being treated, the peptide sequence, peptide concentration, number of doses, time of treatment and route of administration must all be optimized[23,32]. We chose four candidate peptides derived from the α-3 domain of HLA-A2.1. These peptides were chosen from a

list of 53 HLA-A2.1 derived peptides for their relatively low number of polymorphisms within the population and high binding affinity for HLA-DRB1*0401[30]. However, of the 53 HLA-A2.1 peptides, there were multiple peptides that had binding affinities for HLA-DRB*0401 greater than our four chosen peptides. Those peptides were excluded from our list of candidate test peptides as they are from polymorphic regions of the α-1 and α-2 domain, but we can not exclude the possibility that they may represent dominate T cell epitopes that may act as better inducers of tolerance.

An additional challenge to peptide therapy is the administration of peptides into recipient mice under inflammatory conditions. One of the tenets of successful peptide therapy is that peptides must be presented to naïve-T cells in the absence of inflammation. In an HSCT setting, recipient mice have severe systemic inflammation following total body irradiation; in this case, administration of peptides under inflammatory conditions might induce sensitization as opposed to tolerance towards HLA-A2.1 peptides. Furthermore, endotoxin testing of our peptides revealed 0.013-0.108 EU/mL; contamination of LPS in the peptide cocktail is also likely contributing to sensitization of the HLA-DR4^{+} cells.

The next variable to consider moving forward is an appropriate time of treatment. Irradiated mice exhibit signs of radiation sickness between days 7-12 post-transplant followed by a recovery period starting on day 13-14. Reconstitution of donor cells begins around day 14 and is complete by day 21-23[7]. As such we administered peptides on days 9, 16 and 23 post-transplant, however, this timepoint maybe have overlapped with the post-radiation inflammatory phase of recovery. Sampling recipient mice for levels of

inflammatory cytokines and donor cells between days 0 and 21post-transplant may help determine optimal times to start peptide treatment in the future.

The next factor to consider is appropriate peptide dose and route of administration. Our observations indicate 10 ug peptide IP injection does not exacerbate the GvHD phenotype, however, treatment with 10 ug RO injection exacerbated the GvHD response to the point where mice prematurely expired. Whereas RO treatment directly injects peptides into the vascular system, the bioavailability of peptides when IP injected is likely reduced in comparison and may contribute to the differences in phenotype observed between the high dose IP and RO treatment groups.

Finally, following transplantation of HLA-DR4^{+} into HLA-A2^{+} mice, we hypothesize that HLA-A2.1 derived epitopes are presented by donor HLA-DR4^{+} APCs to donor CD4+ T cells through indirect antigen presentation. However, there are likely multiple APC and T cell interactions occurring simultaneously **(Table 2)**. This partially arises from the fact that recipient mice also express endogenous mouse class I MHC, such that donor CD4+ T cells intolerant to MHC I peptides presented in the context of MHC II can be activated. While we did not observe MHC II+ PBMCs at day 56 post-transplant, they may be to present at earlier time points. Furthermore, this result does not preclude their presence in tissues and secondary lymphoid organs.

One solution to address these issues is an in-depth analysis of the T cells from day 60 reconstituted mice. Flow cytometry staining of spleen and/or lymph node cells with MHC

II and/or HLA-DR4 tetramers will reveal the number of peptide-specific effector vs regulatory T cells, and this can also be expanded to test the number of T cells specific for the other 49 HLA-A2.1 peptides identified by *Hanvesakul et al*[30].

In conclusion, use of HLA-A2.1 derived peptides as a treatment to induce transplant tolerance following transplantation of HLA-DR4$^+$ donor cells into irradiated HLA-A2$^+$ mice did not result in the inhibition of GvHD. While some peptide doses exacerbated the disease phenotype, other doses neither significantly improved nor worsened the disease phenotype. Specifically, mice treated with 10 µg of peptides intraperitoneally appeared to be protected from skin lesions but had respiratory mechanics comparable to vehicle mice. As such, this dose of the peptides is likely a good starting point for modulating the treatment protocol. Finally, we have also identified key issues that can be addressed to further improve the protocol moving forward.

Acknowledgments.

We thank the central animal facility (McMaster University, ON, Canada) for their exceptional care and monitoring of the mic. We thank the members of the Larché lab for their continued guidance and support. Finally, we thank, Chandak Upagupta, Hemisha Patel, Nafis Wazed and Spencer D. Revill for their help with the outcome days. This work was performed and funded by the generous support of the Scleroderma Society of Ontario.

Authorship Contributions: Conception and design of study: JI, MI, MK, PM and ML; Conducted experiments: JI, JW; Analysis and interpretations of Data: JI, JW, MI, MK, PM and ML; Drafting the manuscript: JI; Edited and revised manuscript: JI, MI, MK, PM and ML. All authors read and approved the final version.

Conflicts of interest: No conflicts of interests are declared

References

1. Kolb HJ. Graft-versus-leukemia effects of transplantation and donor lymphocytes. *Blood*. 2008;112(12):4371-4383.
2. Spierings E. Minor histocompatibility antigens: past, present, and future. *Tissue Antigens*. 2014;84(4):374-360.
3. Warren EH, Zhang XC, Li S, et al. Effect of MHC and non-MHC donor/recipient genetic disparity on the outcome of allogeneic HCT. *Blood*. 2012;120(14):2796-2806.
4. Schroeder MA, DiPersio JF. Mouse models of graft-versus-host disease: advances and limitations. *Dis Model Mech*. 2011;4(3):318-333.
5. Straub JM, New J, Hamilton CD, Lominska C, Shnayder Y, Thomas SM. Radiation-induced fibrosis: mechanisms and implications for therapy. *Journal of cancer research and clinical oncology*. 2015;141(11):1985-1994.
6. Doe WF. The intestinal immune system. *Gut*. 1989;30(12):1679-1685.
7. Duran-Struuck R, Dysko RC. Principles of bone marrow transplantation (BMT): providing optimal veterinary and husbandry care to irradiated mice in BMT studies. *J Am Assoc Lab Anim Sci*. 2009;48(1):11-22.
8. Alexander KA, Flynn R, Lineburg KE, et al. CSF-1-dependant donor-derived macrophages mediate chronic graft-versus-host disease. *J Clin Invest*. 2014;124(10):4266-4280.
9. Markey KA, Banovic T, Kuns RD, et al. Conventional dendritic cells are the critical donor APC presenting alloantigen after experimental bone marrow transplantation. *Blood*. 2009;113(22):5644-5649.
10. Wysocki CA, Panoskaltsis-Mortari A, Blazar BR, Serody JS. Leukocyte migration and graft-versus-host disease. *Blood*. 2005;105(11):4191-4199.
11. Ferrara JL, Abhyankar S, Gilliland DG. Cytokine storm of graft-versus-host disease: a critical effector role for interleukin-1. *Transplant Proc*. 1993;25(1 Pt 2):1216-1217.
12. Teshima T, Ordemann R, Reddy P, et al. Acute graft-versus-host disease does not require alloantigen expression on host epithelium. *Nat Med*. 2002;8(6):575-581.
13. Young JS, Wu T, Chen Y, et al. Donor B cells in transplants augment clonal expansion and survival of pathogenic CD4+ T cells that mediate autoimmune-like chronic graft-versus-host disease. *J Immunol*. 2012;189(1):222-233.
14. Shimabukuro-Vornhagen A, Hallek MJ, Storb RF, von Bergwelt-Baildon MS. The role of B cells in the pathogenesis of graft-versus-host disease. *Blood*. 2009;114(24):4919-4927.
15. Svegliati S, Olivieri A, Campelli N, et al. Stimulatory autoantibodies to PDGF receptor in patients with extensive chronic graft-versus-host disease. *Blood*. 2007;110(1):237-241.
16. Socie G, Ritz J. Current issues in chronic graft-versus-host disease. *Blood*. 2014;124(3):374-384.
17. Inamoto Y, Flowers ME. Treatment of chronic graft-versus-host disease in 2011. *Curr Opin Hematol*. 2011;18(6):414-420.
18. Billingham RE, Brent L, Medawar PB. Actively acquired tolerance of foreign cells. *Nature*. 1953;172(4379):603-606.
19. Lagaaij EL, Hennemann IP, Ruigrok M, et al. Effect of one-HLA-DR-antigen-matched and completely HLA-DR-mismatched blood transfusions on survival of heart and kidney allografts. *N Engl J Med*. 1989;321(11):701-705.

20. Monneaux F, Muller S. Peptide-based immunotherapy of systemic lupus erythematosus. *Autoimmun Rev*. 2004;3(1):16-24.
21. Steinman RM, Hawiger D, Nussenzweig MC. Tolerogenic dendritic cells. *Annu Rev Immunol*. 2003;21:685-711.
22. Walsh PT, Taylor DK, Turka LA. Tregs and transplantation tolerance. *The Journal of Clinical Investigation*. 2004;114(10):1398-1403.
23. Larché M. Peptide Immunotherapy. *Immunology and Allergy Clinics of North America*. 2006;26(2):321-332.
24. Kaplan DH, Anderson BE, McNiff JM, Jain D, Shlomchik MJ, Shlomchik WD. Target antigens determine graft-versus-host disease phenotype. *J Immunol*. 2004;173(9):5467-5475.
25. Ito K, Bian HJ, Molina M, et al. HLA-DR4-IE chimeric class II transgenic, murine class II-deficient mice are susceptible to experimental allergic encephalomyelitis. *J Exp Med*. 1996;183(6):2635-2644.
26. Kruisbeek AM, Shevach E, Thornton AM. Proliferative assays for T cell function. *Curr Protoc Immunol*. 2004;Chapter 3:Unit 3.12.
27. Irvin CG, Bates JHT. Measuring the lung function in the mouse: the challenge of size. *Respiratory Research*. 2003;4(1):4-4.
28. Hantos Z, Daroczy B, Suki B, Nagy S, Fredberg JJ. Input impedance and peripheral inhomogeneity of dog lungs. *J Appl Physiol (1985)*. 1992;72(1):168-178.
29. Morishima Y, Sasazuki T, Inoko H, et al. The clinical significance of human leukocyte antigen (HLA) allele compatibility in patients receiving a marrow transplant from serologically HLA-A, HLA-B, and HLA-DR matched unrelated donors. *Blood*. 2002;99(11):4200-4206.
30. Hanvesakul R, Maillere B, Briggs D, Baker R, Larche M, Ball S. Indirect recognition of T-cell epitopes derived from the alpha 3 and transmembrane domain of HLA-A2. *Am J Transplant*. 2007;7(5):1148-1157.
31. Smith HJ, Hanvesakul R, Morgan MD, et al. Chronic graft versus host disease is associated with an immune response to autologous human leukocyte antigen-derived peptides. *Transplantation*. 2010;90(5):555-563.
32. Larche M, Wraith DC. Peptide-based therapeutic vaccines for allergic and autoimmune diseases. *Nat Med*. 2005;11(4 Suppl):S69-76.

Tables & Figure Legends

Table 1. List of Synthetic Peptides derived from Class I HLA-A2.1 and the amino acid (AA) location within the full-length HLA-A2.1 protein. The Four peptides were mixed together and dissolved in water and acidified water (peptide 3) and used to Tolerize HLA-DR4 mice at doses of 0.01 ug, 0.1ug, 1ug, and 10 ug.

Table 2 – List of all possible types of APC: T cell interactions following transplantation of HLA-DR4$^+$ donor cells into irradiated HLA-A2$^+$ mice that may lead T cell activation. MHC II is found on recipient APCs, MHC I is found on both donor and recipient cells and APCs, miHC are found in recipient tissues. HLA-DR4 is found on donor APCs, HLA-A2 is found on recipient tissues and APCs.

Figure 1. HLA-DR4$^+$ T cells react against irradiated HLA-A2$^+$ stimulator cells

Mixed lymphocyte reaction using $5x10^5$ spleen cells from HLA-DR4$^+$ mice mixed with $2x10^6$ irradiated (3000 RAD) spleen cells from HLA-A2$^+$ mice in a 96 well microplate for four days and then pulsed with 10µl of 50µCi 3H-Thymidine for 16 hours. HLA-DR4$^+$ cells and irradiated HLA-A2$^+$ cells were treated with 10ng/ml PMA and 0.5 µM Ionomycin as controls. The radioactivity of each well was quantified and the stimulation index was calculated as the ratio of radioactivity of responder cells mixed with stimulator cells to the radioactivity of the responder cells alone. HLA-DR4$^+$ spleen cells mixed with

irradiated HLA-$A2^+$ spleen cells were stimulated 9x (Black Bar) more than HLA-$DR4^+$ spleen cells incubated with media only. HLA-$DR4^+$ spleen cells were stimulated with PMA and Ionomycin, but irradiated HLA-$A2^+$ did not respond to PMA and Ionomycin.

Figure 2. Peptide-treated HLA-$DR4^+$ mice react strongly against irradiated HLA-$A2^+$ stimulator cells

Mixed lymphocyte reaction using $5x10^5$ spleen cells from HLA-$DR4^+$ mice IP or RO injected with 0.01 µg, 0.1 µg, 1 µg or 10 µg of HLA-A2.1 derived peptides, mixed with $2x10^6$ irradiated (3000 RAD) spleen cells from HLA-$A2^+$ mice in a 96 well microplate for four days and then pulsed with 10µl of 50µCi 3H-Thymidine for 16 hours. Peptide-treated HLA-$DR4^+$ cells were treated with 10ng/ml PMA and 0.5 µM Ionomycin as positive controls. The radioactivity of each well was quantified, and the stimulation index was calculated as the ratio of radioactivity of responder cells mixed with stimulator cells to the radioactivity of the responder cells alone. Reconstituted HLA-$A2^+$ mice treated with 0.01 µg of **(A)** IP or **(B)** RO peptide had significantly increased stimulation indices compared to vehicle-treated HLA-$A2^+$ mice. There was no difference between mice treated with 0.1 µg, 1 µg or 10 µg **(C, E, G)** IP or **(D, F, G)** RO peptide. Data were analyzed using an unpaired t-test to compare the stimulation index of peptide-treated mice and vehicle-treated mice. *$p \leq 0.05$, ***$p \leq 0.0005$.

Figure 3. Peptide-treated HLA-DR4^{+} Cells engraft into irradiated HLA-A2^{+} mice

Irradiated C57BL/6(HLA-A2.1) mice reconstituted with $5x10^5$ spleen and $5x10^5$ bone marrow cells from allogeneic B6.129S2-*H2-Ab1^{tm1Gru}* Tg(HLA-DRA/H2-Ea, HLA-DRB1*0401/H2-Eb)1Kito mice and IP or RO injected with 0.01 μg, 0.1 μg, 1 μg or 10 μg of HLA-A2.1 derived peptides on days 9, 16 and 23 post-transplant. C57BL/6(HLA-A2.1) mice were administered saline as controls. Mice were facial bled on day 56 post-transplant and PBMCs were stained with anti-CD4, CD8, CD19, CD11b, MHC II, HLA-A2, and HLA-DR antibodies. **(A)** Representative flowjo gating strategy for assessing HLA-DR vs HLA-A2 staining within CD4+, CD8+ cells and HLA-DR vs MHC II staining in CD11b+, and CD19+. There was no difference in the proportion of HLA-DR+ CD4+ cells treated with 0.01 μg, 0.1 μg, 1 μg or 10 μg of HLA-A2.1 derived peptides injected **(B)** IP or **(C)** RO. There was no difference in the proportion of HLA-DR+ CD8+ cells treated with 0.01 μg, 0.1 μg, 1 μg or 10 μg of HLA-A2.1 derived peptides injected **(D)** IP or **(E)** RO. There was no difference in the proportion of HLA-DR+ CD11b+ cells treated with 0.01 μg, 0.1 μg, 1 μg or 10 μg of HLA-A2.1 derived peptides injected **(F)** IP or **(G)** RO. There was no difference in the proportion of HLA-DR+ CD19+ cells treated with 0.01 μg, 0.1 μg, 1 μg or 10 μg of HLA-A2.1 derived peptides injected **(H)** IP or **(I)** RO. The data were analyzed using a one-way ANOVA with a Dunnett's multiple comparisons test to compare the means of each peptide-treated group against the mean of the vehicle group.

Figure 4. HLA-A2$^+$ mice reconstituted with HLA-DR4$^+$ cells and treated with HLA-A2.1 derived peptides are protected from skin manifestations of GvHD

Irradiated C57BL/6(HLA-A2.1) mice reconstituted with 5x10^5 spleen and 5x10^5 bone marrow cells from allogeneic B6.129S2-*H2-Ab1^{tm1Gru}* Tg(HLA-DRA/H2-Ea, HLA-DRB1*0401/H2-Eb)1Kito mice and IP or RO injected with 0.01 μg, 0.1 μg, 1 μg or 10 μg of HLA-A2.1 derived peptides on days 9, 16 and 23 post-transplant. C57BL/6(HLA-A2.1) mice were administered saline as controls. One of three HLA-A2$^+$ mice reconstituted with HLA-DR4$^+$ donor cells and treated with vehicle developed crusted skin lesions. One of three mice treated with 0.01 μg and 0.1 μg of IP peptides also developed crusted skin lesions. One of three mice treated with 1 μg of IP peptide developed necrotic tail lesions and was amputated **(Mouse #3)**. Mice treated with 10 μg of IP peptide were protected from developing skin lesions. Mice treated with 0.01 μg of RO peptide were protected from developing skin lesions. Mice treated with 0.1 μg, 1 μg and 10 μg of RO peptide developed crusted skin lesions or died prematurely.

Figure 5. HLA-A2$^+$ mice reconstituted with HLA-DR4$^+$ cells and treated with HLA-A2.1 derived peptides have increased lung resistance

Irradiated C57BL/6(HLA-A2.1) mice reconstituted with 5x10^5 spleen and 5x10^5 bone marrow cells from allogeneic B6.129S2-*H2-Ab1^{tm1Gru}* Tg(HLA-DRA/H2-Ea, HLA-DRB1*0401/H2-Eb)1Kito mice and IP or RO injected with 0.01 μg, 0.1 μg, 1 μg or 10 μg of HLA-A2.1 derived peptides on days 9, 16 and 23 post-transplant. C57BL/6(HLA-

A2.1) mice were administered saline as controls. On day 60 post-transplant, a mechanical ventilator was used to assess **(A, B)** total lung resistance, **(C, D)** tissue resistance, and (E, F) conducting airway resistance. Mice treated with 0.01 μg of IP peptide had significantly increased total lung and tissue resistance but not conducting airway resistance compared to mice treated with vehicle only. There was no statistical difference in the total lung, tissue and conducting airway resistance between the vehicle group and mice treated with 0.1 μg, 1 μg or 10 μg of IP peptide and 0.01 μg 0.1 μg, 1 μg or 10 μg of RO peptide. The data were analyzed using a one-way ANOVA with a Dunnett's multiple comparisons test to compare the means of each peptide-treated group against the mean of the vehicle group and represented as +/- SEM; **p≤*0.005,* ***p≤*0.0005.*

Figure 6. Mice reconstituted with HLA-DR4^{+} allogeneic donor cells have decreased lung compliance

Irradiated C57BL/6(HLA-A2.1) mice reconstituted with 5x10^{5} spleen and 5x10^{5} bone marrow cells from allogeneic B6.129S2-*H2-Ab1^{tm1Gru}* Tg(HLA-DRA/H2-Ea, HLA-DRB1*0401/H2-Eb)1Kito mice and IP or RO injected with 0.01 μg, 0.1 μg, 1 μg or 10 μg of HLA-A2.1 derived peptides on days 9, 16 and 23 post-transplant. C57BL/6(HLA-A2.1) mice were administered saline as controls. On day 60 post-transplant, a mechanical ventilator was used to generate **(A, B)** pressure-volume loops and assess **(C, D)** quasi-static lung compliance and (E, F) tissue elastance. The PV loops for mice treated with IP peptides were all lower than PV loop for the vehicle group, whereas, only the mice treated with 10 μg of RO peptide had a PV loop above the vehicle group. Mice treated

with 0.01 μg of IP peptide had significantly decreased quasi-static lung compliance and increased tissue elastance whereas mice treated with 0.1 μg of IP peptide had significantly decreased quasi-static lung compliance but not increased tissue elastance. There was no difference in quasi-static lung compliance between any RO peptide-treated mice and the vehicle group, but mice treated with 0.01 μg and 0.1 μg of RO did have significantly increased tissue elastance. The data were analyzed using a one-way ANOVA with a Dunnett's multiple comparisons test to compare the means of each peptide-treated group against the mean of the vehicle group and represented as +/- SEM; *p≤*0.05,* **p≤*0.005,* ***p≤*0.0005.*

Tables and Figures

Table 1

Peptide Sequence	**AA Number**
HAVSDHEATLRCWAL	Site 192-206
RCWALSFYPAEITLT	Site 202-216
GTFQKWAAVVVPSGQEQR	Site 239-256
KPLTLRWEPSSQPTIPI	Site 268-284

Table 2

Presentation Type	Lymphocyte Type	APC Type	MHC Type	Antigen Type
Direct	CD4	Host	MHC II	HLA-A2
		Host	MHC II	miHC
	CD8	Host	MHC I	HLA-A2
		Host	MHC I	MHC II
		Host	HLA-A2	HLA-A2
		Host	HLA-A2	MHC I
		Host	HLA-A2	MHC II
		Host	HLA-A2	miHC
Indirect	CD4	Donor	HLA-DR4	HLA-A2
		Donor	HLA-DR4	MHC I
		Donor	HLA-DR4	miHC
		Donor	HLA-DR4	MHC II
	CD8	Donor	MHC I	HLA-A2
		Donor	MHC I	MHC II

Figure 1

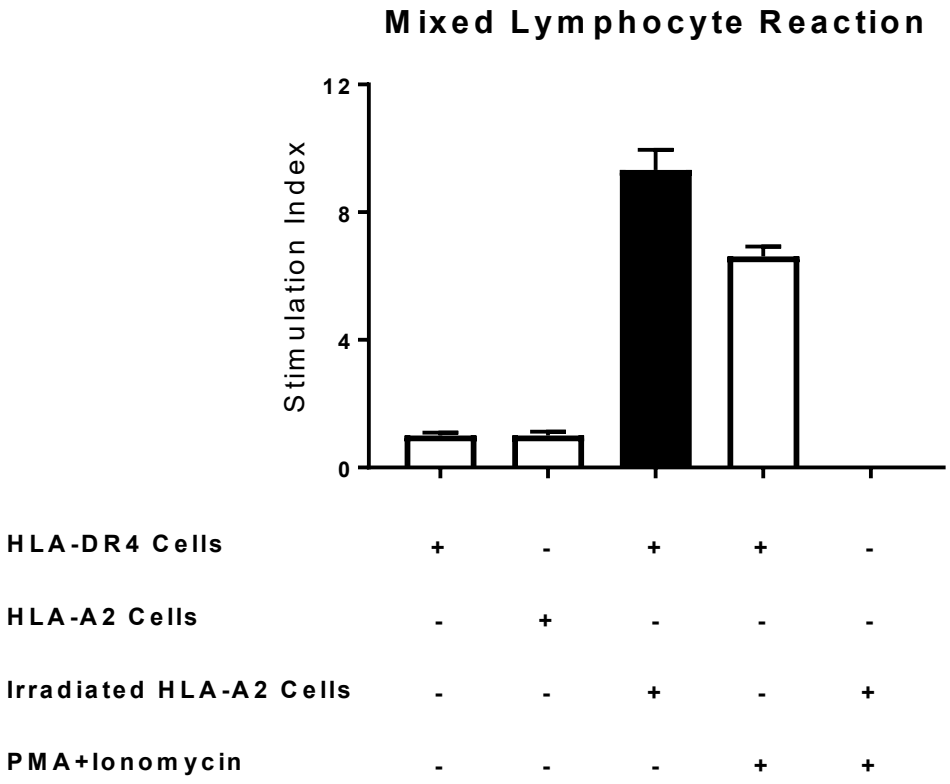
Mixed Lymphocyte Reaction
Stimulation Index
12
8
4
0
HLA-DR4 Cells + - + + -
HLA-A2 Cells - + - - -
Irradiated HLA-A2 Cells - - + - +
PMA+Ionomycin - - - + +

Figure 2

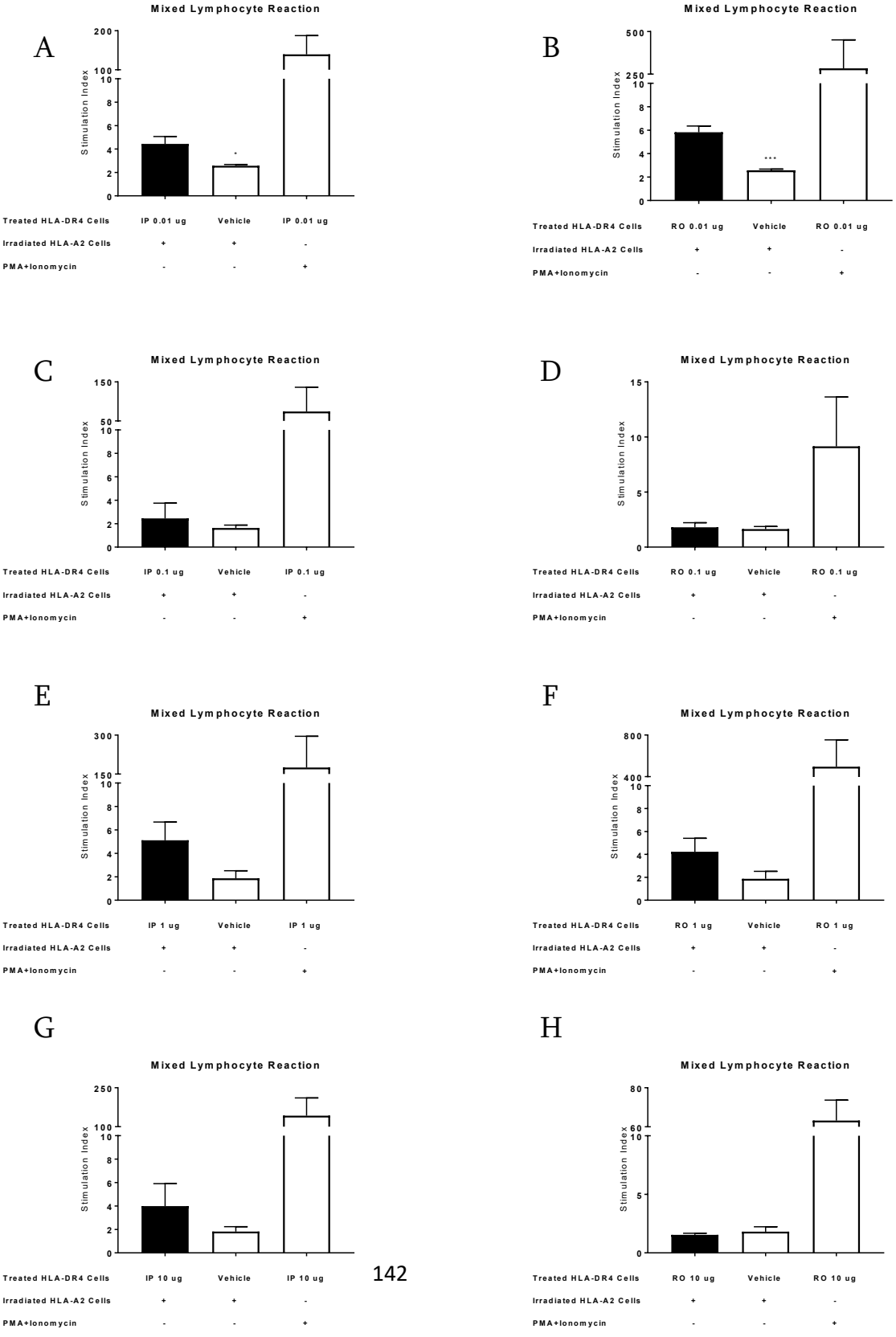
A
Mixed Lymphocyte Reaction
Stimulation Index
Treated HLA-DR4 Cells IP 0.01 ug Vehicle IP 0.01 ug
Irradiated HLA-A2 Cells + + -
PMA+Ionomycin - - +
B
Mixed Lymphocyte Reaction
Stimulation Index
***
Treated HLA-DR4 Cells RO 0.01 ug Vehicle RO 0.01 ug
Irradiated HLA-A2 Cells + + -
PMA+Ionomycin - - +
C
Mixed Lymphocyte Reaction
Stimulation Index
Treated HLA-DR4 Cells IP 0.1 ug Vehicle IP 0.1 ug
Irradiated HLA-A2 Cells + + -
PMA+Ionomycin - - +
D
Mixed Lymphocyte Reaction
Stimulation Index
Treated HLA-DR4 Cells RO 0.1 ug Vehicle RO 0.1 ug
Irradiated HLA-A2 Cells + + -
PMA+Ionomycin - - +
E
Mixed Lymphocyte Reaction
Stimulation Index
Treated HLA-DR4 Cells IP 1 ug Vehicle IP 1 ug
Irradiated HLA-A2 Cells + + -
PMA+Ionomycin - - +
F
Mixed Lymphocyte Reaction
Stimulation Index
Treated HLA-DR4 Cells RO 1 ug Vehicle RO 1 ug
Irradiated HLA-A2 Cells + + -
PMA+Ionomycin - - +
G
Mixed Lymphocyte Reaction
Stimulation Index
Treated HLA-DR4 Cells IP 10 ug Vehicle IP 10 ug
Irradiated HLA-A2 Cells + + -
PMA+Ionomycin - - +
H
Mixed Lymphocyte Reaction
Stimulation Index
Treated HLA-DR4 Cells RO 10 ug Vehicle RO 10 ug
Irradiated HLA-A2 Cells + + -
PMA+Ionomycin - - +

Figure 3

A

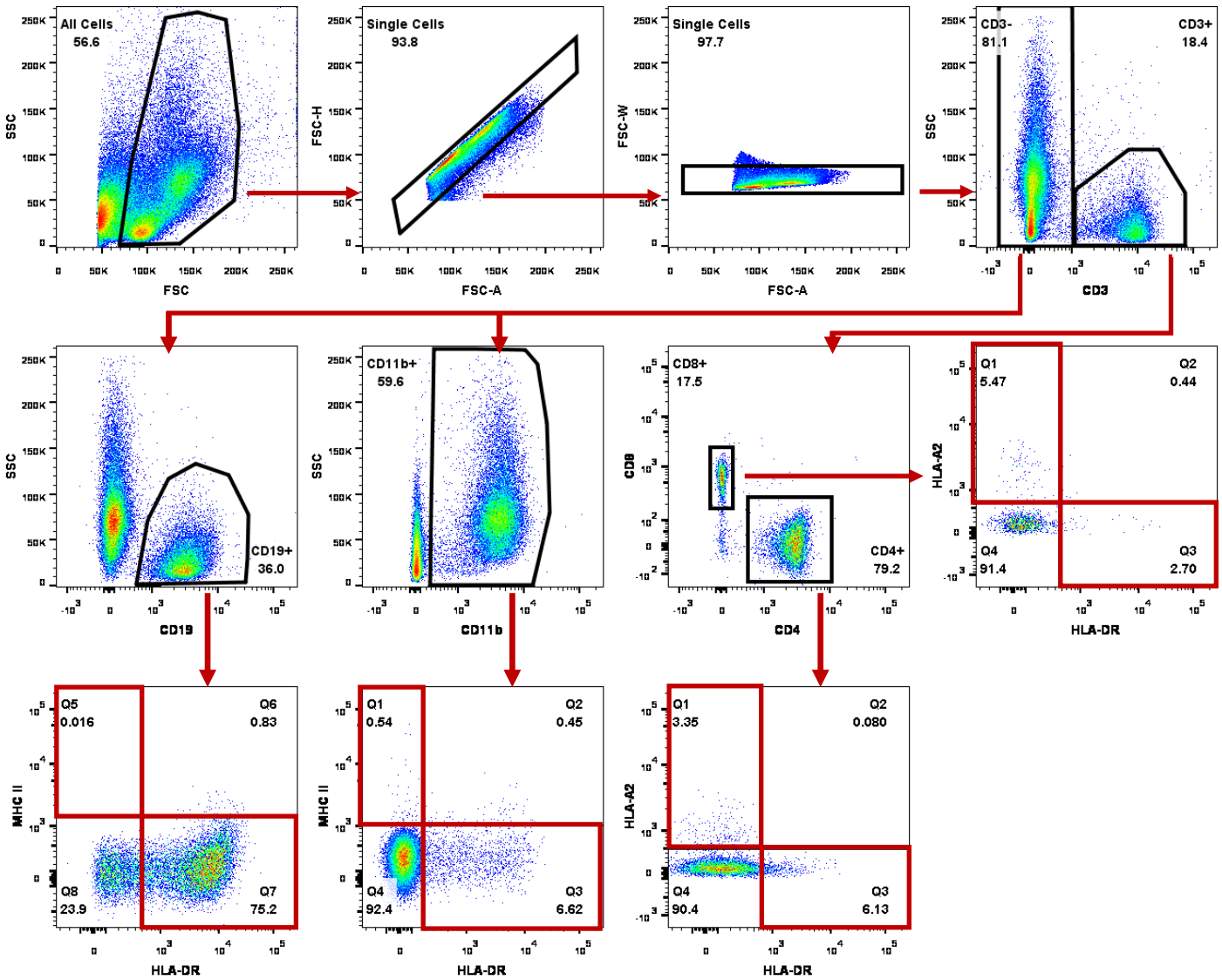
All Cells
56.6
SSC
FSC
Single Cells
93.8
FSC-H
FSC-A
Single Cells
97.7
FSC-W
FSC-A
CD3-
81.1
CD3+
18.4
SSC
CD3
CD19+
36.0
SSC
CD19
CD11b+
59.6
SSC
CD11b
CD8+
17.5
CD8
CD4+
79.2
CD4
Q1
5.47
Q2
0.44
Q4
91.4
Q3
2.70
HLA-A2
HLA-DR
Q5
0.016
Q6
0.83
Q8
23.9
Q7
75.2
MHC II
HLA-DR
Q1
0.54
Q2
0.45
Q4
92.4
Q3
6.62
MHC II
HLA-DR
Q1
3.35
Q2
0.080
Q4
90.4
Q3
6.13
HLA-A2
HLA-DR

Figure 3

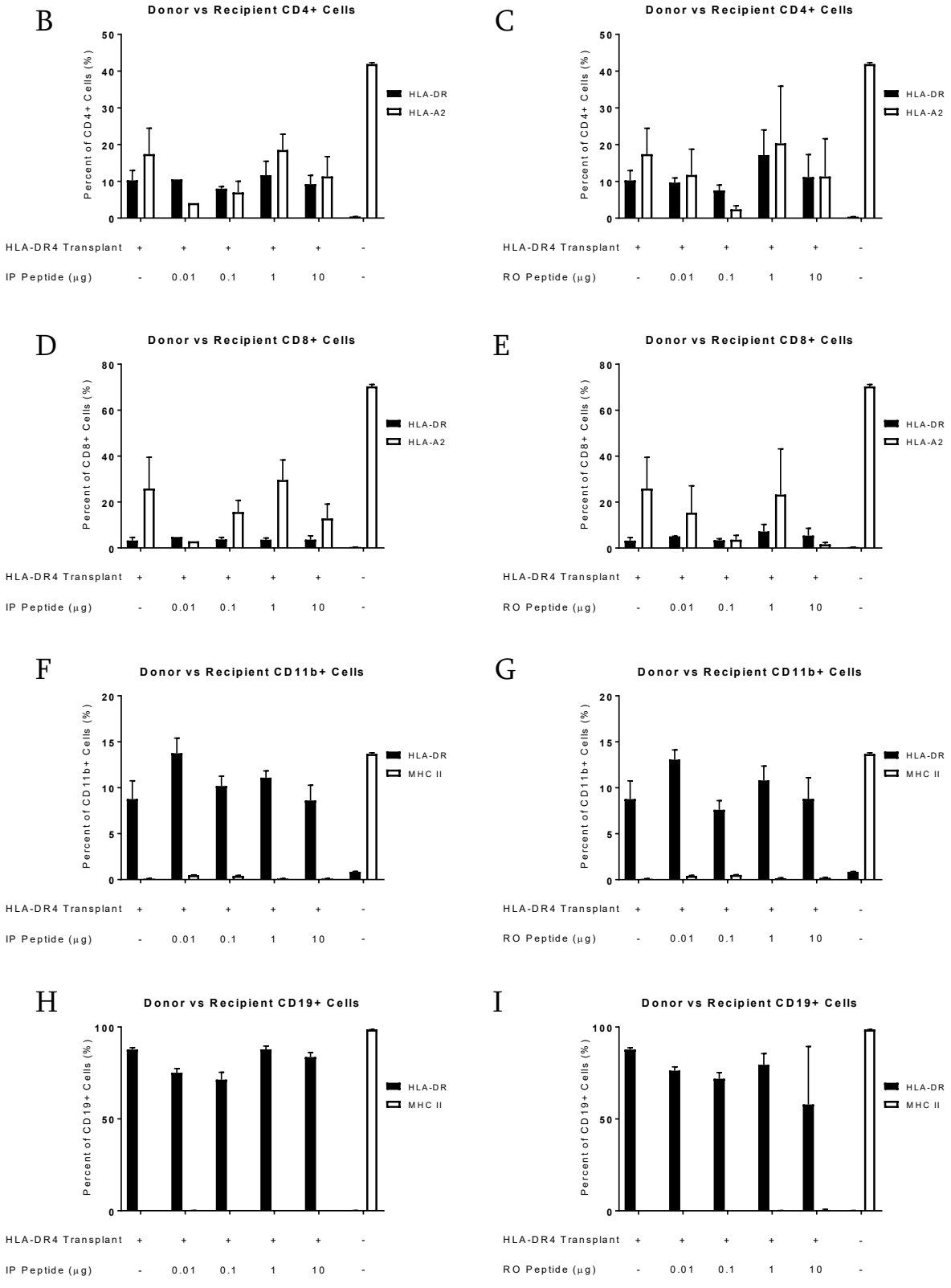
B
Donor vs Recipient CD4+ Cells
Percent of CD4+ Cells (%)
HLA-DR
HLA-A2
HLA-DR4 Transplant + + + + + -
IP Peptide (µg) - 0.01 0.1 1 10 -
C
Donor vs Recipient CD4+ Cells
Percent of CD4+ Cells (%)
HLA-DR
HLA-A2
HLA-DR4 Transplant + + + + + -
RO Peptide (µg) - 0.01 0.1 1 10 -
D
Donor vs Recipient CD8+ Cells
Percent of CD8+ Cells (%)
HLA-DR
HLA-A2
HLA-DR4 Transplant + + + + + -
IP Peptide (µg) - 0.01 0.1 1 10 -
E
Donor vs Recipient CD8+ Cells
Percent of CD8+ Cells (%)
HLA-DR
HLA-A2
HLA-DR4 Transplant + + + + + -
RO Peptide (µg) - 0.01 0.1 1 10 -
F
Donor vs Recipient CD11b+ Cells
Percent of CD11b+ Cells (%)
HLA-DR
MHC II
HLA-DR4 Transplant + + + + + -
IP Peptide (µg) - 0.01 0.1 1 10 -
G
Donor vs Recipient CD11b+ Cells
Percent of CD11b+ Cells (%)
HLA-DR
MHC II
HLA-DR4 Transplant + + + + + -
RO Peptide (µg) - 0.01 0.1 1 10 -
H
Donor vs Recipient CD19+ Cells
Percent of CD19+ Cells (%)
HLA-DR
MHC II
HLA-DR4 Transplant + + + + + -
IP Peptide (µg) - 0.01 0.1 1 10 -
I
Donor vs Recipient CD19+ Cells
Percent of CD19+ Cells (%)
HLA-DR
MHC II
HLA-DR4 Transplant + + + + + -
RO Peptide (µg) - 0.01 0.1 1 10 -

Figure 4

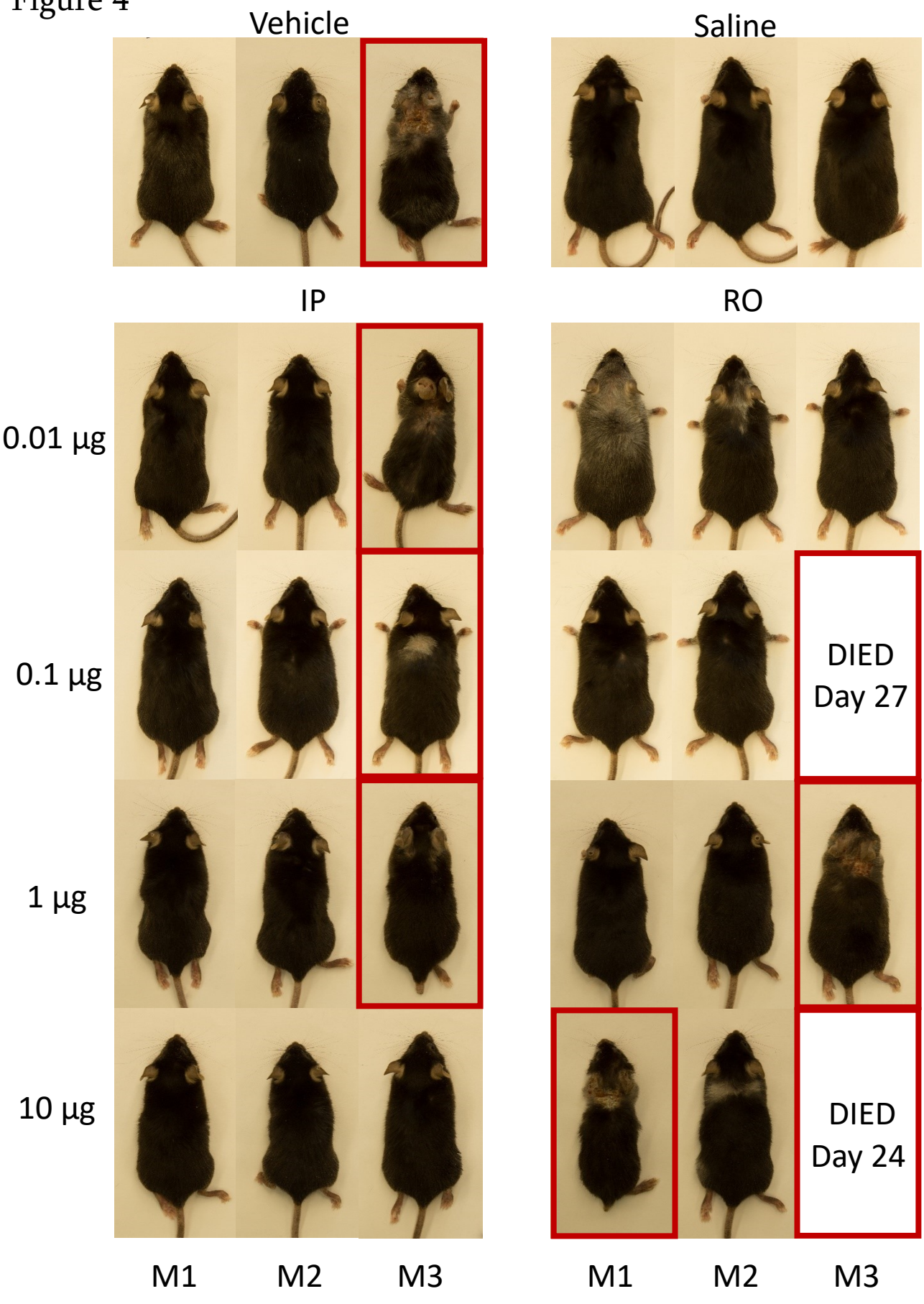
Vehicle
Saline
IP
RO
0.01 µg
0.1 µg
1 µg
10 µg
DIED Day 27
DIED Day 24
M1
M2
M3
M1
M2
M3

Figure 5

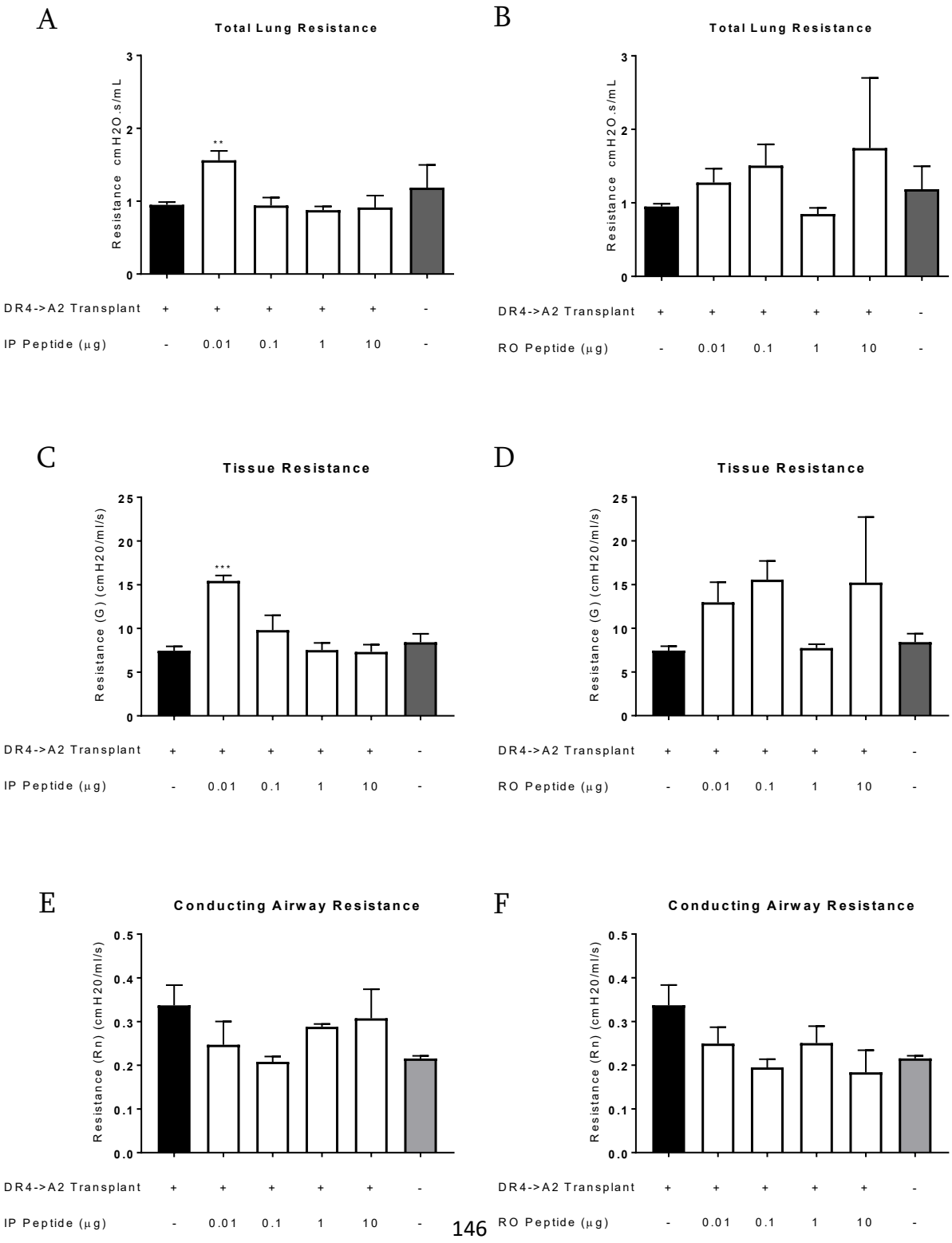
A
Total Lung Resistance
Resistance cmH2O.s/mL
**
DR4->A2 Transplant + + + + + -
IP Peptide (µg) - 0.01 0.1 1 10 -
B
Total Lung Resistance
Resistance cmH2O.s/mL
DR4->A2 Transplant + + + + + -
RO Peptide (µg) - 0.01 0.1 1 10 -
C
Tissue Resistance
Resistance (G) (cmH20/ml/s)
***
DR4->A2 Transplant + + + + + -
IP Peptide (µg) - 0.01 0.1 1 10 -
D
Tissue Resistance
Resistance (G) (cmH20/ml/s)
DR4->A2 Transplant + + + + + -
RO Peptide (µg) - 0.01 0.1 1 10 -
E
Conducting Airway Resistance
Resistance (Rn) (cmH20/ml/s)
DR4->A2 Transplant + + + + + -
IP Peptide (µg) - 0.01 0.1 1 10 -
F
Conducting Airway Resistance
Resistance (Rn) (cmH20/ml/s)
DR4->A2 Transplant + + + + + -
RO Peptide (µg) - 0.01 0.1 1 10 -

Figure 6

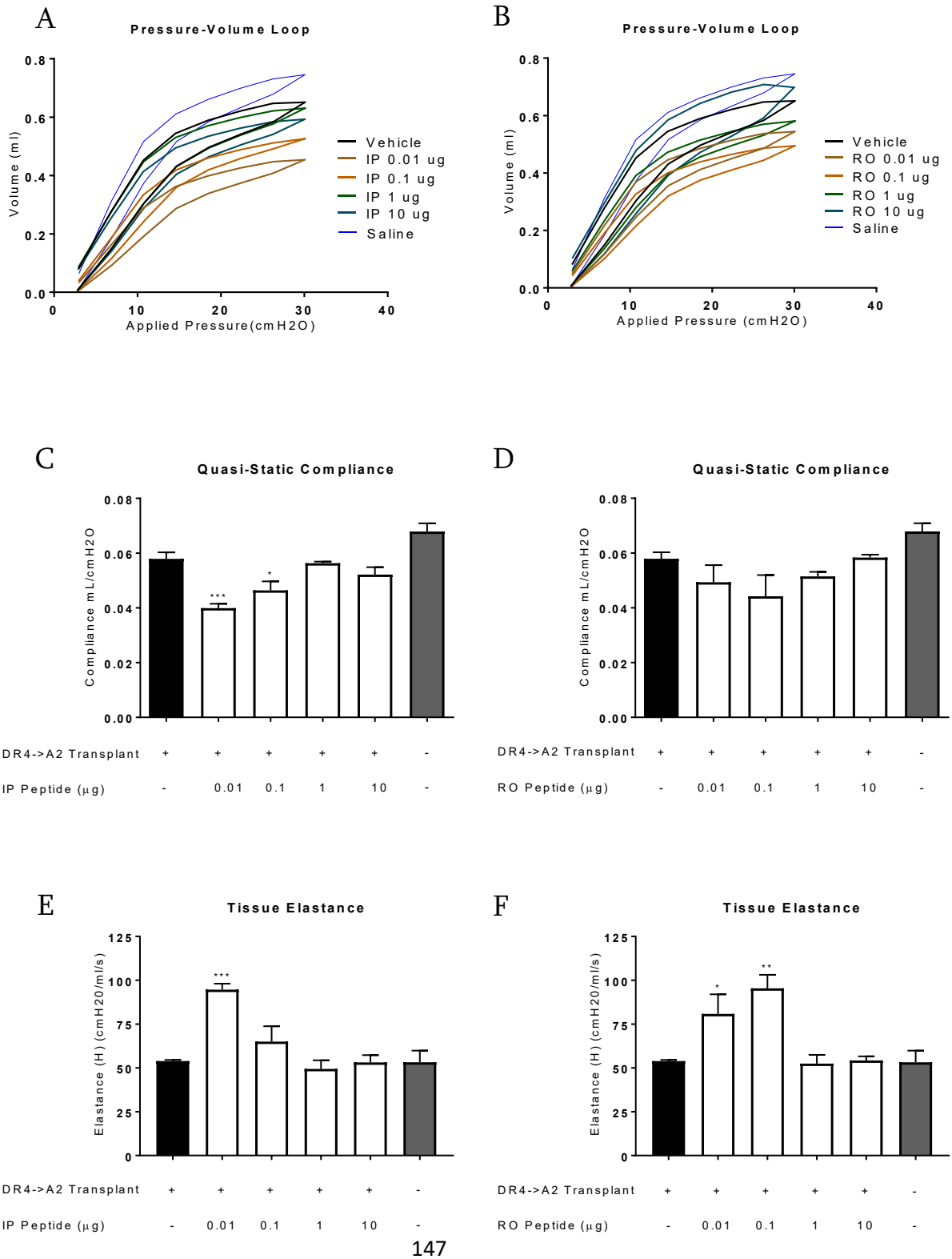
A
Pressure-Volume Loop
Volume (ml)
Applied Pressure(cmH2O)
Vehicle
IP 0.01 ug
IP 0.1 ug
IP 1 ug
IP 10 ug
Saline
B
Pressure-Volume Loop
Volume (ml)
Applied Pressure (cmH2O)
Vehicle
RO 0.01 ug
RO 0.1 ug
RO 1 ug
RO 10 ug
Saline
C
Quasi-Static Compliance
Compliance mL/cmH2O
DR4->A2 Transplant + + + + + -
IP Peptide (µg) - 0.01 0.1 1 10 -
D
Quasi-Static Compliance
Compliance mL/cmH2O
DR4->A2 Transplant + + + + + -
RO Peptide (µg) - 0.01 0.1 1 10 -
E
Tissue Elastance
Elastance (H) (cmH20/ml/s)
DR4->A2 Transplant + + + + + -
IP Peptide (µg) - 0.01 0.1 1 10 -
F
Tissue Elastance
Elastance (H) (cmH20/ml/s)
DR4->A2 Transplant + + + + + -
RO Peptide (µg) - 0.01 0.1 1 10 -

Chapter 5. Discussion

Graft vs Leukemia

The GvL effect is mediated by donor T cells and Natural Killer (NK) cells. Allogeneic T cells can recognize leukemia-associated antigens such as Wilms tumour 1 found in 60-90% of AML patients[136], leukemia-specific antigens that arise through gene mutations, and miHC antigens that are derived exclusively from hematopoietic cells[137]. Peptides derived from these three antigen sources are presented by healthy[138] and leukemia-derived recipient DCs[139] in the context of class I and class II HLA and directly activate donor CD8+ and CD4+ T cells respectively. This leads to the generation of CTLs specific for the leukemia cells and CD4+ T cells that only recognize recipient cells derived from hematopoietic cells. As such, this pathway does not yield traditional GvHD responses against normal tissues.

Following HSCT, NK cells are one of the earliest cells to recover and also contribute to the GvL effect. NK cell functionality is regulated through numerous activating and inhibitory cell surface receptors[140]. The killer-cell immunoglobulin-like (KIR) family of receptors can recognize HLA-A, B, or C on self-cells and inhibit NK cell activity[141,142]. Conversely, other members of the KIR family induce NK cytotoxicity when they recognize class I HLA. In the context of HSCT, NK cell cytotoxicity is regulated by KIR interactions with both matched and mismatched class I HLA on the recipient leukemia cells. If there is an HLA mismatch, signalling through inhibitory KIRs is stopped and the NK cell can lyse the leukemia cell. If the HLA is matched, signalling through activating KIRs induces NK cytotoxicity. This process is further regulated by numerous other inhibitory and activating receptors on the NK cell and the balance between activating and

inhibitory receptors determines the NK cells functionality[143].

GvHD Therapeutic Strategies

Throughout the years, researchers have investigated a number of therapeutic strategies to prevent GvHD. One of the early attempts was modulating the pre-transplant conditioning regiment; studies in mice and canines have shown a correlation between the intensity of TBI and GvHD, with reduced TBI leading to graft rejection, but the use of immunosuppressive drugs lead to successfully engraftment and GvHD[144].

Immunosuppression

Methotrexate was the first drug tested and shown to be effective in canine models[145]. Later on, use of calcineurin inhibitors (cyclosporine A and tacrolimus) in combination with methotrexate were used as prophylactic drugs and were successful in reducing GvHD in canine models[146-148]. Today, The initial treatment for cGVHD involves administration prednisone (glucocorticoid). Secondary treatments are used when the disease progresses[149]. There is no consensus on the choice of secondary drug treatments but commonly used therapies include mycophenolate mofetil, rituximab, sirolimus or imatinib[150]. In general, these treatments act to down-regulate immune responses; however, drug therapies can cause unwanted side effects from prolonged use and in time some patients may become refractory to treatment. Additionally, immunosuppressed patients are susceptible to secondary bacterial or viral infections. However, the most disadvantageous aspect of immunosuppression is the amelioration of the GvL effect. In

clinical trials where suppression was used, patients experienced leukemia relapse and only went back into remission once immunosuppressive drugs were withdrawn[151]

Researchers then attempted to preserve the GvL effect while abolishing the GvHD by transplanting T cell depleted bone marrow followed by subsequent donor lymphocyte infusions (DLI) when required. In early models, canines transplanted with T cell depleted bone marrow could be given DLI up to 2 months post-transplant without developing GvHD[152]. In the clinic, DLI therapy has been tested in various cancers (CML, ALL, AML, MM) but yielded mixed results including the development of GvHD in some patients from repeated DLIs[136].

Bortin et al[153] devised a therapy whereby CBA mice were immunized (sensitized) with leukemia cells from MHC mismatched AKR mice; spleen and lymph node cells from the immunized mice were transplanted into AKR leukemia mice. They observed a significant GvL response but did not observe an augmented GvHD response compared to AKR mice reconstituted with unimmunized CBA donor cells. While they could not explain the underlying mechanisms of the observation at the time, one possibility is that the immunization skewed the donor T cell response towards the leukemia antigens as they may have been immunodominant to the mismatched MHC derived antigens. Indeed when they repeated the experiment using leukemia cells from SJL mice to immunize the CBA mice, the GvL effect was lost but GvHD remained. As such their observations were likely a niche case not applicable as a whole to HSCT. Furthermore, a protocol whereby healthy donors are immunized with cancer cells is unethical and therefore not practical in a

clinical setting.

Targeting Cell Signalling

Recent approaches have investigated the targeting of specific cytokines. TNF-α is a major inflammatory cytokine in the early stages of the disease; in a mouse model of aGvHD, transplantation of LPS resistant donor cells resulted in reduced aGvHD of the GI tract and low serum levels of TNF-α. Subsequent neutralization of TNF-α yielded the same result[154]. In subsequent murine studies, anti-TNF-α treatment was effective at blocking CD4+ mediated GvHD while retaining the GvL response in MHC mismatched models but was only 40% effective in blocking CD8+ mediated GvHD in miHC and MHC mismatched models while retaining the GvL effect[155]. It is important to note, in each of these transplants only CD4+ or CD8+ T cells were transplanted. It remains to be seen how transplant of both CD4+ and CD8+ T cells followed by anti-TNF-α treatment will affect the GvL response. Mouse models of aGvHD have also identified the upregulation of IL-6 and its receptor during the early phase of disease; upon antibody blockade of the IL-6 receptor, aGvHD symptoms were reduced, reconstitution of Treg cells was increased, and the GvL response was not affected[156,157]

IL-2 is another important cytokine that has been targeted, as IL-2 promotes the proliferation of both CD8+ T cells and Tregs; trials investigating the administration of low dose IL-2 in combination with rapamycin have been beneficial in targeting GvHD. As rapamycin blocks mTOR signalling in T cells and B cell but not Tregs[158].

Researchers have also sought to target chemokine-chemokine receptor axes that immune cells utilize to migrate to tissues sites. Antibodies targeting CXCR3, CXCL1 and CCR5 have been tested in mouse models of GvHD with various success. Use of anti-CXCR3[159] or anti-CX3CL1[160] antibodies in mice were shown to reduce aGvHD of the GI Tract, but anti-CCR5 therapy was less effective, likely due to the requirement of Tregs that also utilize CCR5 to migrate[161]. A caveat of these types of therapies is that chemokine and cytokine signalling can be redundant and blocking any specific signal pathway is unlikely to yield significant protection from GvHD.

Studies aimed at blocking T cell co-stimulation have also been investigated. In murine studies, transplantation of CD28 deficient donor T cells was shown to reduce aGvHD symptoms[162], Conversely, use of antibodies towards CD80/CD86 also reduced aGvHD symptoms[163]. Other studies have also targeted the CD40-CD40L[164,165], OX40-OX40L[166], 4-1BB/4-1BBL[167], ICOS/ICOS-L[168], LIGHT/HVEM[169], NKG2D-NKG2D-L[170], DNAM-1/DNAM-1-L[171], and the CD30/CD30L[172] co-stimulation pathways. While many of these therapies were shown to reduce GvHD symptoms, blocking these pathways may also inhibit the GvL effect as well, and needs to be investigated.

Complement C5a

C5 is normally produced by the liver but can be locally produced by macrophages and DCs. Upon secretion it is cleaved by the C5 convertase (C4b2aC3b or C3bBbC3b),

members of the coagulation family of proteins, activated neutrophils, and alveolar macrophages into the cleavage products C5a and C5b[173]. C5b initiates and is a member of MAC while C5a is pleiotropic chemotactic and proinflammatory molecule. Upon binding its receptor C5aR, which is expressed on a number of cells, C5a induces numerous cellular functions that promote inflammation[174].

In T cells, C5a acts as a co-stimulatory molecule that promotes survival and proliferation. When an APC primes a T cell, C5a in addition to its cognate receptor is upregulated by both the T cell and APC[175,176]. If the C5aR is blocked on either the APC or the T cell, this results in inhibited T cell activation in both cases, indicating that C5a signalling in the APC is required to prime the T cell regardless of C5a signalling in the T cell. C5a signalling in the APC may be involved in maturation and activation as well; as upregulation of C5 and C5aR was shown to occur before the upregulation of CD80/CD86. In a mouse model of GvHD, reconstituting recipient mice with T cells deficient for C5aR reduced the GvHD phenotype, conversely, transplantation of Daf1$^{-/-}$ bone marrow cells exacerbated GvHD[177] and this observation was attributed to C5a production[175]. Furthermore, pharmacological blockade of the C5a receptor on human T cells reduced GvHD scores in a xenograft model of disease[178]. In a parent -> F1 mouse model of aGvHD, MACs were found deposited in the skin, liver, lung, and kidney[179]. These data suggest one or both cleavage products of C5 may contribute to the pathology of GvHD. However, as T cell activation is upstream of tissue damage, C5a signalling may be playing a larger role in GvHD than C5b.

In **Chapter 2**, we examined the role of complement protein C5 in a mouse model of GvHD. Specifically, we used B10.D2 donor mice that contain a 2 base pair deletion in the C5 gene. These mice translate a nonfunctional C5 protein that is not secreted out of the cell[180]. We transplanted $1x10^6$ bone marrow and $2x10^6$ RBC free spleen cells from $C5^-$ or congenic $C5^+$ donor mice into irradiated BALB/c recipient mice. We then tracked the recipient mice up to 90 days post-transplant and observed that transplantation of C5 deficient spleen and bone marrow cells did not result in lung manifestations of GvHD. Specifically, the recipient mice did not display perivascular inflammation at day 60 post-transplant and were protected from peribronchiolar fibrosis at day 90. In the mice that were reconstituted with $C5^+$ donor cells, analysis of the lung inflammatory cells at day 60 revealed a significant number of the peribronchiolar infiltrate cells were CD4+ and CD8+ **(Chapter 2. Figure 3& 4).** In contrast, there were no CD4+ or CD8+ cells in the lungs of the mice that were reconstituted with $C5^-$ donor cells. While CD4+ and CD8+ can be expressed on cells (DCs) other than T cells, the migratory nature of the cells we observed in the lungs is line with the reported function of activated T cells in GvHD models[27]. Therefore we believe these inflammatory cells are T cells. Furthermore, confirmation of donor cell engraftment using flow cytometry suggests that the absent inflammation in the $C5^-$ transplant group was a result of absent C5 signalling as opposed engraftment failure. While these findings were not entirely novel given previous reports that C5 mediates alloimmunity in human T cells[178]; it is important to note that recipient mice were C5 sufficient in all cases. The observation that protection from developing GvHD is dependent on donor cell-derived C5 indicates that GvHD in our model is mediated by

donor APCs. As GvL is mediated by recipient APCs and GvHD by donor APCs[138], targetting C5 in the donor cells may represent a new approach to target GvHD while maintaining GvL.

The C5-C5a axis is involved in the pathologies of many diseases including sepsis, rheumatoid arthritis, inflammatory bowel disease, ischemia-reperfusion injury, antiphospholipid syndrome, systemic lupus erythematosus, psoriasis, neurodegenerative disease, age-related macular degeneration, and cancer[181]. As such, there has been a number of agents created and tested to inhibit this pathway. These include synthetic molecules, antibodies or naturally occurring molecules derived from nature that target different points along the C5–C5a receptor axis. These include blocking cleavage of C5 into C5a and C5b, blocking C5a signalling or blocking the C5a receptor. However, despite the numerous research studies that have investigated inhibitors of C5, C5a or C5aR, currently only one antibody, eculizumab has been approved for clinical use[182]. Eculizumab is a mouse-derived humanized antibody, which binds to C5 with high affinity and prevents cleavage of C5 into C5a and C5b[183]. While studies continue investigating these inhibitors, it is important to note that non-specific inhibition of this pathway may have unwanted side effects on host defense. C5a has been shown to protect against glutamate-induced apoptosis in neurons[184], exert anti-inflammatory effects in patients with pancreatitis[185], promote inhibition of angiogenesis[186], and is involved in the early stages of liver regeneration[186]. One strategy to overcome this issue maybe targeted therapy. Macor et al[187] described the use of a C5 neutralizing antibody fused to a small

peptide that only targets inflamed synovium tissues in an arthritis model. In an HSCT setting, one strategy could involve using a similar approach to selectively block the C5aR on donor APCs prior to reconstituting the patient, thereby inhibiting the maturation of donor APCs and preventing donor T cell activation as a consequence. Another approach could utilize gene editing technologies (CRISPR/Cas9) to knock out the C5 and/or C5aR genes in donor APCs. Using these two approaches will leave donor T cell intact to mediate GvL through recipient APCs. In time, as the patient is completely reconstituted and de novo produced T cells are tolerized to recipient antigens in the thymus and periphery, the risk of developing GvHD should decrease.

Future Directions in the C5 Model

Before proceeding with strategies to inhibit C5 signalling in the donor cells. There are a few questions that need to be addressed in our C5 model. We need to first identify if the GvL effect occurs in this model. This can be investigated by first transplanting leukemia cells into the recipient mice and then reconstituting the with $C5^+$ donor cells. We can then monitor the mice for the presence of leukemia cells. Upon confirmation that the GvL effect is occurring, we can follow up this experiment with a second experiment whereby we test if the GvL effect is maintained when $C5^-$ donor cells are used to reconstitute the recipient mice. Next, we need to determine which donor cell(s) is producing C5, as T cells, macrophages, and dendritic cells have all been reported to express C5. This can be investigated by collecting spleen and/or lymph node cells at various time points post-transplant; the different immune cell populations can then be isolated using fluorescence

or magnetically activated cell sorting and then using RNA-seq we can examine the upregulation of C5 and C5aR in both donor and recipient cell types. This data can then be used to determine appropriate target cells for future therapeutic strategies. Another question that should be addressed is if the absence of C5 signalling is sufficient to prevent major mismatch induced GvHD as this is clinically more relevant. There are a number of established and well-described mouse models of major mismatched GvHD that will allow us to easily compare and assess the impact of donor C5 deficiency[27].

Cellular Therapies for GvHD

In addition to pharmacological blockade of GvHD, cellular therapies have also been investigated whereby the donor graft is manipulated to alter the GvHD response.
NK cells are one of two immune cells that mediate the GvL response, but they do not induce GvHD. Use of NK cells in murine models of GvHD have shown that they not only kill leukemia cells but also residual host hematopoietic cells and APCs thereby also preventing aGvHD[188]. In a clinical trial exploring the potential of NK cells therapy for treatment of leukemia, 57 AML patients and 35 ALL patients were transplanted with T cell depleted HLA mismatched $CD34^+$ HSCs. While patients with AML were protected from leukemia relapse and GvHD, patients with ALL were not protected from relapse or GvHD[189]. This observation may be explained by the fact the ALL and AML are different types of cancer and NK cells are only efficient in mediating the GvL response when the

donor-recipient HLA mismatch combination can fully exploit the KIR–MHC mismatch pathway.

Mesenchymal stem cell (MSC) therapy is another possible cell therapy of GvHD. MSCs are non-hematopoietic self-renewing multipotent adult stem cells that can modulate immune responses and differentiate into chondrocytes, osteoblasts, or adipocytes[190]. MSCs can be harvested from skeletal muscle, adipose tissue, umbilical cord, synovium, circulatory system, dental pulp, amniotic fluid, fetal blood, liver, bone marrow, and lung tissues[191]. MSCs express a number of chemokine receptors (CCR2, CCR3, CCR4, and CCL5)[192] that allow them to migrate into activate sites of inflammation and then become activated by IFN-γ, TNF-α or IL-1 β. The activated MSCs can then down-regulate immune responses through the release of microvesicles and anti-inflammatory mediators that inhibit T cell proliferation, maturation of monocyte and activation of macrophages, B cell and APCs [193]. In vitro assays have revealed a number of these immune modulating factors; Nitric oxide (NO), Indoleamine 2, 3-dioxygenase (IDO), Prostaglandin E2 (PGE2) and IL-10[193]. NO inhibits T cell proliferation through STAT5 phosphorylation and induction of apoptosis [194]. IDO catalyzes the degradation of tryptophan, the metabolites generated from tryptophan degradation suppressed T cells[195]. PGE2 suppresses T cells, NK cells, and macrophages activity[196]. Mixed lymphocyte reactions (MLR) using a 1:10 ratio of MSC to lymphocyte[197] have shown that MSCs increase the number of iTregs [198] while also inhibiting the activation of CD4+ and CD8+ T cells. However, adding MSCs to the MLR on day 3 or supplementing the MLR with IL-2

reduces their ability to suppress the activation of T cells[199,200]. This suggests that MSCs only prevent T cell activation but do not suppressive the functional ability of effector T cells.

In addition to regulating immune responses, MSCs also promote tissue repair through secretion of effector molecules including; chemokines, growth factors, microvesicles, and ECM. The ECM molecules provide scaffolding for new cell growth, growth factors can promote the division and migration of endothelial cells to form new blood vessels [201]. Microvesicles which bud off from MSCs have membrane-bound adhesion and signalling molecules and are filled with hundreds of proteins, and modulating mRNA and microRNAs[202,203]. These microvesicles can fuse with target cells and transfer the proteins and genetic material which can reprogram and regulate the target cells.

A key advantage of MSC therapy is that they resistant to lysis by CTLs and NK cells. MSCs express low levels of MHC I, little to no MHC class II and no CD80/86 co-stimulatory molecules. As such, MSCs used for therapeutic interventions can be derived from, autologous, allogeneic or xenogeneic sources without concerns of rejections. MSCs based therapies have been used in the treatment of aGvHD in animal studies[204], but studies of MSC treatments to prevent cGvHD are limited. There is only one mouse study that has shown the use of MSCs to reduce skin involvement in mice with established cGvHD. As both aGvHD and cGvHD are mediated by allogeneic T cells responses, MSC therapies that prevent aGvHD may also prevent murine cGvHD. Additionally, as MSCs promote tissue injury repair and have been shown to reduce skin manifestations in

cGvHD mice, they may be effective at promoting repair of liver and lung tissues as well. However, preclinical animal studies investigating MSC therapy has yielded inconsistent and contrasting results[205].

Cell therapy using Tregs has also been investigated as a treatment option for GvHD given their immunosuppressive capabilities. Tregs are a subset of CD4+ T cells that represent 5–10% of the total T cell pool in human and rodents. When allogeneic HSCT is performed, both Tregs and naïve T cells are simultaneously transplanted. However, when examining patients with cGvHD, the number of Treg is reduced. This may be caused by the proinflammatory environment in GvHD patients which promotes differentiation of naïve T cells into effector T cells[206]. As such, studies investigating transplantation of extra Tregs have been explored; in murine models of allogeneic HSCT, depletion of Tregs from the donor cells was shown to increase aGvHD symptoms, in contrast, when the donor cells were supplemented with extra nTregs, GvHD symptoms were reduced[207,208]. The beneficial effects of Treg transplantation have also been shown in human trials using HLA-matched related donor transplants[209]. Furthermore, Tregs do not appear to inhibit the GvL response. In vitro studies have shown that nTregs do not inhibit the ability of the alloreactive CD8+ T cells to target and kill cancer cells, and this finding was also confirmed in murine models[210]. Murine models of GvHD have shown that Treg therapy is only successful when a minimum of 1:1 Treg to effector T cell is transplanted[211]. However, Tregs are only a small proportion of all the peripheral T cells

and attempts to expand them in vitro while maintaining suppressive activity have produced mixed results.

In contrast, it is possible to efficiently generate iTregs in vitro[212], however, transplantation of in vitro generated iTregs was not shown to protect mice from GvHD. This was shown be a result of the instability of the iTregs in vivo, furthermore, they can lose the expression of FoxP3 along with their immunosuppressive capacity upon transplantation,[213,214] likely due to inflammation-induced reversion back to effector T cells.

We propose that using peptide immunotherapy will overcome the current issues of extracellular Treg therapy by generating iTregs in vivo while also selectively removing alloantigen-specific T cells. This will effectively alter the Treg to effector T cell ratio by removing those T cells that are specific for recipient-derived antigens while simultaneously increasing the number of immunosuppressive Treg cells. A benefit of this approach is that peptide immunotherapy does not target T cells that are specific for leukemia cells and therefore should preserve the GvL effect. As described in **Chapter 4**, we explored the use of peptide immunotherapy as a therapy for GvHD. To test our hypothesis that peptide immunotherapy would inhibit GvHD, we first generated a humanized model of GvHD as described in **Chapter 3**. Using transgenic C57BL/6 donor mice that express mouse MHC I and a hybrid class II MHC/HLA molecule that retains binding specificity of human class II HLA-DRB1*0401; we reconstituted transgenic

C57BL/6 mice that express mouse MHC class I and II and full-length human class I HLA-A2*0201. We hypothesize that upon HSCT, donor CD4+ T cells may be directly activated by recipient APCs expressing mouse MHC II and presenting peptides derived from miHC, MHC I, MHC II, and human HLA-A2*0201. In this scenario, the activated donor CD4+ T cells would only target recipient MHC II expressing cells (In the context of HSCT for a leukemia patient, this is a desirable immune response). Through the indirect pathway, donor CD4+ T cells may be activated by donor APCs expressing HLA-DRB1*0401 and presenting HLA-A2*0201 derived peptides. Donor CD8+ T cells can be indirectly or directly activated by HLA-A2*0201 derived peptides presented by MHC I or directly activated by miHC, MHC I, and HLA-A2*0201 derived peptides presented in the context of HLA-A2*0201. Through a combination of these various donor T cell activation events, the recipient mice should develop GvHD.

Indeed, at day 60 post-transplant, we observed lung inflammation, skin and liver fibrosis in the recipient mice. This suggests that both aGvHD and cGvHD pathways are active in this model, however, future studies investigating the activation status of donor CD8+ and CD4+ T cells are required to confirm this hypothesis. An initial attempt to assess the serum from this mice failed to detect anti-HLA-A2 antibodies. This could be a result of the GvHD response being mediated by antigens other than HLA-A2 or a failure of the assay to detect mouse Ig isotypes. Future studies will need to discern which specific antigens donor T cells are responding against.

Using this model, we then tested peptide immunotherapy as a means of inhibiting or reducing GvHD. We chose 4 peptides derived from the transmembrane domain of HLA-A2*0201 and used them to treat recipient mice following HSCT. One could make the argument that using peptides derived from MHC/HLA molecules is illogical as these proteins are allelically diverse, however, it is important to note that most of the diversity within the HLA molecules lies within the amino acids that generate the peptide binding groove[30]. In contrast, the amino acids that form part of the transmembrane domain are relatively conserved within the population, likely due to structural and functional constraints. We can exploit this feature by choosing peptides that can potentially be used across a range of mismatched transplants. While it is unlikely that a single peptide or pool of peptides will cover the entire population, one can envision a scenario where libraries of different peptide combinations have been characterized and documented to be effective in various combinations of mismatched HSCTs.

One could also argue that using peptides derived from HLA-A2*0201 for immunotherapy would only confer protection against T cells specific for HLA-A2*0201. However, given that MHC molecules are co-dominantly expressed on APCs, we believe that iTregs specific for HLA-A2*0201 will expand the number of anergized alloreactive T cells and new iTregs through linked suppression and infectious tolerance mechanisms such that in time, donor T cells will be tolerant of all recipients derived antigens. This phenomenon has been documented in animal models of skin[215] and heart transplant[216] and may also

function in HSCT as the mechanisms of rejection in organ transplant and GvHD is similar.

Future Directions in the humanized Model

As described in **Chapter 4,** our first attempt at peptide immunotherapy did not yield favorable results. In some cases, use of peptides exacerbated the GvHD response, this suggests that T cells may have become sensitized against HLA-A2 as opposed to tolerized, therefore it suggests that GvHD in our model is at least partially mediated by anti-HLA-A2 responses. We have discussed some possibilities as to why peptide therapy may have failed in **Chapter 4.** Briefly, we believe the biggest reason was the timing of treatment. Recipient mice were administered peptides between days 9 and 23 post-transplant when rampant inflammation likely persisted. An alternative approach may be to pre-tolerize the donor mice and then perform the HSCT. In this scenario, naïve T cells would be presented with HLA-A2 derived peptides under non-inflammatory conditions and alloantigen-specific T cells would be anergized. A simplified version of this approach is described in **Chapter 4 Figure 2** whereby spleen cells from peptide-treated HLA-DR4^{+} donor mice were used in an MLR with spleen cells from HLA-A2^{+} recipient mice. The results of this assay were inconclusive as the magnitude of the MLR response from untreated donor mice did not match the response observed in **Chapter 4 Figure 1.** A key difference between the experiments in **Chapter 4 Figure 1** and **Chapter 4 Figure 2** is that the peptide treated donor cells were cryopreserved prior to conducting the MLR. It is possible this extra freeze-thaw step altered the phenotype and/or functionality of the

peptide-treated cells. Interestingly, in a study investigating the use of CD4+CD25+FoxP3^{+} T regulatory cells to treat GvHD, cryopreservation of the Tregs was shown to reduce CD62L expression and these Tregs were incapable of protecting mice against GvHD[217]. While CD62L is unlikely to play a major role during in vitro MLRs. It is not inconceivable that cryopreservation may alter other aspects of Treg biology as well. Furthermore, as mentioned in the discussion of chapter 4, the peptides were found to be contaminated with endotoxin. As such, this warrants a repeat of the pre-tolerization protocol using "cleaner" peptides. However, a practical and cost-effective alternative approach to determining the efficacy of peptide treatment would be to first assess the peptide treated donor mice for the presence and frequency of peptide-specific Tregs using HLA-DRB1*0401 tetramers and flow cytometry. This approach will likely speed up the discovery of optimal peptides and doses prior to testing in long-term animal studies. Finally, once we can show that peptide therapy is effective in preventing GvHD, we need to establish that the GvL effect can occur in this model as well and peptide therapy does not abolish it.

Concluding Statements

Graft vs Host disease was serendipitously discovered when allogeneic bone marrow and lymph node cells were used to transplant irradiated mice with leukemia. Interestingly, the graft vs leukemia effect was also discovered during this investigational study. Over the years, the work of numerous researchers and studies conducted throughout the world have characterized both GvHD and GvL. Studies in canines and mice have characterized the role of TBI, the requirement of MHC matching, the contribution of donor CD8+ T cells, CD4+ T cells and B cells. They have also defined the two main subtypes of GvHD, (acute and chronic), and the target organs and degree of involvement in each tissue. The results of these studies have been instrumental in guiding clinicians and scientist in developing efficient bone marrow transplant protocols that have improved the survival rate from 0% in 1957 to over 70% and have helped thousands of cancer patients worldwide as international transplants centers have been established. However, in the nearly 70 years since GvHD was discovered, an effective strategy to prevent and or inhibit the disease remains elusive. As the fundamental principles of allogeneic rejection that promote the desired Graft vs leukemia effect also promote the rejection of healthy tissues, it has been difficult designing therapies that selectively target GvHD while not affecting the GvL effect. As scientists have begun to tease out the differences between GvHD and GvL, this has facilitated the development of newer drugs and strategies to tackle the issue of GvHD. As of July 2018, a query of “GvHD” on the NIH clinical trial's website (www.clinicaltrials.gov/), a database of worldwide clinical trials, yields a search result of 740 ongoing and completed trials conducted for the therapy of GvHD. As described

above, many of these therapies have been shown to be effective in preclinical animal models, however, in the clinic, results have usually varied. This discrepancy between preclinical animal models and clinical trials may be due to compounding factors such as patient age, cancer burden, the sensitivity of cancer to GvL, the degree of HLA mismatch, and secondary infections and use of immunosuppressive therapies. Unlike in humans, these factors can be tightly controlled and regulated in the laboratory animals. Furthermore, given the immense complexity and incredible redundancy that exists within the allogeneic immune response; from multiple proinflammatory cytokines that can activate the recipient and donor APCs, numerous chemokine signalling pathways, multiple target alloantigens antigens and co-stimulatory molecules involved in activating alloreactive T cells, it is unlikely that single drug or therapy will completely abolish or prevent GvHD. Rather, a combination therapy is likely required to target multiple arms of the alloresponse such that it will destabilize the entire response.

The studies and mouse models described in this thesis do not add to the body of knowledge of how GvHD is initiated or which organs are involved but rather examines two new approaches to target GvHD. However, of the two proposed strategies, peptide immunotherapy is perhaps the most alluring. Unlike pharmacological inhibitors that try to block and work against the natural immune response, Peptide therapy exploits a natural feature of the immune system and works with it to achieve its intended purpose. Simply put, transplant rejection and GvHD is caused by a glitch in the evolutionary code of the immune system, and rather than try to block the code, the fix may lie in exploiting the natural features within the code itself.

References For Chapter 1 and 5

1. Jacobson LO, Simmons EL, Marks EK, Eldredge JH. Recovery from radiation injury. *Science*. 1951;113(2940):510-511.
2. Ford CE, Hamerton JL, Barnes DWH, Loutit JF. Cytological Identification of Radiation-Chimæras. *Nature*. 1956;177:452.
3. Lorenz E, Uphoff D, Reid TR, Shelton E. Modification of irradiation injury in mice and guinea pigs by bone marrow injections. *J Natl Cancer Inst*. 1951;12(1):197-201.
4. Becker AJ, Mc CE, Till JE. Cytological demonstration of the clonal nature of spleen colonies derived from transplanted mouse marrow cells. *Nature*. 1963;197:452-454.
5. Barnes DW, Loutit JF. Treatment of murine leukaemia with x-rays and homologous bone marrow. II. *Br J Haematol*. 1957;3(3):241-252.
6. Uphoff DE. Genetic factors influencing irradiation protection by bone marrow. I. The F1 hybrid effect. *J Natl Cancer Inst*. 1957;19(1):123-130.
7. Snell GD. The Nobel Lectures in Immunology. Lecture for the Nobel Prize for Physiology or Medicine, 1980: Studies in histocompatibility. *Scand J Immunol*. 1992;36(4):513-526.
8. Thomas ED, Lochte HL, Jr., Lu WC, Ferrebee JW. Intravenous infusion of bone marrow in patients receiving radiation and chemotherapy. *N Engl J Med*. 1957;257(11):491-496.
9. Thomas ED, Lochte HL, Jr., Cannon JH, Sahler OD, Ferrebee JW. Supralethal whole body irradiation and isologous marrow transplantation in man. *J Clin Invest*. 1959;38:1709-1716.
10. Thomas ED, LeBlond R, Graham T, Storb R. Marrow infusions in dogs given midlethal or lethal irradiation. *Radiat Res*. 1970;41(1):113-124.
11. Bull MI, Herzig GP, Graw RG, Jr., Krueger GR, Bowles CA. Canine allogeneic bone marrow transplantation. Technique and variables influencing engraftment. *Transplantation*. 1976;22(2):150-159.
12. Kolb HJ, Rieder I, Bodenberger U, et al. Dose rate and dose fractionation studies in total body irradiation of dogs. *Pathol Biol (Paris)*. 1979;27(6):370-372.
13. Storb R, Raff RF, Appelbaum FR, et al. What radiation dose for DLA-identical canine marrow grafts? *Blood*. 1988;72(4):1300-1304.
14. Storb R, Epstein RB, Rudolph RH, Thomas ED. Allogeneic canine bone marrow transplantation following cyclophosphamide. *Transplantation*. 1969;7(5):378-386.
15. Kolb HJ, Storb R, Weiden PL, et al. Immunologic, toxicologic and marrow transplantation studies in dogs given dimethyl myleran. *Biomedicine*. 1974;20(5):341-351.
16. Appelbaum FR, Brown P, Sandmaier B, et al. Antibody-radionuclide conjugates as part of a myeloablative preparative regimen for marrow transplantation. *Blood*. 1989;73(8):2202-2208.
17. Sullivan RD, Stecher G, Sternberg SS. Value of bone marrow and spleen cell suspensions for survival of lethally irradiated dogs. *J Natl Cancer Inst*. 1959;23:367-383.
18. Appelbaum FR. Hemopoietic reconstitution following autologous bone marrow and peripheral blood mononuclear cell infusions. *Exp Hematol*. 1979;7 Suppl 5:7-11.
19. Storb R, Deeg HJ, Raff R, et al. Prevention of graft-versus-host disease. Studies in a canine model. *Ann N Y Acad Sci*. 1995;770:149-164.
20. Thomas ED, Buckner CD, Rudolph RH, et al. Allogeneic marrow grafting for hematologic malignancy using HL-A matched donor-recipient sibling pairs. *Blood*. 1971;38(3):267-287.

21. Thomas ED, Buckner CD, Banaji M, et al. One hundred patients with acute leukemia treated by chemotherapy, total body irradiation, and allogeneic marrow transplantation. *Blood*. 1977;49(4):511-533.
22. Thomas ED, Buckner CD, Clift RA, et al. Marrow transplantation for acute nonlymphoblastic leukemia in first remission. *N Engl J Med*. 1979;301(11):597-599.
23. Henig I, Zuckerman T. Hematopoietic stem cell transplantation-50 years of evolution and future perspectives. *Rambam Maimonides Med J*. 2014;5(4):e0028.
24. Billingham RE. Studies on the reaction of injected homologous lymphoid tissue cells against the host. *Ann N Y Acad Sci*. 1958;73(3):782-788.
25. Lonai P, Eliraz A, Wekerle H, Feldman M. Depletion of specific graft-versus-host reactivity following adsorption of nonsensitized lymphocytes on allogeneic fibroblasts. *Transplantation*. 1973;15(4):368-374.
26. Quantitative studies on tissue transplantation immunity IV. Induction of tolerance in newborn mice and studies on the phenomenon of runt disease. *Philosophical Transactions of the Royal Society of London Series B, Biological Sciences*. 1959;242(694):439-477.
27. Schroeder MA, DiPersio JF. Mouse models of graft-versus-host disease: advances and limitations. *Disease Models & Mechanisms*. 2011;4(3):318-333.
28. Higo S, Shimizu A, Masuda Y, et al. Acute graft-versus-host disease of the kidney in allogeneic rat bone marrow transplantation. *PLoS One*. 2014;9(12):e115399.
29. Nagler RM, Laufer D, Nagler A. Parotid gland dysfunction in a murine model of acute graft versus host disease [aGVHD]. *Head Neck*. 1998;20(1):58-62.
30. Imanguli MM, Alevizos I, Brown R, Pavletic SZ, Atkinson JC. Oral graft-versus-host disease. *Oral diseases*. 2008;14(5):396-412.
31. Dertschnig S, Hauri-Hohl MM, Vollmer M, Hollander GA, Krenger W. Impaired thymic expression of tissue-restricted antigens licenses the de novo generation of autoreactive CD4+ T cells in acute GVHD. *Blood*. 2015;125(17):2720-2723.
32. Min CK. The pathophysiology of chronic graft-versus-host disease: the unveiling of an enigma. *Korean J Hematol*. 2011;46(2):80-87.
33. Joseph RW, Couriel DR, Komanduri KV. Chronic graft-versus-host disease after allogeneic stem cell transplantation: challenges in prevention, science, and supportive care. *J Support Oncol*. 2008;6(8):361-372.
34. Ferrara JLM, Levine JE, Reddy P, Holler E. Graft-versus-Host Disease. *Lancet*. 2009;373(9674):1550-1561.
35. Giridhar P, Mallick S, Rath GK, Julka PK. Radiation induced lung injury: prediction, assessment and management. *Asian Pac J Cancer Prev*. 2015;16(7):2613-2617.
36. Brittan M, Wright NA. Gastrointestinal stem cells. *J Pathol*. 2002;197(4):492-509.
37. Doe WF. The intestinal immune system. *Gut*. 1989;30(12):1679-1685.
38. Duran-Struuck R, Dysko RC. Principles of bone marrow transplantation (BMT): providing optimal veterinary and husbandry care to irradiated mice in BMT studies. *J Am Assoc Lab Anim Sci*. 2009;48(1):11-22.
39. R Hill G. Inflammation and Bone Marrow Transplantation. Vol. 15; 2008.
40. Roncarolo MG, Battaglia M. Regulatory T-cell immunotherapy for tolerance to self antigens and alloantigens in humans. *Nat Rev Immunol*. 2007;7(8):585-598.
41. Wysocki CA, Panoskaltsis-Mortari A, Blazar BR, Serody JS. Leukocyte migration and graft-versus-host disease. *Blood*. 2005;105(11):4191-4199.

42. Murai M, Yoneyama H, Ezaki T, et al. Peyer's patch is the essential site in initiating murine acute and lethal graft-versus-host reaction. *Nature Immunology*. 2003;4:154.
43. Xia G, Truitt RL, Johnson BD. Graft-versus-leukemia and graft-versus-host reactions after donor lymphocyte infusion are initiated by host-type antigen-presenting cells and regulated by regulatory T cells in early and long-term chimeras. *Biol Blood Marrow Transplant*. 2006;12(4):397-407.
44. Burman AC, Banovic T, Kuns RD, et al. IFNgamma differentially controls the development of idiopathic pneumonia syndrome and GVHD of the gastrointestinal tract. *Blood*. 2007;110(3):1064-1072.
45. Iclozan C, Yu Y, Liu C, et al. T helper17 cells are sufficient but not necessary to induce acute graft-versus-host disease. *Biol Blood Marrow Transplant*. 2010;16(2):170-178.
46. Yu Y, Wang D, Liu C, et al. Prevention of GVHD while sparing GVL effect by targeting Th1 and Th17 transcription factor T-bet and RORgammat in mice. *Blood*. 2011;118(18):5011-5020.
47. Teshima T, Ordemann R, Reddy P, et al. Acute graft-versus-host disease does not require alloantigen expression on host epithelium. *Nat Med*. 2002;8(6):575-581.
48. Watanabe Y, Kawakami H, Kawamoto H, et al. Effect of neonatal thymectomy on experimental autoimmune hepatitis in mice. *Clinical and Experimental Immunology*. 1987;67(1):105-113.
49. Tung KS, Smith S, Matzner P, et al. Murine autoimmune oophoritis, epididymoorchitis, and gastritis induced by day 3 thymectomy. Autoantibodies. *Am J Pathol*. 1987;126(2):303-314.
50. Sakoda Y, Hashimoto D, Asakura S, et al. Donor-derived thymic-dependent T cells cause chronic graft-versus-host disease. *Blood*. 2007;109(4):1756-1764.
51. Na IK, Lu SX, Yim NL, et al. The cytolytic molecules Fas ligand and TRAIL are required for murine thymic graft-versus-host disease. *J Clin Invest*. 2010;120(1):343-356.
52. Wu T, Young JS, Johnston H, et al. Thymic damage, impaired negative selection, and development of chronic graft-versus-host disease caused by donor CD4+ and CD8+ T cells. *J Immunol*. 2013;191(1):488-499.
53. Hauri-Hohl MM, Keller MP, Gill J, et al. Donor T-cell alloreactivity against host thymic epithelium limits T-cell development after bone marrow transplantation. *Blood*. 2007;109(9):4080-4088.
54. Allison AC, Denman AM, Barnes RD. Cooperating and controlling functions of thymus-derived lymphocytes in relation to autoimmunity. *Lancet*. 1971;2(7716):135-140.
55. Cooke KR, Luznik L, Sarantopoulos S, et al. The Biology of Chronic Graft-versus-Host Disease: A Task Force Report from the National Institutes of Health Consensus Development Project on Criteria for Clinical Trials in Chronic Graft-versus-Host Disease. *Biology of Blood and Marrow Transplantation*. 2017;23(2):211-234.
56. Zeiser R, Blazar BR. Pathophysiology of Chronic Graft-versus-Host Disease and Therapeutic Targets. *N Engl J Med*. 2017;377(26):2565-2579.
57. Svegliati S, Olivieri A, Campelli N, et al. Stimulatory autoantibodies to PDGF receptor in patients with extensive chronic graft-versus-host disease. *Blood*. 2007;110(1):237-241.
58. Socié G, Schmoor C, Bethge WA, et al. Chronic graft-versus-host disease: long-term results from a randomized trial on graft-versus-host disease prophylaxis with or without anti–T-cell globulin ATG-Fresenius. *Blood*. 2011;117(23):6375-6382.
59. Finke J, Bethge WA, Schmoor C, et al. Standard graft-versus-host disease prophylaxis with or without anti-T-cell globulin in haematopoietic cell transplantation from matched

unrelated donors: a randomised, open-label, multicentre phase 3 trial. *The Lancet Oncology*. 2009;10(9):855-864.
60. Luznik L, Bolaños-Meade J, Zahurak M, et al. High-dose cyclophosphamide as single-agent, short-course prophylaxis of graft-versus-host disease. *Blood*. 2010;115(16):3224-3230.
61. Kanakry CG, Tsai H-L, Bolaños-Meade J, et al. Single-agent GVHD prophylaxis with posttransplantation cyclophosphamide after myeloablative, HLA-matched BMT for AML, ALL, and MDS. *Blood*. 2014;124(25):3817-3827.
62. Schroeder MA, DiPersio JF. Mouse models of graft-versus-host disease: advances and limitations. *Dis Model Mech*. 2011;4(3):318-333.
63. Ralph DD, Springmeyer SC, Sullivan KM, Hackman RC, Storb R, Thomas ED. Rapidly progressive air-flow obstruction in marrow transplant recipients. Possible association between obliterative bronchiolitis and chronic graft-versus-host disease. *Am Rev Respir Dis*. 1984;129(4):641-644.
64. Chien JW, Duncan S, Williams KM, Pavletic SZ. Bronchiolitis Obliterans Syndrome After Allogeneic Hematopoietic Stem Cell Transplantation - An Increasingly Recognized Manifestation of Chronic Graft-versus-Host Disease. *Biology of blood and marrow transplantation : journal of the American Society for Blood and Marrow Transplantation*. 2010;16(1 Suppl):S106-S114.
65. Phan SH. Biology of Fibroblasts and Myofibroblasts. *Proceedings of the American Thoracic Society*. 2008;5(3):334-337.
66. Levi-Schaffer F, Piliponsky AM. Tryptase, a novel link between allergic inflammation and fibrosis. *Trends in Immunology*. 2003;24(4):158-161.
67. Hart J. Inflammation. 1: Its role in the healing of acute wounds. *J Wound Care*. 2002;11(6):205-209.
68. Wah TM, Moss HA, Robertson RJ, Barnard DL. Pulmonary complications following bone marrow transplantation. *Br J Radiol*. 2003;76(906):373-379.
69. Kitko CL, White ES, Baird K. Fibrotic and sclerotic manifestations of chronic graft-versus-host disease. *Biol Blood Marrow Transplant*. 2012;18(1 Suppl):S46-52.
70. Hamilton PJ, Pearson AD. Bone marrow transplantation and the lung. *Thorax*. 1986;41(7):497-502.
71. Davis RE, Smoller BR. T lymphocytes expressing HECA-452 epitope are present in cutaneous acute graft-versus-host disease and erythema multiforme, but not in acute graft-versus-host disease in gut organs. *The American Journal of Pathology*. 1992;141(3):691-698.
72. Esteban JM, Somlo G. Skin biopsy in allogeneic and autologous bone marrow transplant patients: a histologic and immunohistochemical study and review of the literature. *Mod Pathol*. 1995;8(1):59-64.
73. Hogan WJ, Maris M, Storer B, et al. Hepatic injury after nonmyeloablative conditioning followed by allogeneic hematopoietic cell transplantation: a study of 193 patients. *Blood*. 2004;103(1):78-84.
74. McDonald GB, Shulman HM, Sullivan KM, Spencer GD. Intestinal and hepatic complications of human bone marrow transplantation. Part II. *Gastroenterology*. 1986;90(3):770-784.
75. Epstein O, Thomas HC, Sherlock S. Primary biliary cirrhosis is a dry gland syndrome with features of chronic graft-versus-host disease. *Lancet*. 1980;1(8179):1166-1168.
76. Goker H, Haznedaroglu IC, Chao NJ. Acute graft-vs-host disease: pathobiology and management. *Exp Hematol*. 2001;29(3):259-277.

77. McDonald GB, Sullivan KM, Schuffler MD, Shulman HM, Thomas ED. Esophageal abnormalities in chronic graft-versus-host disease in humans. *Gastroenterology*. 1981;80(5 pt 1):914-921.
78. Chaplin DD. Overview of the Immune Response. *The Journal of allergy and clinical immunology*. 2010;125(2 Suppl 2):S3-23.
79. Lind EF, Prockop SE, Porritt HE, Petrie HT. Mapping precursor movement through the postnatal thymus reveals specific microenvironments supporting defined stages of early lymphoid development. *J Exp Med*. 2001;194(2):127-134.
80. Zúñiga-Pflücker JC. When Three Negatives Made a Positive Influence in Defining Four Early Steps in T Cell Development. *The Journal of Immunology*. 2012;189(9):4201-4202.
81. Ciofani M, Zuniga-Pflucker JC. Determining gammadelta versus alphass T cell development. *Nat Rev Immunol*. 2010;10(9):657-663.
82. Ciofani M, Zuniga-Pflucker JC. The thymus as an inductive site for T lymphopoiesis. *Annu Rev Cell Dev Biol*. 2007;23:463-493.
83. Starr TK, Jameson SC, Hogquist KA. Positive and negative selection of T cells. *Annu Rev Immunol*. 2003;21:139-176.
84. Anderson MS, Venanzi ES, Chen Z, Berzins SP, Benoist C, Mathis D. The cellular mechanism of Aire control of T cell tolerance. *Immunity*. 2005;23(2):227-239.
85. Derbinski J, Gabler J, Brors B, et al. Promiscuous gene expression in thymic epithelial cells is regulated at multiple levels. *J Exp Med*. 2005;202(1):33-45.
86. Gallegos AM, Bevan MJ. Central tolerance to tissue-specific antigens mediated by direct and indirect antigen presentation. *J Exp Med*. 2004;200(8):1039-1049.
87. Koble C, Kyewski B. The thymic medulla: a unique microenvironment for intercellular self-antigen transfer. *J Exp Med*. 2009;206(7):1505-1513.
88. Aschenbrenner K, D'Cruz LM, Vollmann EH, et al. Selection of Foxp3+ regulatory T cells specific for self antigen expressed and presented by Aire+ medullary thymic epithelial cells. *Nat Immunol*. 2007;8(4):351-358.
89. Hanabuchi S, Ito T, Park WR, et al. Thymic stromal lymphopoietin-activated plasmacytoid dendritic cells induce the generation of FOXP3+ regulatory T cells in human thymus. *J Immunol*. 2010;184(6):2999-3007.
90. Sakaguchi S, Miyara M, Costantino CM, Hafler DA. FOXP3+ regulatory T cells in the human immune system. *Nat Rev Immunol*. 2010;10(7):490-500.
91. Liu Y, Zhang P, Li J, Kulkarni AB, Perruche S, Chen W. A critical function for TGF-beta signaling in the development of natural CD4+CD25+Foxp3+ regulatory T cells. *Nat Immunol*. 2008;9(6):632-640.
92. Wang F, Huang C-Y, Kanagawa O. Rapid deletion of rearranged T cell antigen receptor (TCR) Vα-Jα segment by secondary rearrangement in the thymus: Role of continuous rearrangement of TCR α chain gene and positive selection in the T cell repertoire formation. *Proceedings of the National Academy of Sciences of the United States of America*. 1998;95(20):11834-11839.
93. Santori FR, Arsov I, Lilic M, Vukmanovic S. Editing autoreactive TCR enables efficient positive selection. *J Immunol*. 2002;169(4):1729-1734.
94. Mueller DL, Jenkins MK, Schwartz RH. Clonal expansion versus functional clonal inactivation: a costimulatory signalling pathway determines the outcome of T cell antigen receptor occupancy. *Annu Rev Immunol*. 1989;7:445-480.

95. Keir ME, Butte MJ, Freeman GJ, Sharpe AH. PD-1 and its ligands in tolerance and immunity. *Annu Rev Immunol*. 2008;26:677-704.
96. Fletcher AL, Lukacs-Kornek V, Reynoso ED, et al. Lymph node fibroblastic reticular cells directly present peripheral tissue antigen under steady-state and inflammatory conditions. *J Exp Med*. 2010;207(4):689-697.
97. Bjorkman PJ. MHC restriction in three dimensions: a view of T cell receptor/ligand interactions. *Cell*. 1997;89(2):167-170.
98. Niedermann G. Immunological functions of the proteasome. *Curr Top Microbiol Immunol*. 2002;268:91-136.
99. Momburg F, Tan P. Tapasin-the keystone of the loading complex optimizing peptide binding by MHC class I molecules in the endoplasmic reticulum. *Mol Immunol*. 2002;39(3-4):217-233.
100. Joffre OP, Segura E, Savina A, Amigorena S. Cross-presentation by dendritic cells. *Nat Rev Immunol*. 2012;12(8):557-569.
101. Turley SJ, Inaba K, Garrett WS, et al. Transport of peptide-MHC class II complexes in developing dendritic cells. *Science*. 2000;288(5465):522-527.
102. Van Kaer L. Accessory proteins that control the assembly of MHC molecules with peptides. *Immunol Res*. 2001;23(2-3):205-214.
103. Sadegh-Nasseri S, Chen M, Narayan K, Bouvier M. The convergent roles of tapasin and HLA-DM in antigen presentation. *Trends Immunol*. 2008;29(3):141-147.
104. Chen L, Flies DB. Molecular mechanisms of T cell co-stimulation and co-inhibition. *Nat Rev Immunol*. 2013;13(4):227-242.
105. June CH, Ledbetter JA, Gillespie MM, Lindsten T, Thompson CB. T-cell proliferation involving the CD28 pathway is associated with cyclosporine-resistant interleukin 2 gene expression. *Mol Cell Biol*. 1987;7(12):4472-4481.
106. del Rio ML, Lucas CL, Buhler L, Rayat G, Rodriguez-Barbosa JI. HVEM/LIGHT/BTLA/CD160 cosignaling pathways as targets for immune regulation. *J Leukoc Biol*. 2010;87(2):223-235.
107. Denoeud J, Moser M. Role of CD27/CD70 pathway of activation in immunity and tolerance. *J Leukoc Biol*. 2011;89(2):195-203.
108. Boomer JS, Green JM. An enigmatic tail of CD28 signaling. *Cold Spring Harb Perspect Biol*. 2010;2(8):a002436.
109. Ricklin D, Hajishengallis G, Yang K, Lambris JD. Complement: a key system for immune surveillance and homeostasis. *Nat Immunol*. 2010;11(9):785-797.
110. Kemper C, Atkinson JP. T-cell regulation: with complements from innate immunity. *Nat Rev Immunol*. 2007;7(1):9-18.
111. Longhi MP, Harris CL, Morgan BP, Gallimore A. Holding T cells in check--a new role for complement regulators? *Trends Immunol*. 2006;27(2):102-108.
112. Suresh M, Molina H, Salvato MS, Mastellos D, Lambris JD, Sandor M. Complement component 3 is required for optimal expansion of CD8 T cells during a systemic viral infection. *J Immunol*. 2003;170(2):788-794.
113. Peng Q, Li K, Sacks SH, Zhou W. The role of anaphylatoxins C3a and C5a in regulating innate and adaptive immune responses. *Inflamm Allergy Drug Targets*. 2009;8(3):236-246.
114. Groscurth P, Filgueira L. Killing Mechanisms of Cytotoxic T Lymphocytes. *Physiology*. 1998;13(1):17-21.

115. Romagnani S. T-cell subsets (Th1 versus Th2). *Ann Allergy Asthma Immunol*. 2000;85(1):9-18; quiz 18, 21.
116. Lamb JR, Skidmore BJ, Green N, Chiller JM, Feldmann M. Induction of tolerance in influenza virus-immune T lymphocyte clones with synthetic peptides of influenza hemagglutinin. *J Exp Med*. 1983;157(5):1434-1447.
117. Briner TJ, Kuo MC, Keating KM, Rogers BL, Greenstein JL. Peripheral T-cell tolerance induced in naive and primed mice by subcutaneous injection of peptides from the major cat allergen Fel d I. *Proceedings of the National Academy of Sciences*. 1993;90(16):7608-7612.
118. Hoyne GF, O'Hehir RE, Wraith DC, Thomas WR, Lamb JR. Inhibition of T cell and antibody responses to house dust mite allergen by inhalation of the dominant T cell epitope in naive and sensitized mice. *The Journal of Experimental Medicine*. 1993;178(5):1783-1788.
119. L. B, B. B, B. J-S, et al. Modulation of the allergic immune response in BALB/c mice by subcutaneous injection of high doses of the dominant T cell epitope from the major birch pollen allergen Bet v 1. *Clinical & Experimental Immunology*. 1997;107(3):536-541.
120. King TP, Lu G, Agosto H. Antibody responses to bee melittin (Api m 4) and hornet antigen 5 (Dol m 5) in mice treated with the dominant T-cell epitope peptides. *Journal of Allergy and Clinical Immunology*. 1998;101(3):397-403.
121. Monneaux F, Muller S. Peptide-based immunotherapy of systemic lupus erythematosus. *Autoimmun Rev*. 2004;3(1):16-24.
122. Critchfield JM, Racke MK, Zuniga-Pflucker JC, et al. T cell deletion in high antigen dose therapy of autoimmune encephalomyelitis. *Science*. 1994;263(5150):1139-1143.
123. Gaur A, Wiers B, Liu A, Rothbard J, Fathman CG. Amelioration of autoimmune encephalomyelitis by myelin basic protein synthetic peptide-induced anergy. *Science*. 1992;258(5087):1491-1494.
124. Ku G, Kronenberg M, Peacock DJ, et al. Prevention of experimental autoimmune arthritis with a peptide fragment of type II collagen. *Eur J Immunol*. 1993;23(3):591-599.
125. Daniel D, Wegmann DR. Protection of nonobese diabetic mice from diabetes by intranasal or subcutaneous administration of insulin peptide B-(9-23). *Proc Natl Acad Sci U S A*. 1996;93(2):956-960.
126. Bockova J, Elias D, Cohen IR. Treatment of NOD Diabetes with a Novel Peptide of the hsp60 Molecule Induces Th2-type Antibodies. *Journal of Autoimmunity*. 1997;10(4):323-329.
127. Raz I, Elias D, Avron A, Tamir M, Metzger M, Cohen IR. β-cell function in new-onset type 1 diabetes and immunomodulation with a heat-shock protein peptide (DiaPep277): a randomised, double-blind, phase II trial. *The Lancet*. 2001;358(9295):1749-1753.
128. Prakken BJ, Samodal R, Le TD, et al. Epitope-specific immunotherapy induces immune deviation of proinflammatory T cells in rheumatoid arthritis. *Proceedings of the National Academy of Sciences*. 2004;101(12):4228-4233.
129. Kretschmer K, Apostolou I, Hawiger D, Khazaie K, Nussenzweig MC, von Boehmer H. Inducing and expanding regulatory T cell populations by foreign antigen. *Nat Immunol*. 2005;6(12):1219-1227.
130. Kretschmer K, Heng TS, von Boehmer H. De novo production of antigen-specific suppressor cells in vivo. *Nat Protoc*. 2006;1(2):653-661.
131. Dornmair K, Goebels N, Weltzien H-U, Wekerle H, Hohlfeld R. T-Cell-Mediated Autoimmunity: Novel Techniques to Characterize Autoreactive T-Cell Receptors. *The American Journal of Pathology*. 2003;163(4):1215-1226.

132. Suchin EJ, Langmuir PB, Palmer E, Sayegh MH, Wells AD, Turka LA. Quantifying the frequency of alloreactive T cells in vivo: new answers to an old question. *J Immunol*. 2001;166(2):973-981.
133. Ezkurdia I, Juan D, Rodriguez JM, et al. Multiple evidence strands suggest that there may be as few as 19 000 human protein-coding genes. *Human Molecular Genetics*. 2014;23(22):5866-5878.
134. C. OJ, R. KN, S. BJ. Direct versus Indirect Allorecognition: Visualization of Dendritic Cell Distribution and Interactions During Rejection and Tolerization. *American Journal of Transplantation*. 2006;6(10):2488-2496.
135. Gould DS, Auchincloss H, Jr. Direct and indirect recognition: the role of MHC antigens in graft rejection. *Immunology Today*. 1999;20(2):77-82.
136. Dickinson AM, Norden J, Li S, et al. Graft-versus-Leukemia Effect Following Hematopoietic Stem Cell Transplantation for Leukemia. *Frontiers in Immunology*. 2017;8(496).
137. Marijt WA, Heemskerk MH, Kloosterboer FM, et al. Hematopoiesis-restricted minor histocompatibility antigens HA-1- or HA-2-specific T cells can induce complete remissions of relapsed leukemia. *Proc Natl Acad Sci U S A*. 2003;100(5):2742-2747.
138. Matte CC, Liu J, Cormier J, et al. Donor APCs are required for maximal GVHD but not for GVL. *Nat Med*. 2004;10(9):987-992.
139. Woiciechowsky A, Regn S, Kolb HJ, Roskrow M. Leukemic dendritic cells generated in the presence of FLT3 ligand have the capacity to stimulate an autologous leukemia-specific cytotoxic T cell response from patients with acute myeloid leukemia. *Leukemia*. 2001;15(2):246-255.
140. Chan CJ, Smyth MJ, Martinet L. Molecular mechanisms of natural killer cell activation in response to cellular stress. *Cell Death Differ*. 2014;21(1):5-14.
141. Wagtmann N, Biassoni R, Cantoni C, et al. Molecular clones of the p58 NK cell receptor reveal immunoglobulin-related molecules with diversity in both the extra- and intracellular domains. *Immunity*. 1995;2(5):439-449.
142. Colonna M, Samaridis J. Cloning of immunoglobulin-superfamily members associated with HLA-C and HLA-B recognition by human natural killer cells. *Science*. 1995;268(5209):405-408.
143. Caligiuri MA. Human natural killer cells. *Blood*. 2008;112(3):461-469.
144. Xun CQ, Thompson JS, Jennings CD, Brown SA, Widmer MB. Effect of total body irradiation, busulfan-cyclophosphamide, or cyclophosphamide conditioning on inflammatory cytokine release and development of acute and chronic graft-versus-host disease in H-2-incompatible transplanted SCID mice. *Blood*. 1994;83(8):2360-2367.
145. Thomas ED, Collins JA, Herman EC, Jr., Ferrebee JW. Marrow transplants in lethally irradiated dogs given methotrexate. *Blood*. 1962;19:217-228.
146. Deeg HJ, Storb R, Weiden PL, et al. Cyclosporin A and methotrexate in canine marrow transplantation: engraftment, graft-versus-host disease, and induction of intolerance. *Transplantation*. 1982;34(1):30-35.
147. Deeg HJ, Storb R, Appelbaum FR, Kennedy MS, Graham TC, Thomas ED. Combined immunosuppression with cyclosporine and methotrexate in dogs given bone marrow grafts from DLA-haploidentical littermates. *Transplantation*. 1984;37(1):62-65.
148. Deeg HJ, Storb R, Weiden PL, Graham T, Atkinson K, Thomas ED. Cyclosporin-A: effect on marrow engraftment and graft-versus-host disease in dogs. *Transplant Proc*. 1981;13(1 Pt 1):402-404.

149. Socie G, Ritz J. Current issues in chronic graft-versus-host disease. *Blood*. 2014;124(3):374-384.
150. Inamoto Y, Flowers ME. Treatment of chronic graft-versus-host disease in 2011. *Curr Opin Hematol*. 2011;18(6):414-420.
151. Collins RH, Jr., Rogers ZR, Bennett M, Kumar V, Nikein A, Fay JW. Hematologic relapse of chronic myelogenous leukemia following allogeneic bone marrow transplantation: apparent graft-versus-leukemia effect following abrupt discontinuation of immunosuppression. *Bone Marrow Transplant*. 1992;10(4):391-395.
152. Weiden PL, Storb R, Tsoi MS, Graham TC, Lerner KG, Thomas ED. Infusion of donor lymphocytes into stable canine radiation chimeras: implications for mechanism of transplantation tolerance. *J Immunol*. 1976;116(5):1212-1219.
153. Bortin MM, Truitt RL, Rimm AA, Bach FH. Graft-versus-leukaemia reactivity induced by alloimmunisation without augmentation of graft-versus-host reactivity. *Nature*. 1979;281(5731):490-491.
154. Cooke KR, Hill GR, Crawford JM, et al. Tumor necrosis factor- alpha production to lipopolysaccharide stimulation by donor cells predicts the severity of experimental acute graft-versus-host disease. *J Clin Invest*. 1998;102(10):1882-1891.
155. Korngold R, Marini JC, de Baca ME, Murphy GF, Giles-Komar J. Role of tumor necrosis factor-α in graft-versus-host disease and graft-versus-leukemia responses. *Biology of Blood and Marrow Transplantation*. 2003;9(5):292-303.
156. Tawara I, Koyama M, Liu C, et al. Interleukin-6 modulates graft-versus-host responses after experimental allogeneic bone marrow transplantation. *Clin Cancer Res*. 2011;17(1):77-88.
157. Chen X, Das R, Komorowski R, et al. Blockade of interleukin-6 signaling augments regulatory T-cell reconstitution and attenuates the severity of graft-versus-host disease. *Blood*. 2009;114(4):891-900.
158. Shin HJ, Baker J, Leveson-Gower DB, Smith AT, Sega EI, Negrin RS. Rapamycin and IL-2 reduce lethal acute graft-versus-host disease associated with increased expansion of donor type CD4+CD25+Foxp3+ regulatory T cells. *Blood*. 2011;118(8):2342-2350.
159. He S, Cao Q, Qiu Y, et al. A New Approach to the Blocking of Alloreactive T Cell-Mediated Graft-versus-Host Disease by In Vivo Administration of Anti-CXCR3 Neutralizing Antibody. *The Journal of Immunology*. 2008;181(11):7581-7592.
160. Ueha S, Murai M, Yoneyama H, et al. Intervention of MAdCAM-1 or fractalkine alleviates graft-versus-host reaction associated intestinal injury while preserving graft-versus-tumor effects. *Journal of Leukocyte Biology*. 2006;81(1):176-185.
161. Wysocki CA, Jiang Q, Panoskaltsis-Mortari A, et al. Critical role for CCR5 in the function of donor CD4⁺CD25⁺ regulatory T cells during acute graft-versus-host disease. *Blood*. 2005;106(9):3300-3307.
162. Yu X-Z, Bidwell SJ, Martin PJ, Anasetti C. CD28-Specific Antibody Prevents Graft-Versus-Host Disease in Mice. *The Journal of Immunology*. 2000;164(9):4564-4568.
163. Blazar BR, Sharpe AH, Taylor PA, et al. Infusion of anti-B7.1 (CD80) and anti-B7.2 (CD86) monoclonal antibodies inhibits murine graft-versus-host disease lethality in part via direct effects on CD4+ and CD8+ T cells. *The Journal of Immunology*. 1996;157(8):3250-3259.
164. Durie FH, Aruffo A, Ledbetter J, et al. Antibody to the ligand of CD40, gp39, blocks the occurrence of the acute and chronic forms of graft-vs-host disease. *The Journal of Clinical Investigation*. 1994;94(3):1333-1338.

165. Hargreaves REG, Monk NJ, Jurcevic S. Selective depletion of activated T cells: the CD40L-specific antibody experience. *Trends in Molecular Medicine*. 2004;10(3):130-135.
166. Blazar BR, Sharpe AH, Chen AI, et al. Ligation of OX40 (CD134) regulates graft-versus-host disease (GVHD) and graft rejection in allogeneic bone marrow transplant recipients. *Blood*. 2003;101(9):3741-3748.
167. Nozawa K, Ohata J, Sakurai J, et al. Preferential Blockade of CD8⁺ T Cell Responses by Administration of Anti-CD137 Ligand Monoclonal Antibody Results in Differential Effect on Development of Murine Acute and Chronic Graft-Versus-Host Diseases. *The Journal of Immunology*. 2001;167(9):4981-4986.
168. Taylor PA, Panoskaltsis-Mortari A, Freeman GJ, et al. Targeting of inducible costimulator (ICOS) expressed on alloreactive T cells down-regulates graft-versus-host disease (GVHD) and facilitates engraftment of allogeneic bone marrow (BM). *Blood*. 2005;105(8):3372-3380.
169. Xu Y, Flies AS, Flies DB, et al. Selective targeting of the LIGHT-HVEM costimulatory system for the treatment of graft-versus-host disease. *Blood*. 2007;109(9):4097-4104.
170. Karimi MA, Bryson JL, Richman LP, et al. NKG2D expression by CD8⁺ T cells contributes to GVHD and GVT effects in a murine model of allogeneic HSCT. *Blood*. 2015;125(23):3655-3663.
171. Nabekura T, Shibuya K, Takenaka E, et al. Critical role of DNAX accessory molecule-1 (DNAM-1) in the development of acute graft-versus-host disease in mice. *Proceedings of the National Academy of Sciences*. 2010;107(43):18593-18598.
172. Blazar BR, Levy RB, Mak TW, et al. CD30/CD30 Ligand (CD153) Interaction Regulates CD4⁺ T Cell-Mediated Graft-versus-Host Disease. *The Journal of Immunology*. 2004;173(5):2933-2941.
173. Amara U, Rittirsch D, Flierl M, et al. Interaction Between the Coagulation and Complement System. *Advances in experimental medicine and biology*. 2008;632:71-79.
174. Manthey HD, Woodruff TM, Taylor SM, Monk PN. Complement component 5a (C5a). *Int J Biochem Cell Biol*. 2009;41(11):2114-2117.
175. Lalli PN, Strainic MG, Yang M, Lin F, Medof ME, Heeger PS. Locally produced C5a binds to T cell-expressed C5aR to enhance effector T-cell expansion by limiting antigen-induced apoptosis. *Blood*. 2008;112(5):1759-1766.
176. Strainic MG, Liu J, Huang D, et al. Locally produced complement fragments C5a and C3a provide both costimulatory and survival signals to naive CD4+ T cells. *Immunity*. 2008;28(3):425-435.
177. Kwan WH, Hashimoto D, Paz-Artal E, et al. Antigen-presenting cell-derived complement modulates graft-versus-host disease. *J Clin Invest*. 2012;122(6):2234-2238.
178. Cravedi P, Leventhal J, Lakhani P, Ward SC, Donovan MJ, Heeger PS. Immune cell-derived C3a and C5a costimulate human T cell alloimmunity. *Am J Transplant*. 2013;13(10):2530-2539.
179. Niculescu F, Niculescu T, Nguyen P, et al. Both apoptosis and complement membrane attack complex deposition are major features of murine acute graft-vs.-host disease. *Exp Mol Pathol*. 2005;79(2):136-145.
180. Wetsel RA, Fleischer DT, Haviland DL. Deficiency of the murine fifth complement component (C5). A 2-base pair gene deletion in a 5'-exon. *J Biol Chem*. 1990;265(5):2435-2440.
181. Woodruff TM, Nandakumar KS, Tedesco F. Inhibiting the C5-C5a receptor axis. *Mol Immunol*. 2011;48(14):1631-1642.

182. Dmytrijuk A, Robie-Suh K, Cohen MH, Rieves D, Weiss K, Pazdur R. FDA report: eculizumab (Soliris) for the treatment of patients with paroxysmal nocturnal hemoglobinuria. *Oncologist*. 2008;13(9):993-1000.
183. Matis LA, Rollins SA. Complement-specific antibodies: designing novel anti-inflammatories. *Nat Med*. 1995;1(8):839-842.
184. Mukherjee P, Pasinetti GM. Complement anaphylatoxin C5a neuroprotects through mitogen-activated protein kinase-dependent inhibition of caspase 3. *J Neurochem*. 2001;77(1):43-49.
185. Bhatia M, Saluja AK, Singh VP, et al. Complement factor C5a exerts an anti-inflammatory effect in acute pancreatitis and associated lung injury. *Am J Physiol Gastrointest Liver Physiol*. 2001;280(5):G974-978.
186. Langer HF, Chung KJ, Orlova VV, et al. Complement-mediated inhibition of neovascularization reveals a point of convergence between innate immunity and angiogenesis. *Blood*. 2010;116(22):4395-4403.
187. Macor P, Durigutto P, De Maso L, et al. Prevention of antigen-induced arthritis by targeting synovial endothelium with a neutralizing recombinant antibody to C5. Vol. 46; 2009.
188. Ruggeri L, Capanni M, Urbani E, et al. Effectiveness of Donor Natural Killer Cell Alloreactivity in Mismatched Hematopoietic Transplants. *Science*. 2002;295(5562):2097-2100.
189. Dickinson AM, Norden J, Li S, et al. Graft-versus-Leukemia Effect Following Hematopoietic Stem Cell Transplantation for Leukemia. *Frontiers in Immunology*. 2017;8:496.
190. Pittenger MF, Mackay AM, Beck SC, et al. Multilineage potential of adult human mesenchymal stem cells. *Science*. 1999;284(5411):143-147.
191. Kalinina NI, Sysoeva VY, Rubina KA, Parfenova YV, Tkachuk VA. Mesenchymal stem cells in tissue growth and repair. *Acta Naturae*. 2011;3(4):30-37.
192. Yagi H, Soto-Gutierrez A, Parekkadan B, et al. Mesenchymal stem cells: Mechanisms of immunomodulation and homing. *Cell Transplant*. 2010;19(6):667-679.
193. Le Blanc K, Ringden O. Immunomodulation by mesenchymal stem cells and clinical experience. *J Intern Med*. 2007;262(5):509-525.
194. Sato K, Ozaki K, Oh I, et al. Nitric oxide plays a critical role in suppression of T-cell proliferation by mesenchymal stem cells. *Blood*. 2007;109(1):228-234.
195. Mellor AL, Munn DH. IDO expression by dendritic cells: tolerance and tryptophan catabolism. *Nat Rev Immunol*. 2004;4(10):762-774.
196. Spaggiari GM, Capobianco A, Abdelrazik H, Becchetti F, Mingari MC, Moretta L. Mesenchymal stem cells inhibit natural killer-cell proliferation, cytotoxicity, and cytokine production: role of indoleamine 2,3-dioxygenase and prostaglandin E2. *Blood*. 2008;111(3):1327-1333.
197. Le Blanc K, Tammik L, Sundberg B, Haynesworth SE, Ringden O. Mesenchymal stem cells inhibit and stimulate mixed lymphocyte cultures and mitogenic responses independently of the major histocompatibility complex. *Scand J Immunol*. 2003;57(1):11-20.
198. Maccario R, Podesta M, Moretta A, et al. Interaction of human mesenchymal stem cells with cells involved in alloantigen-specific immune response favors the differentiation of CD4+ T-cell subsets expressing a regulatory/suppressive phenotype. *Haematologica*. 2005;90(4):516-525.

199. Rasmusson I, Ringden O, Sundberg B, Le Blanc K. Mesenchymal stem cells inhibit the formation of cytotoxic T lymphocytes, but not activated cytotoxic T lymphocytes or natural killer cells. *Transplantation*. 2003;76(8):1208-1213.
200. Angoulvant D, Clerc A, Benchalal S, et al. Human mesenchymal stem cells suppress induction of cytotoxic response to alloantigens. *Biorheology*. 2004;41(3-4):469-476.
201. Rubina K, Kalinina N, Efimenko A, et al. Adipose stromal cells stimulate angiogenesis via promoting progenitor cell differentiation, secretion of angiogenic factors, and enhancing vessel maturation. *Tissue Eng Part A*. 2009;15(8):2039-2050.
202. Lavoie JR, Rosu-Myles M. Uncovering the secretes of mesenchymal stem cells. *Biochimie*. 2013;95(12):2212-2221.
203. Kim HS, Choi DY, Yun SJ, et al. Proteomic analysis of microvesicles derived from human mesenchymal stem cells. *J Proteome Res*. 2012;11(2):839-849.
204. Toubai T, Paczesny S, Shono Y, et al. Mesenchymal stem cells for treatment and prevention of graft-versus-host disease after allogeneic hematopoietic cell transplantation. *Curr Stem Cell Res Ther*. 2009;4(4):252-259.
205. Boieri M, Shah P, Dressel R, Inngjerdingen M. The Role of Animal Models in the Study of Hematopoietic Stem Cell Transplantation and GvHD: A Historical Overview. *Frontiers in Immunology*. 2016;7:333.
206. Zorn E, Kim HT, Lee SJ, et al. Reduced frequency of FOXP3+ CD4+CD25+ regulatory T cells in patients with chronic graft-versus-host disease. *Blood*. 2005;106(8):2903-2911.
207. Cohen JL, Trenado A, Vasey D, Klatzmann D, Salomon BL. CD4(+)CD25(+) immunoregulatory T Cells: new therapeutics for graft-versus-host disease. *J Exp Med*. 2002;196(3):401-406.
208. Hoffmann P, Ermann J, Edinger M, Fathman CG, Strober S. Donor-type CD4(+)CD25(+) regulatory T cells suppress lethal acute graft-versus-host disease after allogeneic bone marrow transplantation. *J Exp Med*. 2002;196(3):389-399.
209. Rezvani K, Mielke S, Ahmadzadeh M, et al. High donor FOXP3-positive regulatory T-cell (Treg) content is associated with a low risk of GVHD following HLA-matched allogeneic SCT. *Blood*. 2006;108(4):1291-1297.
210. Edinger M, Hoffmann P, Ermann J, et al. CD4+CD25+ regulatory T cells preserve graft-versus-tumor activity while inhibiting graft-versus-host disease after bone marrow transplantation. *Nat Med*. 2003;9(9):1144-1150.
211. Taylor PA, Panoskaltsis-Mortari A, Swedin JM, et al. L-Selectin(hi) but not the L-selectin(lo) CD4+25+ T-regulatory cells are potent inhibitors of GVHD and BM graft rejection. *Blood*. 2004;104(12):3804-3812.
212. Fantini MC, Becker C, Monteleone G, Pallone F, Galle PR, Neurath MF. Cutting Edge: TGF-β Induces a Regulatory Phenotype in CD4⁺CD25[−] T Cells through Foxp3 Induction and Down-Regulation of Smad7. *The Journal of Immunology*. 2004;172(9):5149-5153.
213. Beres A, Komorowski R, Mihara M, Drobyski WR. Instability of Foxp3 expression limits the ability of induced regulatory T cells to mitigate graft versus host disease. *Clin Cancer Res*. 2011;17(12):3969-3983.
214. Koenecke C, Czeloth N, Bubke A, et al. Alloantigen-specific de novo-induced Foxp3+ Treg revert in vivo and do not protect from experimental GVHD. *Eur J Immunol*. 2009;39(11):3091-3096.

215. Qin S, Cobbold SP, Pope H, et al. "Infectious" transplantation tolerance. *Science*. 1993;259(5097):974-977.
216. Niimi M, Shirasugi N, Ikeda Y, Wood KJ. Oral antigen induces allograft survival by linked suppression via the indirect pathway. *Transplantation Proceedings*. 2001;33(1):81.
217. Florek M, Schneidawind D, Pierini A, et al. Freeze and Thaw of CD4+CD25+Foxp3+ Regulatory T Cells Results in Loss of CD62L Expression and a Reduced Capacity to Protect against Graft-versus-Host Disease. *PLOS ONE*. 2015;10(12):e0145763.